

Latest Advances in Cryogel Technology for Biomedical Applications

*Adnan Memic, Thibault Colombani, Mahboobeh Rezaeeyazdi, Loek Eggermont, Joseph Steingold, Zach Rogers, Kasturi J. Navare, Halimatu S. Mohammed, Sidi A. Bencherif**

Prof. A. Memic

Center of Nanotechnology, King Abdulaziz University, Jeddah 21589, Saudi Arabia

Center for Biomedical Engineering, Department of Medicine, Brigham and Women's Hospital, Harvard Medical School, Cambridge, MA 02139, USA

Prof. A. Memic, M. Rezaeeyazdi, Dr. T. Colombani, Z. Rogers, Dr. K. Joshi Navare, Dr. H. S. Mohammed, Prof. S. A. Bencherif

Department of Chemical Engineering, Northeastern University, Boston, MA 02115, USA

Dr. L. Eggermont

Department of Tumor Immunology, Oncode Institute, Radboud Institute for Molecular Life Sciences, Radboud University Medical Center, Nijmegen 6500, the Netherlands

J. Steingold

Department of Pharmaceutical Sciences, Northeastern University, Boston, MA 02115, USA

Prof. S. A. Bencherif

Department of Bioengineering, Northeastern University, Boston, MA 02115, USA

Harvard John A. Paulson School of Engineering and Applied Sciences, Harvard University, Cambridge, MA 02138, USA

Sorbonne University, UTC CNRS UMR 7338, Biomechanics and Bioengineering (BMBI), University of Technology of Compiègne, Compiègne 60159, France

E-mail: s.bencherif@northeastern.edu

Keywords: cryogels; biomaterials; bioseparation; tissue engineering; immunotherapy

Abstract:

There exists a technological need for advanced materials with improved properties for emerging biomedical applications. Recent developments in macroporous materials have demonstrated their applicability as indispensable tools in biomedical research. Cryogels, which are materials with a macroporous three-dimensional structure, are produced as a result of controlled freezing during polymerization with a highly interconnected polymer network. Cryogels' interest lies in their ability to address some of the limitations of their hydrogel analogues. In this review, we first discuss basic hydrogel and cryogel concepts as a short primer for readers unfamiliar with the cryogels literature. Next, we provide a general overview of the methods for synthesis and characterization of cryogels, highlighting key concepts relevant to cryogels and explaining their unique properties. Finally, we provide an in-depth overview of specific technologies and fields where cryogels have been applied. We illustrate how the latest advances in cryogel technologies are able to address challenges in bioseparation, tissue engineering, and other emerging bioengineering disciplines.

1. Introduction

The next generation of biomedical advances require materials with unique properties. The utility and versatility of gels has placed them at the forefront of biomedical research. Gels can be defined as materials consisting of a network component and a swelling agent. Hydrogels are gels in which the network component are hydrophilic polymers and the swelling agent is water.^[1] Hydrogels can be classified according to several parameters, which, in addition to several listed in an excellent review by Ahmed,^[2] include porosity^[3] and particle network type^[4] (**Table 1**). It is worth noting that although “supermacroporous” is not an official International Union of Pure and Applied Chemistry (IUPAC) term, it has been used informally in the hydrogel literature to describe pore diameters ranging from 10–200 μm , where excellent mass flow and significant interaction with biomolecules become feasible.^[5] In various applications, efforts to utilize hydrogels have been undermined by their lack of a highly elastic interconnected macroporous network. A prominent method for introducing interconnected macroporous networks in hydrogels is the utilization of materials that cause disruptions in the gel or “porogens” such as crystalline particles,^[6] immiscible solvent,^[7] gas bubbles,^[8] and photolithography molds,^[9] which all must later be removed from the resulting materials. Porogen-based syntheses have yielded interconnected pores up to and including the supermacroporous level in diameter. However, the resulting hydrogels manifest inherent risks when used as biomaterials. Remnant porogens not only represent potential cytotoxins, but they also present potential physical barriers in tissue engineering by blocking cell infiltration.^[10]

Cryogels can be defined as hydrogels in which a controlled polymerization occurs at subzero temperatures, yielding an elastic interconnected network of macropores^[11]. Cryogels can be traced back as early as the 1940s^[12]. However, significant interest in cryogels arguably did not occur until the 1980s^[13]. Paradigm shifts in cryogel science that are highly relevant to this review include: i) increased interest in the unique aspects of cryogel synthesis and characterization; key findings from the 1980s on the freezing behavior of polyacrylamide cryogels, for example, still influence modern research on these systems^[14]. ii) The then-novel accomplishment of whole cell entrapment in cryogels

(specifically of microbes), also in the 1980s^[15]. This particular achievement implicated cryogels both as chromatography monoliths, which remains their most popular application, and as tissue engineering scaffolds, which as of 2016, is their fastest growing application^[16]. Advances in polymer chemistry continue to lead to advances in cryogel synthesis.^[17]

In this review, we first provide a mechanistic explanation of cryogel synthesis, including sections on physical and chemical cross-links and specifically addressing the limitations of each. We then describe different types of cryogels, especially novel approaches to generate composite and stimuli-responsive materials. We emphasize cryogels' physical properties and their characterization. In the subsequent sections, we focus on specific applications of cryogels. Initially, cryogels were used in bioseparation as chromatography monoliths. We aim to provide a detailed account of bioseparation-related applications of cryogels, including biomolecule and cell separation, bioanalytical chemistry, cell immobilization, and biocatalysis. Next, we emphasize the importance of cryogels in tissue engineering applications. We focus on the use of cryogels in mimicking various tissues and the advances that have resulted in the application of cryogels, even when fabricated using traditionally non-biocompatible precursors and as cryogel based bioreactors. Finally, we provide an overview of other relevant bioengineering applications of cryogels. For example, cryogels are presented as a solution to the limitations of cell-based therapies, as cancer vaccines and as drug delivery vehicles. We have set out to demonstrate that materials with unique biophysical properties can lead to various novel biological applications, and that advanced cryogels represent an effective and dynamic solution to these challenges.

2. Overview of cryogels

Cryogels, which are advanced forms of hydrogels, have revolutionized the field of biomedical research. The highly interconnected, macroporous structure of cryogels has proven to be essential for many biomedical applications. Unique cryogel properties that include high water content, porosity,

and soft consistency make them capable of closely simulating natural living tissue.^[2, 18, 19] Various types of cryogels can be synthesized through different techniques and various characterization methods can be used to describe their properties, such as their interconnected macroporous architecture.^[20, 21]

2.1 Synthesis of cryogels

Cryogel synthesis circumvents the need for porogens by utilization of frozen solvent for pore formation. Frozen solvent leaves behind pores after removal (**Figure 1**). Freeze-thawing also tends to be less time- and resource-consuming.^[22] However, when done at a specific pressure and temperature, freeze-drying can optimize the efficiency of cryogel monoliths by introducing nanospines in the cryogel.^[23] Various parameters of the cryogelation process can be tampered with to customize cryogels for their intended use, several of which are listed in an excellent review by Henderson *et al.* (**Table 2**).^[10] One other method of cryogel customization include cyclic cryogelation, which utilizes cycles of temperature increases and decreases after the freezing step. Each cycle results in a net gain of hydrogen bonds in the polymer network, yielding mechanically stronger cryogels with high polymer network uniformity and thermal conductivity.^[24] Cryogels can also be made mechanically stronger using so-called “cryogelation within cryogelation,” in which cryogelation occurs within pores formed via cryogelation.^[25] Another advantage of cryogels relative to hydrogels include gelation at lower initiator concentrations than their hydrogel counterparts, yielding more economically produced cryogels.^[26]

2.1.1. Cryogelation vs. conventional fabrication methods

Over the last 20 years, macroporous scaffolds used for different biomedical applications have been fabricated through numerous techniques:^[27, 28] salt/porogen templating,^[29, 30, 31, 32, 33] gas foaming,^[34-40] 3D printing,^[41-43, 44, 45] freeze-drying,^[46, 47] and cryogelation^[48, 49-51] are the most common among these methods. However, cryogelation is the only fabrication method through which

a highly interconnected 3D macroporous matrix can be obtained. In addition, cryogelation is the easiest and least time consuming technique that can be used for fabricating injectable macroporous scaffolds as large as 64 mm³.^[52] Here, we will review the above methods in detail, noting their limitations and inconveniences (**Figure 2**).

2.1.2. Salt/Porogen Templating

Salt/porogen templating due to its low cost and simplicity has been one of the most common methods used in preparing macroporous 3D scaffolds.^[28] In this technique, salt particles or polymeric microbeads can be used as a template to create micro-/macrosized pores within hydrogels. The salt particles or polymeric microbeads can be further dissolved by submersion in an appropriate solvent, leading to the formation of a porous network. Historically, salt particles have been used in this technique owing to their availability, ease in handling, low price, and stability during processing under various conditions.^[53] Due to the bio-inertness of sodium chloride crystals, they have been the most commonly used type of salts for the fabrication of porous hydrogels.^[32]

Various polymer precursors—including poly (ethyleneglycol) (PEG), poly (ε-caprolactone) (PCL)^[54], oligo (PEG) fumarate,^[55] alginate-g-poly (N-isopropylacrylamide),^[55] and poly (2-hydroxyethyl methacrylate) (PHEMA)^[56]—can be used to fabricate scaffolds with an interconnected and highly porous morphology. These scaffolds exhibit improved swelling properties when synthesized in the presence of NaCl-based salt templating, generating pore sizes of 180–400 μm. However, a high concentration of salt is required for this fabrication technique, which decreases the purity of the final scaffold and can cause a high osmolarity. Furthermore, the possibility of the salt crystals remaining undissolved within the hydrogel scaffold has limited this technique's applicability to biomedical applications.^[28] To overcome these limitations, researchers have investigated degradable polymeric microbeads to be used as alternative porogens for the fabrication of macroporous polymeric scaffolds.^[28] In one study, Delaney *et al.* integrated well-defined geometric microspheres made of calcium alginate into hydrogels, taking advantage of their reversible gel state;

these alginate microgels could subsequently be solubilized and removed, resulting in the formation of an open macroporous network.^[57] In another study, Hwang *et al.* used the thermoresponsive gelling property of gelatin in order to produce gelatin beads as large as 150–300 μm to formulate macroporous alginate hydrogels which can be utilized for cell encapsulation.^[58] An important consideration when using porogens during scaffold fabrication is that they are not only nontoxic and cytocompatible, but that they also have controlled degradation times relevant to their application.^[59] Challenges associated with complete elimination of porogens from the polymer network limits the applications of this technique to the fabrication of only relatively thin scaffolds (usually $<500\text{ }\mu\text{m}$ thick). It should be noted that as the salt/porogen templating technique mostly relies on the use of cytotoxic organic solvents that require a long drying process to ensure complete purification of the salt/porogen, this technique may not result in a perfectly biocompatible biomaterial matrix. Furthermore, the need for extraction of salt/porogen and the subsequent purification steps make salt/porogen templating a relatively time-consuming method.

2.1.3. *Gas foaming*

Gas foaming is another well-known and common method for fabricating macroporous hydrogels. In this technique, the polymer network forms around gas bubbles that have been captured throughout the matrix. The gas bubbles can be formed within the precursor solution through active bubbling or in-situ generation of gas bubbles.^[34-40] The most common gas forming agent used is sodium bicarbonate, since it produces CO_2 gas in an acidic environment.^[31] However, alternative types of carbonates and nitrates, such as ammonium and potassium carbonates and sodium nitrite,^[37] could also be utilized for such purposes. Foaming agents are mostly chosen based on their cost, safety, by-product generation, and the type of residual products that remain within a scaffold post-fabrication. Factors influencing the size of pores within scaffolds when using foaming agents include the amount of gas that is dissolved initially and the rate of pressure variation.^[60] However, low to moderate solubility of gasses such as CO_2 in water can limit the final porosity of the fabricated

scaffold, which is a major drawback of the gas foaming technique.^[61] Similar to salt/porogen templating, the washing steps required to remove the residues of gas foaming agents following gas bubbling can be very technically challenging. In addition, unlike the salt/porogen templating technique, which leads to a defined and reproducible pore size and shape, scaffolds made using gas foaming often exhibit a highly heterogeneous distribution of pore sizes and shapes.^[28] However, when combining these two techniques, the disadvantages of both techniques can be reduced, yielding gels with a more uniform macroporous architecture and higher surface area.^[39, 62] Besides the limitations mentioned for each approach above, the key drawback common to all these techniques is the lack of a fully continuous pore structure and pore connectivity, a shortcoming which makes the fabricated macroporous scaffolds suitable for only limited applications.^[28]

2.1.4. *Freeze-drying*

A search of studies published on polymeric cryogels possessing highly interconnected macropores reveals that there are two different types of cryogels: (i) polymeric cryogels produced from several freeze-drying cycles of freshly-made conventional nanoporous hydrogels, and (ii) cryogels produced in a frozen solvent through cryogelation from synthetic and natural polymers or proteins. Both techniques use ice microcrystallites as porogens in order to fabricate microporous cryogels.^[22]

During freeze-drying, also known as lyophilization, a freshly-made nanoporous hydrogel undergoes a freezing cycle, resulting in the growth of ice crystals, which can be subsequently eliminated through vacuum drying. Freeze-drying techniques can be used to generate interconnected porous structures with scaffolds made of both natural^[63, 64, 65-67] and synthetic^[46, 68-70] polymers. In some studies, freeze-drying is used as an ice templating technique for producing ordered macroporous materials from freshly-made hydrogels.^[71] In this technique, hydrogels are quickly immersed into a cold bath, where micrometer-sized ice crystals form within the matrices of these premade networks. These ice spheres then act as templates for the creation of three-dimensionally interconnected

macroporous scaffolds.^[71] The freezing temperature prior to freeze-drying has been shown to play an important role in determining the size and the shape of the pores within the scaffolds, which can consequently affect the characteristics of the resulting porous cryogels. For instance, Wu *et al.* observed open pore structures after lyophilization of samples frozen at -20°C and -80°C and pores with parallel sheet structure throughout samples frozen at -196°C (in liquid N₂) following freeze-drying.^[72] To guide axonal regeneration by tuning pore properties, Stokols *et al.* used a modified version of this freeze-drying technique to generate linear pores within agarose hydrogels which were subsequently used to study spinal cord injury repair.^[73] The technique used by Stokols *et al.* causes ice crystals to form in an oriented manner in the direction of the uniaxial thermal gradient (i.e. subjecting only a single end of the agarose pillar to dry ice immersed in liquid). As a result, upon removal of ice through lyophilization, it is possible to generate highly aligned networks of porous channels. Despite the development of these novel techniques for cryogel fabrication through freeze-drying, these scaffolds generally possess low structural stability and other weak mechanical properties. Depending on the type of cryogelation (i.e. freeze-drying or freeze-thawing), the mechanical properties of the cryogels can vary from rigid and brittle gels (e.g. cryogels fabricated through freeze-drying) to soft and elastic sponges with shape memory properties (e.g. freeze-thawed cryogels).^[22]

2.1.5. *Cryopolymerization or freeze-thawing*

To address some of these challenges, researchers developed a novel freeze-gelation process called cryopolymerization to fabricate highly elastic and mechanically robust cryogels. This technique involves a simple strategy for the preparation of macroporous polymeric scaffolds with a high degree of pore interconnectivity and toughness. This approach highlights cryogels' capability in tolerating extreme compression, elongation and torsion forces which has attracted a great deal of attention for the past 15 years.^[74] The formation of cryogels via cryopolymerization (i.e. freeze-thawing) involves the cross-linking of an initial polymer mixture at an optimized subzero temperature

followed by subsequent defrosting at room temperature. Due to the phase separation that occurs during the ice crystal formation at subzero temperatures, the solvent in the pre-polymer solution crystallizes within a highly concentrated monomer solution which subsequently forms around the resulting ice crystals. Further incubation at subzero temperature results in cross-linking of the highly concentrated pre-polymer solution around the ice crystals. Upon removal of the ice crystals at room temperature, a macroporous 3D structure containing interconnected pores is the result.^[28] Chemical cross-linking through free radical polymerization during incubation at subzero temperature is the most common method for production of cryogels. The highly interconnected macrostructure of cryogels fabricated through freeze-thawing is a result of the organized fractal nature of ice crystal formation within the pre-polymer solution at subzero temperature. Therefore, cryogelation retains the advantages of techniques that use salt/porogen templated fabrication while overcoming the limitations of that approach such as poor pore interconnectivity and the need for salt/porogen elimination. Depending on the desired application, cryogels can be fabricated in different shapes and sizes, including monoliths, rods, sheets, discs, spherical particles, etc. (**Figure 3**).^[43, 44, 51, 65, 75, 76] It was once believed that the subzero temperature processing required for cryogel fabrication would represent a limitation when cell loading of scaffolds was required, such as applications in tissue engineering and regenerative medicine. However, when Vrana *et al.* combined cell cryoprotectants in conjunction with a cryogelation process, they showed that a cell-loaded macroporous gel scaffold can be successfully fabricated, which can then be used for the storage and transportation of mammalian cells.^[77, 78]

2.2 Fabrication of cryogels using different cross-linking strategies

Polymeric cryogels can be synthesized through two main mechanisms: the cross-linking of hydrophilic and hydrophobic monomers in the presence of a large quantity of water (up to 99 wt.%) through either chemical or physical means. Chemical cross-linking is cross-linking that takes place via a chemical reaction linking polymer chains into a cryogel. On the other hand, physical interactions

such as ionic or hydrophobic bonding between polymer chains that lead to cryogel formation are referred to as physical cross-linking.^[2] Chemical cross-linking of cryogels takes place while the polymer solution is at subzero temperatures.^[52, 79] However, physical cross-linking of cryogels occurs during the thawing step (in the case of using freeze-thawing or cryogelation), or, alternatively, before freeze-drying occurs (in the case of utilizing freeze-drying for cryogel fabrication).^[80, 81]

2.2.1. Physical cross-linking

Physical cross-linking can take place through either (i) hydrophobic or electrostatic interactions among different parts of polymer chains, or (ii) ions present in the solvent. As the formation of molecular networks through these interactions is purely physical, gel formation through physical cross-linking can be reversible.^[82] There are two primary criteria for selecting a suitable polymer for cryogel fabrication through physical cross-linking: (i) the presence of a strong interaction between the polymer chains causing the formation of semi-permanent junctions throughout the polymer walls, and (ii) the formation of strong polymer walls which can hold large amount of water molecules.

As physical cross-linking usually takes place through ion exchange or interaction, it is a fast process that can happen in a few seconds. Therefore, physical cross-linking usually cannot take place during cryogelation, as it would happen before the ice crystal formation and growth, which would result in a nanoporous hydrogel. There are two exceptions through which physically cross-linked cryogels can be fabricated: (i) physical cross-linking, which is very slow and/or takes place after ice crystal formation and growth,^[83] and (ii) freeze-thawing, by which the cryogel is generated from an already physically cross-linked hydrogel.^[84]

Although stable and strong macroporous scaffolds can be formed through physical cross-linking, the final pore size of the cryogel thus generated measures less than 10 μm , which, for tissue engineering applications, is considered too small. Offeddu *et al.* investigated the properties of responsive polyvinyl alcohol cryogels in order to recapitulate charge regeneration properties found

in cartilage and discovered that this matrix can provide a biomimetic environment for three-dimensional cell cultures aimed at repairing cartilage.^[84] In another study, Ciolacu *et al.* prepared porous cellulose matrices through both physical and chemical cross-linking.^[81] The structural characterization of their scaffolds revealed that physical gelation results in a heterogeneous network of thick polymer walls as well as a large pore size distribution, while chemical bonding can act as a spacer between chains, disrupting the self-association of thick polymer walls.^[81]

2.2.2. *Chemical cross-linking*

Physical cross-linking can be a very simple and rapid process for cryogel fabrication, as it is performed without the use of cross-linking entities or chemical modifications. However, there exist reports that physical cross-linking can lead to inconsistent performance during *in vivo* experiments, as the control over experimental conditions such as gelation time and chemical modification is limited—a factor which results in decreased control over pore size and degradation.^[85] In contrast, chemical cross-linking allows for the incorporation, encapsulation, and controlled release of drugs and bioactive molecules within the cryogel network without significant dissolution and termination of the scaffold.

The preparation of cryogels through the chemical cross-linking of monomer precursors is one of the most extensively-used pathways for cryogel fabrication. Among the different methods available for chemical cross-linking during cryogelation process, free radical polymerization has received the most attention in the last two decades.^[21] Free radical polymerization involves the formation of free radicals and their reaction with the polymer chains, which results in formation of a continuous polymer network.^[86] The free radicals required for this polymerization pathway can be generated through the decomposition of an initiator component by light, heat, or redox reaction. Free radical polymerization can only take place in cases where the monomer functional groups remain unsaturated (i.e., double or triple bonds present between two adjacent carbon atoms within the molecular structure of the polymer). The radical groups generated during free radical polymerization react with the double

bond of the unsaturated monomers, growing the polymer network. The main characteristic of free radical polymerization is its reaction rate, which is high due to the extreme reactivity of the radical groups generated during the reaction. Free radical polymerization is always a three-step process: initiation, propagation, and termination. The initiation step includes formation of free radicals due to the presence of an initiator. Different types of natural and synthetic polymers—such as hyaluronic acid,^[87, 88] gelatin,^[89] alginate,^[52, 90] and PEG—can be functionalized with vinylic groups in order to cross-link through a free radical polymerization pathway. Ammonium persulfate (APS) is the most common initiator system used for free radical polymerization of cryogels.

2.2.3.1 *Photo-cross-linking*

Photopolymerization is another type of free radical polymerization, in which a photo-initiator decomposes when subjected to UV light in order to produce free radicals for cross-linking.^[91, 92] This is the most common cross-linking method for generating nanoporous hydrogels; however, only a few literature reports are available on photopolymerization-based cryogel fabrication. A complicated system is needed to utilize light at subzero temperatures to make cryophotopolymerization possible. Ozmen *et al.* reported on obtaining highly compressive PDMS cryogels which were polymerized at -18°C through free radical polymerization using UV or sunlight.^[93] In another study, Kahveci *et al.*^[94] utilized a special photoreactor for the preparation of poly(acrylamide) cryogels through photopolymerization at -13°C of monomeric precursors.

2.2.3.2 *Cryo-polymerization based approaches*

Another chemical cross-linking pathway among the most frequently applied during cryopolymerization includes a combination of 1-ethyl-3-(3-dimethyl aminopropyl)carbodiimide (EDC) and N-hydroxysuccinimide (NHS).^[95] This cross-linking pathway can only occur in the presence of gelatin^[44, 96] or other amine-containing reagents.^[68, 97]

There exist other common cross-linking pathways for cryopolymerization of gels, such as Michael addition, which is a versatile synthetic method that conjugates electrophilic olefins to nucleophiles, typically in the presence of a base catalyst. Michael addition is used to synthesize various polymer architectures including linear, branched and network polymers.^[98] The Michael addition type reactions that functionalize biologically active polymers are often meant to generate bioconjugates for biomedical and pharmaceutical applications.^[99] For example, Wang *et al.* showed that hyperbranched amine-terminated polyamidoamine (PAMAM) dendrimer can react with linear PEG diacrylate (PEGDA) via the aza-Michael addition reaction at -20°C, resulting in fabrication of a macroporous superelastic dendrimer cryogel.^[79] The cryogels fabricated using this technique have superelasticity, high resilience, pH-dependent swelling and degradation, and an extremely high recovery rate after storage at various temperatures, which makes them a promising new class of materials for drug delivery and tissue engineering applications.

2.3 Different types of cryogels

The simplest types of cryogels are made from only natural and/or synthetic polymers.^[100, 101] Natural polymers are those derived from plants or animals, e.g. polysaccharides, proteins, and polyesters. These polymers closely mimic the physical and chemical characteristics of the extracellular matrix (ECM).^[102] Recently, 3D structured scaffolds fabricated from naturally-derived polymers have attracted attention for both *in vivo* and *in vitro* growth and proliferation of mammalian cells.^[103] Chitosan,^[40, 104] collagen,^[65] gelatin,^[37, 38, 51, 63, 89, 105, 106] alginate,^[83, 107, 108] hyaluronic acid,^[87, 97, 109-112] silk,^[67, 113, 114, 115] and starch,^[116] as well as cellulose,^[81, 117] rubber,^[118] and their derivatives are some of the naturally occurring biomaterials that have been extensively utilized for cryogel fabrication. Although natural polymers have a long history as hydrogel and cryogel polymer precursors, synthetic polymers are relatively new, having entered into use with applications in the 1960s.^[101, 119] Several synthetic polymers have tunable physical and degradation properties that make them appealing for a variety of biomedical applications.^[103] For example, polyethylene glycol

(PEG),^[68, 70, 79, 120, 121] poly(L-lactic) (PLLA),^[122-124] and poly(vinyl alcohol) (PVA),^[121, 124-126] are some of the most common synthetic polymers that have been widely investigated for the fabrication of cryogels owing to their ability to degrade in biological environments. The rate of degradation for these polymers through hydrolytic breakdown of the ester bonds can be modified by changing the molar mass and molar ratios of the monomers. The main limitation of the synthetic polymers when used for biomedical applications is their lack of bioactivity and bio-adhesive properties, which can be compensated for through covalent linkage of synthetic peptides^[127] or bioadhesive moieties^[68, 123] during cross-linking as well as combination with natural polymers.^[120, 125, 128-130]

2.3.1. *Composite cryogels*

Composite cryogels are made of a mixture of one or several types of polymers along with other kinds of materials such as nano- or macroparticles.^[90, 106, 112, 131, 132] The final composite cryogel possesses unique characteristics which can be suitable for various biomedical applications. In a recent study, Koshy *et al.* designed an injectable nanocomposite alginate-based cryogel platform for the bioactive and sustained release of various encapsulated proteins.^[90] By incorporating and modifying charged laponite nanoparticles within the polymer walls, the researchers were able to tune the kinetics of protein release in a controlled manner. This protein release strategy could potentially simplify the design of cryogel drug delivery systems. Another interesting example of composite cryogels is given by the conductive, magnetic, highly flexible and resilient injectable hybrid cryogels result. For example, Liu *et al.* used cryogelation of methacrylated elastin peptide, methacrylate gelatin, and multiwall carbon nanotubes to create a novel nanocomposite cryogel.^[129] Their observations shows that incorporating rigid conductive polypyrrole (Ppy) or iron oxide magnetic nanoparticles (IONP) can yield multifunctional cryogels with shape memory that are highly elastic, injectable, conductive, and magnetic.

2.3.2. *Hybrid cryogels*

Hybrid cryogels contain various types of polymers (natural or synthetic) with different physical, chemical, and biological properties can result in a versatile cryogel platforms that offer unique properties.^[66, 87, 106, 111, 130, 133, 134] Such platforms can combine the advantageous properties of each polymer precursor used in the fabrication of hybrid cryogels. Neo *et al.* combined PVA and silk in order to simultaneously improve the cell-hosting capability of PVA and the physical properties of silk cryogels for applications in nucleus pulposus (NP) replacement.^[130] In another study, Han *et al.* developed, using free radical polymerization, a cryogel which was found to be capable of supporting cartilage-specific ECM production through combining ECM-based polymers with PEGDA.^[111]

2.3.3. *Stimuli responsive (Magnetic and/or conductive cryogels)*

Investigations into the impact of electricity on living subjects began in 1792, when Luigi Galvani observed contractions in muscle fibers of a frog caused by an accidental spark discharge.^[75] The role of bioelectricity in cell division, signaling, and differentiation, and in wound healing or angiogenesis, is now well understood.^[106, 135-139] These advancements have led to the invention of conductive biomaterials which can be used in regenerative medicine and tissue engineering (**Figure 4**). For example, integration of conductive elements within macroporous cryogels could be used for cell function monitoring in real-time. A 3D macroporous scaffold with such capability could lead to the design and fabrication of hybrid 3D tissue-electronic biomaterials and novel lab-on-a-chip pharmacological screening systems.^[121] However, a macroporous biomaterial is required in order to allow for the 3D interpenetration of conductive elements within the biomaterials.^[137] Zhang *et al.* have combined directional freezing with an ice-segregation-induced self-assembly (ISISA) approach to fabricate a 3D macroporous architecture of PEDOT-PSS cryogels.^[135] Their results revealed that novel conductive macroporous cryogels can play a significant role in the development of electronic components for tissue regeneration purposes. In another study, Wang *et al.* reported on their development a mussel-inspired engineered cardiac patch (ECP) built using a DOPA-derived conductive polypyrrole cryogel.^[136] Cardiomyocyte-encapsulating patches were then implanted into

infarcted myocardia of rats, which resulted in the migration of Ppy nanoparticles into the cardiomyocytes from the scaffold, leading to improved cardiac function.^[136] Tian *et al.* integrated flexible nanowires within macroporous collagen, alginate, and poly(lactic-*co*-glycolic acid) scaffolds in order to produce conductive scaffolds capable of providing nanoscale electrical sensory components in three dimensions.^[137] Deng *et al.* fabricated an electrically conductive and thermally responsive hybrid cryogel through incorporating conductive polymers such as polyaniline and polypyrrole within scaffolds made of poly(N-isopropylacrylamide) (PNIPAm).^[139] Their multifunctional cryogel could be used for numerous stimuli-responsive biomedical applications owing to both its rapid response rate to NIR light and temperature and to its shape memory behavior.^[139] In another study, Liu *et al.* investigated the conductivity and magnetic response of highly elastic, hybrid cryogels fabricated through cryogelation of a mixture of methacrylated elastin peptide, methacrylate gelatin, and multiwall carbon nanotubes.^[129] These iron oxide magnetic nanoparticles (IONP) incorporating cryogels were not only injectable with shape memory but were also conductive and magnetically responsive and hence could have potential applications as syringe-injectable biosensors.

2.3.4. Thermoresponsive cryogels

Thermoresponsive polymers undergo cross-linking as a response to temperature change. The sensitivity of this class of polymers to changes in temperature is useful, considering that temperature cross-linking does not require additional chemical treatment. These polymers have attracted a great deal of attention in biomedical research, as they can undergo gelation upon injection into the body.^[139-141] Among the different types of thermoresponsive polymers, ionic poly(N-isopropylacrylamide-*co*-sodium acrylate) P(NIPA-*co*-NaA) has drawn attention due to its unique properties: for example, P(NIPA-*co*-NaA) is more sensitive to temperature-induced conformational transition than other similar polymers.^[139, 140] Using P(NIPA-*co*-NaA) and other conductive polymers (i.e. polyaniline or polypyrrole nanoaggregates), Deng *et al.* developed a multifunctional, thermally responsive hybrid

cryogel.^[139] The final hybrid cryogels fabricated in their study exhibited good cytocompatibility, photothermal properties, and both native and pressure dependent conductivity. The combination of these properties within a single cryogel makes them desirable candidates as novel actuators, sensors, as well as electrical components and elements within biomedical devices.^[139]

2.4. Physical properties of cryogels

The physical properties of cryogels, which include mechanical properties, swelling ratio, and percentage of interconnected pores, determine the physical stability of the cryogels.^[142] For example, cryogels' mechanical properties can be determined using methods such as combination of atomic force microscopy and nanoindentation^[143] or rheological analyses.^[144] Superior mechanical strength^[145] and swelling ability^[146] are the some of the most important advantages of cryogels relative to hydrogels. Cryogels fabricated through the cryogelation (i.e. freeze-thawing) process are very elastic and have a sponge-like morphology which is the result of their highly interconnected pore structure.^[21] Due to the high pore interconnectivity and elasticity, these cryogels can adopt their initial shape after mechanical compression or collapsing; this property is called the shape memory effect.^[52]

2.4.1. Mechanical properties

As cryogels combine interconnected macropores with densely cross-linked polymer walls, investigating the mechanical properties of these systems requires specific measurements.^[21] Depending on the specific biomedical application, a number of mechanical characterizations can be performed.^[142] Determination of bulk tensile and compressive strength behavior is often required when cryogels are intended for tissue engineering applications. In addition, these measurements are essential for assessing the injectability of cryogels.^[52, 80, 90, 133] Other parameters, such as compressive modulus and dynamic shear, can be used to characterize the bulk elastic properties of cryogels. However, these measurements are not ideal, as the impact of the highly porous cryogel structure on their mechanical properties is neglected during such characterizations.^[21] Local elasticity and

toughness of the polymer wall can also play a crucial role, particularly in determining matrix-cell interactions. Furthermore, local matrix stiffness can affect cellular behavior, including proliferation and differentiation as well as adhesion and migration.^[147] However, mechanical properties often relate properties of bulk cryogels that might not fully reflect the local properties of polymer walls sensed by cells.^[21] Even though several methods exist for the local measurement of the mechanical properties of nanoporous hydrogels, these methods often cannot be used for assessing cryogels. Other characterization methods, including atomic force microscopy (AFM) and nanoindentation, are methods that can be used to assess local mechanical properties of polymer walls within cryogels. For example, AFM has been utilized to measure the local mechanical properties of PNIPAm macroporous hydrogels of with pores <10 μm .^[148] Since AFM predominately determines surface topology, it is still difficult to fully quantify the mechanical properties of the polymer walls. Another technique for the local mechanical characterization of microporous hydrogels' polymer walls is nanoindentation.^[149, 150] As these measurements are done while the macroporous hydrogels are in their fully hydrated states, technical problems such as surface tension forces and difficulties identifying the point of zero force due to presence of water are limitations on this technique.^[150] An alternative method reported by Welzel *et al.* characterized local mechanical properties of macroporous starPEG-heparin cryogels measured by an AFM-based nanoindentation methodology.^[143] This study showed that AFM-based nanoindentation can be combined with uniaxial stress-strain compression in order to provide valuable insights regarding the effect of cryogelation parameters on local scaffold mechanics.

2.4.2. *Swelling ratio*

Swelling ratio is described as the fractional increase in the weight of a cryogel upon absorption of a solvent (e.g. water). When a cryogel undergoes swelling, the pores within the cryogel network rapidly fill with the solvent used for this purpose. However, it must be considered that a fraction of the solvent diffuses through the polymer walls as well. Thus, cryogel swelling consists of two distinct

processes: (i) filling of the pores by the solvent, and (ii) swelling of the polymer walls.^[142] Cryogels possess a much higher swelling capability than nanoporous hydrogels owing to their macro-scale pore size (compared to the nano-sized pores of hydrogels) as well as a high degree of pore connectivity within the cryogels in comparison with hydrogels.^[52] The swelling ratio of the cryogels has been calculated with the following equations:

$$Q_v = \frac{D}{D_{dry}} \quad (1)$$

$$Q_w = \frac{m}{m_{dry}} \quad (2)$$

where D , D_{dry} , m , and m_{dry} are the gel diameters and weights in equilibrium swollen and dry states, respectively.

The equilibrium weight swelling ratio (Q_w) represents the quantity of solvent taken up by pores and polymer walls. However, if we assume that the pore volume within cryogels stays constant during swelling, then the cryogel volume swelling ratio (Q_v) is determined by polymer wall solvation. In this case, Q_v is the solvent quantity absorbed by the polymer walls within the cryogel. Therefore, if the difference between Q_w and Q_v is high, then the pore volume is large in the swollen cryogels.^[142] Degree of cross-linking of the cryogels has been shown to have the most effect on their swelling ratio.^[52, 80] It is hypothesized that the degree of cross-linking can affect the density of the polymer walls within the cryogel, which can in turn affect their ability to absorb a given quantity of solvent.

2.4.3. Porosity and pore interconnectivity

Interconnectivity and pore size are both important cryogel parameters which can affect cryogels' potential to recapitulate the ECM, facilitate nutrition transport, and promote blood vessel ingrowth—and therefore their likelihood to be considered as a scaffold for biomedical applications.^[20, 21, 142] The main method used for measuring the porosity of cryogels requires comparing the weight of the completely swollen cryogel to its weight in the completely dehydrated state. Dehydration for this purpose usually happens through the mechanical squeezing of the cryogel without destroying the

macrostructure of the gel. The rough estimation involved in this method is assuming that the total volume of the solvent released during mechanical squeezing accurately equals the volume of total porosity present within the cryogel. However, in the case of nanoporous hydrogels, water retention from the gel usually causes damage to the gel structure.^[142]

2.5. Parameters controlling physical properties of cryogels

The process of cryogelation includes the following steps: separation of polymer phase from the water, ice crystal formation and growth, and cross-linking followed by ice crystal thawing, which leads to the formation of an interconnected macroporous 3D network. There are a number of factors in this process that determine and influence the physical properties of cryogels, including the composition of the polymer solution, the temperature of the pre-polymer solution, the cryogelation temperature, and the freezing rate.

2.5.1. *Impact of temperature*

Temperature can have a considerable impact on the properties and ultimately the applications of cryogels. The effect of temperature on both on the cryogelation process and the physical properties of the final cryogel is detailed. Selection of an optimum cryogelation temperature as well as an optimum cooling rate are crucial, as these choices can directly influence the ice crystal formation rate and the polymerization rate, which can affect pore size and distribution as well as polymer wall thickness and distribution, which can in turn have a significant impact on the physical properties of the fabricated cryogels.^[142] The role of cryogelation temperature on pore size and distribution has been investigated for many types of polymers, as the cryogels can have different applications depending on the pore size. The size of ice crystals, which directly determines the final pore size, can be tuned by adjusting the cooling and freezing temperature. For instance, in order to produce larger pores, it is generally recommended that the highest possible freezing temperature and the lowest possible cooling rate be used. On the other hand, to produce small pores within the cryogel, freezing

needs to take place at a high cooling rate and at the lowest freezing temperature possible. When these principles are applied to the polymer solution, they reduce the ice crystal growth time.^[41, 50, 65, 83, 97, 118, 133, 151, 152] Based on classical nucleation theory, at lower cryogelation temperatures, the rate of crystallization increases, causing the nucleation of a larger number of smaller solvent crystals. Note that there is an optimum freezing temperature (i.e. cryogelation temperature) at which pore size is maximized; this optimum temperature depends on viscosity.^[96, 100] To demonstrate this effect, Yetriskin *et al.* prepared anisotropic silk fibroin cryogels through a combined directional freezing cryogelation method; these cryogels exhibited anisotropic mechanical properties and microstructure, leading to an exceptionally high Young's modulus.^[115] Since numerous tissues display anisotropic hierarchical morphologies, the high-strength anisotropic fibroin cryogels fabricated in Yetriskin *et al.* can be used for a wide variety of bioengineering applications, including bioseparation, tissue engineering, and creating organo-electronic devices. To optimize cryogel properties, Zhang *et al.* investigated the effect of different cryogelation temperature steps, starting temperature, and cryogelation period at each subzero temperature on the shape, size, and distribution of the final pores within alginate cryogels (**Figure 5**).^[83] Their team observed that the cryogelation temperature predominately affects pore shape, whereas the pre-polymer temperature and cryogelation period at each subzero temperature mostly affects pore size. Similarly, they showed that pore size and shape can be easily controlled through a stage cooling approach and that cryogels with gradient morphology could be generated.

The temperature at which cryogels will be used post-fabrication can also influence cryogel performance independent of initial fabrication conditions. Wang *et al.* reported the effect of temperature on the mechanical properties of hyperbranched amine-terminated polyamidoamine (PAMAM) dendrimer cryogels.^[79] Their results show that dendrimer-based cryogels have exceptional rebound performance and do not exhibit substantial stress relaxation during cyclic deformation under broad temperature ranges (-80 to 100 °C).

2.5.2. Impact of solute concentration

The final pore size of a cryogel can be also influenced by the type of polymer used its molecular weight and concentration during gel fabrication. With a fixed polymer concentration, a lower molecular weight of polymers will lead to the development of larger pores within the final cryogel.^[153] These observations can be explained by the Mark–Kuhn–Houwink equation, which indicates that as the molecular weight of the polymer increases, the free water content in the polymer solution decreases, which results in smaller pores and thicker polymer walls within the fabricated cryogel.^[21] In addition, an increase in the concentration of the polymer solution at constant molecular weight results in an increase in the availability of cross-linkable groups and a decrease in the availability of free water, which will lead to a decrease in the pore size of the final cryogel.^[110, 154]

2.5.3. Impact of cooling rate

To generate a highly interconnected macroporous architecture within the cryogels, it is essential that the formation of ice crystals take place before the polymerization of the highly concentrated polymer between the ice crystals starts. However, this condition can be difficult to achieve for two reasons: firstly, the presence of monomers within water in the polymer solution can lower the freezing temperature of the water (i.e. the freeze point depression effect), and secondly, phase separation within the polymer, which is essential for ice crystal formation during cryogelation, can take longer as the concentration of monomers increases. If the cross-linking happens faster than the ice crystal formation, polymerization will take place without porogens (i.e. ice crystals) and a nanoporous hydrogel will be achieved instead of a highly interconnected cryogel. On the contrary, bigger pores could be achieved by slowing the rate of cross-linking to facilitate ice crystal formation and growth. It should be noted that the temperature of the initial polymer solution determines the cooling rate to which the polymer solution is subjected, which can directly affect the pore size and distribution of the fabricated cryogels.^[41] As the temperature of the initial polymer solution increases, the temperature difference between the polymer solution and the cryogelation temperature increases;

based on thermodynamic principles,^[142] this difference can lead to more ice nucleation and more ice crystal formation, and therefore to smaller pore size and more uniform pores. In other words, the lower the cooling rate, the larger the size of the growing ice crystals, leading to cryogels with larger pore size. Serex *et al.* studied the effects of pre-polymer temperature on the local pore size changes of 3D-printed cryogels used for tissue regeneration purposes.^[41] Their experiments revealed that the pore size of the 3D printed cryogels decreases with a decreasing cryogelation temperature (from -20°C to -80°C). Moreover, they showed that the temperature of the polymer solution before starting the freezing process can exert a major effect on the final pore size within these cryogels; a higher pre-polymer solution temperature results in the development of smaller ice crystals throughout the polymer structure, which leads to smaller pores within the final cryogel. The authors' interpretation of this result was that when the temperature of the pre-polymer solution increases, the cross-linking reaction rate increases, resulting in the production of a more viscous pre-polymer. This pre-cross-linking prevents the formation of large ice crystals, as ice crystals cannot grow within the polymer solution beyond a certain viscosity threshold; therefore, the final cryogel has an overall smaller pore size.

2.5.4. Injectability (shape memory properties)

Bolus injection is the conventional method of cell transplantation for tissue repair and regeneration. However, incorrectly localized or disorganized grafting as well as poor cell survival can occur as a result of shear forces applied during the course of the injection, leading to poor cell engraftment.^[155] Therefore, minimally invasive surgical approaches for polymeric biomaterial delivery could present an effective alternative aimed at lowering the risk and complications accompanying surgical implantation and overcoming the current limitations of bolus injection (**Figure 6**).^[20, 52, 68, 80, 96, 97, 114, 155, 156] Conventional injectable hydrogels have attracted the attention of biomaterial scientists for tissue engineering applications, owing to their ability to form any desired shape to match irregular defects.^[91] However, these injectable hydrogels can cause a number of

complications, such as the requirement that proper gelation conditions be maintained and the need for mechanical strength, biocompatibility, and the ability to retain encapsulated protein, drugs, or cells in adverse environments.^[52] In order to address these concerns, hydrogels with shear-thinning behaviors have been recently developed;^[157] however, these hydrogels still lack defined macrostructures and the researchers cannot precisely control gel location.^[52] On the other hand, injectable cryogels possess several advantages over conventional injectable hydrogels. These pre-formed injectable cryogels have the ability to form well-defined macro- and micro-structures post-injection as well as maintaining a defined gel volume at the site of injection, bypassing the need for gelation following injection. Furthermore, as the injectable cryogels are cross-linked prior to injection, they can be subjected to several washing steps, a factor which makes it possible to remove any potentially toxic precursors and cross-linking materials before injection.^[80] In order for the cryogels to be injectable, they must be compressible under moderate forces, retain sufficient strength during injection, rapidly regain their initial size and shape after being collapsed during injection, and maintain encapsulated cells or biomolecules during the injection.^[52] A highly interconnected macroporous structure, a high degree of cross-linking, and an optimum pore-to-polymer wall ratio can make it possible for the cryogels to be injectable through a conventional needle-syringe system.^[142]

2.6. Characterization of cryogels

Characterization of cryogel tissue scaffolds is essential, as physical properties can affect their performance in supporting the *in vitro* or *in vivo* formation of native tissue.^[158] Furthermore, comprehensive characterization of the physical properties of cryogels is crucial in order to understand and predict cells' responses to these materials. Physical characterization includes pore size and distribution, pore connectivity, bulk and local gel mechanics, solvent absorption efficiency, etc. Here, we review the most common techniques utilized for the physical characterization of macroporous cryogels.

2.6.1. Structural characterization

Lack of standard methods for the structural characterization of soft cryogel materials makes it challenging to fully characterize the structure of these systems. Although optical microscopy, confocal laser scanning microscopy (CLSM), and environmental scanning electron microscopy (ESEM) are useful for the structural and morphological characterization of cryogels in their complete hydrated states, these methods are not powerful enough to reveal all aspects of cryogel structure and function. For the biomedical application of cryogels, it may be necessary to determine pore volume, specific surface area, pore size distribution, polymer wall thickness and distribution, pore connectivity, and tortuosity. However, quantitative characterization of the aforementioned structural details can be difficult due to the soft nature and strong hydration of the polymeric cryogels in their native state. Therefore, the structural and textural characterizations performed for cryogels in most published studies took place only at the qualitative or semi-quantitative level. The typical characterization measurements that are done in most studies are limited to microscopic images of freeze-dried cryogels without calculation of pore volume, specific surface area, or polymer wall thickness. These analyses have been performed with the assumption that freeze-drying does not result in an alteration of the pore structures, as the ice crystals required for this process only form within the pores of the cryogels and have minimum damage to the dense polymer walls of the cryogels. However, in some studies, more textural characteristics were analyzed in detail through mercury porosimetry^[30, 158, 159, 160] and image analysis software.^[35, 41, 158] In these reports, CLSM, SEM, and other microscopic techniques were performed, followed with further quantitative analysis of images.^[161] Recently, various new methods have been used for quantitative structural characterization of cryogels. For example, since a poor solvent for polymer can only be taken up by the pores and not by the polymer walls, the total volume of the pores of a cryogel system can be estimated through measuring the volume of a poor solvent such as methanol or acetone uptaken by the cryogel.^[142] V_p (the volume of pores in 1 g of dry polymer network in mL) can be calculated as:

$$V_p = \frac{m_{ns} - m_{dry}}{m_{dry} d_1} \quad (3)$$

where m_{ns} and m_{dry} represent the weight of the swollen cryogel in the poor solvent and its weight in the completely dry state, respectively, and d_1 is the solvent density. Similarly, Wang *et al.* used a hexane uptake-based method to calculate the porosity of dendrimer cryogels by the ratio of mass to volume of the cylindrical cryogels with defined dimensions.^[79]

2.6.2. Thermal characterization

Thermogravimetry (TG) methods are used to estimate the water content and the temperature profile of substrate water desorption. Thermogravimetric methods are used in thermoporometric calculations of pore size distribution of cryogels based on the fact that water desorption from smaller pores occurs at higher temperatures than that of the big pores.^[158, 162] In addition, TG results of scaffolds prepared with different fabrication methods revealed that the thermal stability of scaffolds made of one specific material changes with fabrication method.^[163] Furthermore, the TG results can be used to compare the pore size of scaffolds fabricated from a specific material through different methods.^[163] TG measurements have also been used in order to investigate the impact of organic or inorganic additives on the cross-linking of cryogels.^[106, 132, 164] One of the most common TG methods used for the characterization of polymeric cryogels is differential scanning calorimetry (DSC). DSC analyses on cryogels from their freezing state to the water desorption state are used to estimate the pore size distribution of polymeric cryogels.^[165]

2.6.3. Chemical characterization

Proton nuclear magnetic resonance (^1H NMR) spectroscopy is a method used by researchers as an analytical tool to determine the chemical structure of organic materials as well as to study and control the chemical reactions occurring during cryogel preparation.^[158] In addition, researcher use this tool to study the chemical modification of macroporous networks of cryogels to investigate the

progress of the polymerization reaction or confirm the completion of the cryogelation process.^[52, 133, 166] ¹H NMR spectroscopy has been also utilized to investigate the structural and thermodynamic properties of polymeric material systems such as hydrogels and cryogels.^[167] However, NMR spectroscopy has rarely been used as a quantitative structural characterization method for cryogels.

3. Cryogels as versatile tools for bioseparation

There is a continuous demand for effective, robust, and cost-efficient technologies for the separation of biomolecules in several fields of study, including biotechnology, medicine, molecular biology, and biochemistry. The superior mechanical strength of cryogels compared to hydrogels has also been noted in bioseparation experiments; cryogels can exhibit significantly more stability than corresponding hydrogels in response to saturation by an analyte.^[168] Due to their large, interconnected pores, cryogels have superior mass transport properties but consequently have lower binding capacities compared to conventional mediums. Several technologies and approaches including functionalization of cryogels have been developed to address this issue and improve separation outcomes. The advancements made thus far have led to the commercialization of cryogel monoliths (e.g. by Protista Biotechnology AB, Lund, Sweden). Through affinity chromatography (e.g. immobilized metal affinity chromatography (IMAC)) or molecular imprinting, cryogels can be utilized for the separation of cells (mammalian, bacterial and yeast), proteins, viruses and plasmids. Other promising applications include protein depletion for proteomics and biosensors.

3.1. Benefits of cryogels as a chromatographic medium

A prominent technique in bioseparation, chromatography, conventionally uses a stationary phase consisting of porous particles (i.e. beads) in a packed bed. Due to the mechanism by which molecules diffuse into the bead pores, this medium has significant diffusion resistance, limiting the

separation speed.^[169] Another limitation is the packed bed interparticle void volume, which lowers separation efficiency due to band broadening.^[169]

Addressing these limitations, cryogel monoliths exist as a single, large particle, achieving purely convective transport with no interparticulate voids.^[170] Monoliths are typically comprised of synthetic polymers (e.g. polyacrylamide, polymethacrylate, polystyrene), natural polymers (e.g. agarose, cellulose) or inorganic materials (e.g. silica).^[169] Cryogels represent the newest generation of monoliths, achieving 100–1000-fold larger pore sizes compared to those in other gels.^[171]

Due to pore sizes in the 10–100 μm range, cryogel monoliths are capable of processing non-clarified, viscous feedstreams, including blood, plasma, fermentation broth, and plant and animal extracts.^[172–174] Traditional chromatography mediums cannot process these feedstreams without high backpressures or clogging. Because pore size can be controlled,^[21, 175] cryogels can be tailored to separate a vast range of biomolecules, including nanoparticles (e.g. plasmids, cell organelles, viruses, protein inclusion bodies, macro-molecular assemblies) and microparticles (e.g. proteins, bacterial cells, yeast cells, mammalian cells).^[172, 174]

Another important property of cryogels relevant to chromatographic applications is their high elasticity and compressibility, which allows for lab operation at high velocities with low backpressure, decreasing processing time. Under high compression, the cryogel pores remain open, preventing backpressure formation (**Figure 7A**). Plieva *et al.* demonstrated the high compressibility of commercial polyacrylamide (pAAm) cryogel monoliths (Protista Biotechnology AB) by applying uniaxial force and measuring compression.^[175] Their cryogel monoliths showed very little deformation at up to 60% compression (**Figure 7B**). In comparison, traditional pAAm hydrogels are destroyed when deformed less than 30%.^[175] In the same study, it was demonstrated that the monoliths did not show an increase in backpressure up to 50–60% compression, a finding which was in agreement with the force-compression curve (**Figure 7C**).^[170]

Furthermore, cryogels are chemically stable due to the hydrophilic nature of their polymers, leading to minimal non-specific interactions.^[172] Additionally, cryogels have high mechanical

strength due to the high polymer concentration at the pore walls. During cryogelation, freezing of porogen displaces polymer from the pore to the pore wall, increasing concentration and thus strength.^[176] Due to these properties, cryogels can withstand numerous cleaning and regeneration cycles.^[172] Several studies have demonstrated no loss in adsorption capacity after performing 10 adsorption-desorption cycles in a series.^[177-179, 180, 181] In addition, because cryogels can be dried and re-swollen quickly without their structure being affected, they can be stored for long periods of time in their dried state.^[176]

Because cryogels are so chemically stable, the medium is chemically inert and thus must be functionalized for a specific chromatographic type.^[182] Generally, there are two approaches to functionalization: physical entrapment (embedding) or covalent coupling (immobilization) of the ligand.^[172] In physical entrapment, a functional group is copolymerized with the cryogel monomer. Covalent coupling involves chemically attaching a ligand to a pre-formed cryogel. Several limitations are associated with embedding. For instance, there are a limited number of functional monomers that are suitable for cryogelation.^[183] In addition, high concentrations of functional monomer can lead to brittle, non-elastic cryogel formation.^[176] Lastly, not all the functional groups are accessible by the mobile phase when embedded. In one study, acrylamide, N,N'-methylenebis(acrylamide) (MBAAm) and DMAEMA were copolymerized to form anion-exchange pAAm monoliths. Although a low enough concentration of DMAEMA was used to conserve cryogel elasticity, low bovine serum albumin (BSA) binding capacity was achieved (0.1–0.2 mg/mL).^[184]

3.2. Improving cryogel binding capacity

Although cryogels are a promising chromatographic medium, they can suffer from low binding capacity. For chromatographic mediums, the higher the porosity, the greater the surface area of pore walls. Because cryogels have porosities up to 0.9 (by comparison: packed bed porosity is typically 0.45), there is limited surface area for the introduction of functional ligands and consequently the absorption of target molecules.^[171, 182, 185] An example of this consideration is the

comparison of a commercial resin (SP Sepharose Big Beads) to commercial pAAm monoliths for the extraction of proteins from raw milk, a non-clarified feedstream. Although the pAAm monoliths achieved low backpressures at moderate flow velocities (300–525 cm/h) of raw milk, the protein binding capacity of pAAm monoliths compared to the commercial resin was found to be 25-fold less.^[186]

An ideal solution would increase functional surface area without changing the hydrodynamic properties of the cryogel. To this end, several approaches, including immobilization of metal affinity ions (IMAC),^[49, 177, 178, 187, 188, 189] surface grafting of ligands,^[190, 191] formation of a cryogel within a cryogel,^[192] and embedding or immobilizing functionalized particles (leading to the formation of a composite cryogel),^[177, 189, 193] are possible alternatives.

In surface grafting, an initiator forms active sites on the cryogel backbone, followed by formation of polymer chains on the monolith surface. Savina *et al.* functionalized pAAm monoliths with pDMAEMA (anion-exchanger) using 1-step (co-incubation of the initiator and monomer) and 2-step (initiator, then monomer incubation) grafting procedures.^[191] The binding capacity of a low molecular-weight target (e.g. metal ion, dye) did not impact the grafting procedure type. However, the 2-step procedure in conjunction with a high pDMAEMA density achieved the highest BSA capacity (12 mg/mL), attributed to the long, flexible pDMAEMA grafts capable of multipoint interactions with BSA.^[191]

Composite cryogels are formed by embedding or immobilizing nano- or microparticles into the monolith cryogel matrices.^[173] For example, Acet *et al.* copolymerized Ni(II)-attached O-carboxymethyl-chitosan Schiff base complexes with 2-hydroxyethyl methacrylate (HEMA) monomer.^[189] The chitosan-based particle contains several functional groups (e.g. amino, hydroxyl, Ni(II)) for protein adsorption, but has poor solubility without cryogel embedding. Lysozyme, which serves as an anti-microbial agent and therapeutic, was purified from chicken egg whites using the composite PHEMA, achieving a binding capacity of 244.6 mg/g. The resulting binding capacity was 16-fold higher compared to the binding capacity achieved by the non-composite Ni(II)-PHEMA.^[189]

To compare the properties between embedded and immobilized composite cryogels, Hajizadeh *et al.* used both methods with amino- or epoxy-activated particles to synthesize composite pAAm-AGE monoliths.^[194] The immobilized composites were synthesized by circulating particles through pre-made cryogels in a glass column to ensure uniform particle distribution. SEM images confirmed that circulation time (1 to 24 hours) impacted the amount of available immobilized particle. Compared to the immobilized monoliths, the embedded monoliths had fewer particles available for adsorption (**Figure 8A-B**), a more aligned structure (**Figure 8C-D**), and lower elasticity. Lastly, researchers demonstrated that the immobilized composite had a higher binding capacity than that of Cu(II), Orange G, and His-tagged exoglucanase. The difference in structure and function of the embedded cryogel was attributed to the particle's impact on ice crystal formation.^[194]

3.3. Protein separation applications

Several methods have been developed for protein and biomolecular separation using cryogels. Functionalization of cryogels can significantly improve separation outcome. Various approaches based on cryogel functionalization that include affinity chromatography as well as molecular imprinting can be used for efficient purification of proteins using their ligands. In this section, we describe the most commonly used approaches for the separation of various biomolecules.

3.3.1. Affinity chromatography

Affinity chromatography selectively isolates biomolecules of interest (proteins, nucleic acids, etc.) by immobilizing a ligand to an insoluble, porous support (e.g. a cryogel) which adsorbs the target molecule.^[195] Cryogels have been used as a chromatographic medium for affinity chromatography of proteins in numerous applications. Peptide ligands are commonly used for affinity chromatography, but they are complicated and costly to produce. An alternative to peptide ligands are bacteriophages, which are produced to selectively bind a target protein using a method called biopanning. However, phages cannot be immobilized to conventional mediums due to their large size (1 μm). To address

this issue, Noppe *et al.* covalently coupled phages with affinity to human lactoferrin (HuLF) and von Willebrand factor (vWF) to epoxy-activated PHEMA cryogels.^[196] These mediums successfully captured and eluted HuLF and vWF from raw milk and whole blood, respectively. Noppe *et al.* not only demonstrated the ability of PHEMA cryogels to process particulate-containing feeds: they also illustrate the potential of phage affinity chromatography as a cost-effective, straightforward approach.^[196]

Highly purified immunoglobulin (IgG) is required for applications in immunodiagnostics, therapeutics, and immunochromatography. From human plasma, IgG is commercially purified using ethanol precipitation, which has low selectivity and can cause denaturation.^[197] As an alternative method, Alkan *et al.* covalently-attached protein A to a PHEMA cryogel using cyanogen bromide activation (CNBr) and achieved an adsorption capacity of 88.1 mg/g with 85% purity from human blood (**Figure 9**).^[198] The adsorption capacity was higher than that of conventional mediums coupled to protein A and that of PHEMA cryogel coupled to other ligands.^[198]

3.3.2 Molecular imprinting

Molecular imprinting is a technique used to impart molecular recognition properties to a synthetic polymer matrix.^[199] In the pre-polymer mixture, which includes monomers and template molecule, the spatial arrangement of the molecule is determined by its interactions with the monomer. This arrangement is then fixed during polymerization of monomer and cross-linker. When the template molecule is removed, the result is a chemically and sterically complementary imprint in the polymer network, which can rebind the template with high specificity.^[200] Applications of molecularly imprinted polymers (MIPs) include chemical and biological separations, immunoassays, artificial enzymes, and biosensors.^[200] MIPs have been successfully employed for the separation of compounds of low molecular weight.^[201]

Regarding biological separations, MIPs hold several advantages over affinity chromatography methods, including longer usable life, decreased cost, greater efficiency of production, and the

absence of ligand leaching.^[202] However, molecularly imprinting biomolecules remains a challenge: biomolecules are large, complex structures with sensitivity to pH, temperature, and salt concentration. Consequently, they have a tendency to undergo denaturation and conformational changes during polymerization when exposed to organic solvents or high temperatures.^[202] Another challenge is developing optimal conditions for the removal and binding of the template molecule, because the outcome of its interaction with the polymer depends on a multitude of factors, including intermolecular interactions (e.g. electrostatic and van der Waals forces, H-bonding) and the physical and chemical nature of the molecule (e.g. flexibility, accessibility of the binding site, shape of the material).^[203]

Cryogels address some of these limitations, since they are polymerized in aqueous solutions and at low temperatures, conserving template molecules during polymerization. Cryogels and composite cryogels have been used in conjunction with MIP technology for several applications in the separation or capture of proteins. Examples will be discussed using various cryogel platforms.

Recombinant human interferon- α (hIFN- α) is used for the treatment of AIDS-related Kaposi's sarcoma and chronic hepatitis B and C. Introducing a new purification method, Ertürk *et al.* copolymerized hIFN- α with HEMA monomer to synthesize hIFN- α -MIPs.^[199] The concentration of hIFN- α introduced during copolymerization was directly proportional to the specific hIFN- α surface area (BET analysis) and consequently proportional to the amount of hIFN- α adsorbed from the aqueous solution. However, the removal of template hIFN- α was consistently 85% when a 1M sodium chloride wash was performed. After optimizing adsorption conditions (e.g. pH, ionic strength, flow rate), hIFN- α -MIPs purified hIFN- α from human gingival fibroblast culture to achieve specific activity rates of $3.45\text{--}3.75 \times 10^8$ IU/mg.^[199]

3.3.2.1 Composite molecularly imprinted polymers (MIPs)

To synthesize a composite MIP, a technique called surface imprinting is used, in which micro- or nanoparticles are molecularly imprinted and then embedded or immobilized to cryogel matrices.

This technique improves binding capacity, mass transfer, and ease of template removal.^[203] For example, Asliyuce *et al.* developed an anti-hepatitis B surface antibody (HBsAb)-imprinted PHEMA composite cryogel.^[204] HBsAbs, which are purified from human donors, animal plasma, and transgenic plants, can be used as a vaccine for hepatitis B, a global health concern causing diseases such as liver cirrhosis and hepatocellular carcinoma.^[85] Asliyuce *et al.* dried, ground and sieved HBsAb-imprinted PHEMA monolith into 20–63 μm particles. These particles were mixed with HEMA monomer and poured between two glass plates and then copolymerized to form composite cryogel membranes (CMs) (**Figure 10**). HBsAb positive plasma samples were loaded onto CMs to evaluate chromatographic performance. The theoretical plate number (N), capacity factor (CF), resolution (Rs) and separation performance (α) were 1153.9, 5.48, 1.72 and 6.02 (respectively), indicating CMs as a promising alternative for HBsAb capture.^[204]

Blood transfusions have several limitations, including lack of healthy blood donors, short shelf life, and risk of transmitting pathogens. One alternative is the use of blood substitutes, an example being hemoglobin-based oxygen carriers (HBOCs). MIPs have the potential to purify HBOCs from human and bovine feedstreams. An example of this, Hajizadeh *et al.* prepared silica particles imprinted with hemoglobin (Hb) using Pickering emulsion polymerization.^[205]

These particles were then used to prepare two types of composite cryogels: (1) pAAm with particles covalently-immobilized to a pre-formed gel, and (2) pAAm with particles embedded during cryogelation. The adsorption capacities of Hb were 5.2 mg/g and 3.6 mg/g, respectively. The lower capacity of the embedded composite was attributed to the large size and heavy weight of the silica particles.^[205]

3.4. Cell separation applications

Separation of a distinct type of cells from a heterogeneous population is applicable to biological and biomedical research, clinical therapy, and diagnostics.^[206] An optimal separation results in high purity and yield without loss of cell function. To achieve this end, an affinity-based

approach can be used, targeting cell-surface molecules. Two prominent affinity-based techniques are fluorescent-activated cell sorting (FACS) and magnetic bead separation—yet these approaches can be time-consuming and expensive.^[207] A viable alternative, affinity chromatography, represents a cost-effective, efficient, and scalable method for cell separation. There is a need for suitable affinity matrices to provide large pore sizes, high flow velocities, and low shear on cells.^[207] The inherent properties of cryogels meet these requirements, and thus their efficacy was demonstrated in several applications of cell separation.

Kumar *et al.* evaluated cell separation performance between commercial polystyrene-core beads (TentaGel), PVA cryogel beads and N, N'-dimethylacrylamide (DMAAm) monolithic cryogels, all covalently coupled to protein A (protein A binds the F_c region of IgG-coated cells).^[208] The potential for DMAAm monolithic cryogels to fractionate B and T lymphocytes had been demonstrated previously.^[209] In the first experiment of this study, all mediums were evaluated in the B and T lymphocyte fractionation from human peripheral blood; B cells express IgG on their surface and are thus captured while T lymphocytes are concentrated in the flow-through. The TentaGel beads, PVA cryogel beads and DMAAm monolithic cryogels achieved 60%, 74%, and 91% cell binding, respectively. In the second experiment of this study, cryogel beads and monoliths were tested for the capture of CD34⁺ human acute myeloid leukemia cells (incubated with anti-CD34⁺ antibodies), achieving 76% and 95% cell binding, respectively. Both experiments demonstrate the potential of cryogel beads and monoliths in multiple cell separation applications.^[208]

Building upon this research, Kumar *et al.* developed an all-encompassing approach to separate cells using a polyacrylamide-based cryogel monolith.^[210] Kumar *et al.* performed two demonstrations: hematopoietic stem cell (CD34⁺) capture and B and T lymphocyte fractionation. In CD34⁺ capture, protein A was covalently coupled to epoxy-activated monoliths using a two-step derivatization procedure. Umbilical cord blood (UCB) was sedimented and incubated with anti-CD34 antibodies to label the target cells (**Figure 11A**). Sedimented-UCB was loaded onto the monolith and a mechanical deformation was performed followed by a buffer wash to elute bound material (**Figure**

11B), which achieved a 90% yield of CD34⁺ cells. Interestingly, further cryogel compression during elution (>70%) increased yield but consequently decreased viability. Fluorescent microscopy determined that eluted cells maintained viability and retained CD34⁺ cell-surface marker expression.^[210]

3.5. Protein depletion

Protein depletion of serum, a necessary step for the field of proteomics, has employed both affinity and molecularly imprinted cryogels as efficient, cost-effective methods. Proteomics is the large-scale study of protein properties, including expression levels and post-translational modifications and interactions, in order to provide an integrated view of processes occurring at the protein level.^[211] The characterization of human serum proteins holds the potential to yield markers for several diseases and conditions (e.g. infection, inflammation, cancer, diabetes, malnutrition, cardiovascular diseases, Alzheimer's and autoimmune diseases).^[212] However, the proteins in human serum have an extraordinarily dynamic concentration range (i.e. up to 10 orders of magnitude), making detection of less abundant proteins challenging.^[213] Thus, there is a demand for cost-efficient separation techniques to remove highly abundant proteins, making the discovery of less represented proteins more possible. Due to their favorable cost and their hydrodynamic and mass transport properties, both affinity and molecularly imprinted cryogels have been employed for human serum protein depletion, including hemoglobin, albumin and IgG.^[180, 181, 214, 215]

For the depletion of human serum albumin (HSA) from human serum, Andac *et al.* developed albumin-imprinted PGMA beads and copolymerized them with HEMA monomer poly(GMA-*co*-HEMA).^[180] Using BET analysis, the PGMA-*co*-PHEMA surface area was determined to be 232.0 m²/g (on average), which was 10-fold larger than that of non-composite PHEMA. The increased surface area led to an absorption capacity of 98.2 mg/g of HSA from aqueous solution and 85% HSA depletion from human serum,^[180] which were higher than that of APBA imprinted beads (58%)^[216] but slightly lower than that of imprinted multiwalled carbon nanotubes (92–97%).^[217]

A novel approach was taken by Yang *et al.* to *per se* imprint cryogels by mixing human serum and monomer during polymerization.^[214] This approach allowed for the molecular imprinting of proteins above a threshold concentration, whereas less abundant proteins would remain unimprinted. SDS-PAGE, peptide fingerprint analysis, and MALDI-TOF revealed that several other proteins were depleted (hemopexin, clusterin, alpha-1-acid glycoprotein 1, and apolipoprotein C-I) in addition to albumin and immunoglobulins.^[214]

3.6. Biosensor

A biosensor is an analytical device that uses a biological component in combination with a physicochemical detector. Compared to other detection methods, biosensors typically have fast responses, high sensitivities, low limits of detection (LOD), low costs of construction, and small sizes.^[218] When coupled with a detector, molecularly imprinted cryogels represent cost-effective biosensors.

HSA, a protein normally found in human blood, leaks into the urine when the kidneys are damaged, indicating diseases such as chronic kidney disease^[219]. To detect HSA in urine, Fatoni *et al.* synthesized a biosensor wherein HSA binding to a molecularly imprinted pAAm cryogel oxidizes ferrocene, transmitting a signal to a gold electrode to be detected by differential pulse voltammetry (DPV).^[218] A composite MIP was formed by adding chitosan, AAm, MBAAm, graphene, ferrocene and HSA to a gold electrode and incubating at -20°C. The HSA template was removed by soaking in acetic acid, followed by SDS (**Figure 12**). The SEM images indicated MIP pore sizes of 5–20 µm and MIPs with a rough surface from the embedded molecules. To optimize biosensor performance, several composite MIPs were formed with varying graphene concentrations (graphene increased electron transfer). The composite MIP with a graphene concentration of 0.75 mg/mL had the highest sensitivity (oxidation peak per amount of analyte added).

Using the optimized biosensor, the linear range of HSA concentration and oxidation peak were between 1.0×10^{-4} mg/L and 1 mg/L, with a LOD of 5.0^{-5} mg/L. These values are wider and

lower (respectively) than conventional HSA detection methods. When the researchers were testing the selectivity of the sensor, a concentration of 10 mg/L of BSA, which is closely related to HSA, gave a signal that was below the LOD. Lastly, urine samples were diluted by a factor of 10^4 and applied to the biosensor. The biosensor was used to measure HSA concentration of six urine samples, demonstrating results comparable to the standard hospital method for HSA detection (i.e. immunoturbidometric assay).^[218]

3.7. Molecular biology and microbiology applications

In many biological systems, the interaction of biomolecules with liquid–solid interfaces, including cell adsorption to column surfaces, occurs via affinity binding that is polyvalent in nature. Such polyvalent interactions comprise concurrent binding of various receptors on the surface of biological particles such as DNA, cells, and viruses to multiple ligands on the column surface. Polyvalent interactions, when combined, can produce stronger and more specific binding as compared to monovalent interactions. Conventional separation and detachment techniques or solvent elution may cause cell damage resulting from shear forces. On the other hand, mechanically compressing a cryogel column can lead to the disruption of multiple bonds holding bound particles to the affinity cryogel surface, thus releasing detached particles in the liquid eluate, as displayed in **Figure 13**, while retaining high viability/activity.^[18]

3.8. Separation of plasmid DNA (pDNA)

Plasmid DNA is widely required for DNA vaccination, cloning, gene therapy purposes, enzymatic modification, and industrial-scale protein production.^[23, 220] The commercial manufacturing of pDNA involves fermentation, cell destruction, clarification, purification, refinement, final formulation, and filling. Liquid chromatography had been the method of choice for downstream operation, giving optimal resolution, which is essential for pDNA production for therapeutic applications.^[221] Around 1990, another class of chromatographic supports known as

monoliths were introduced for DNA purification.^[222] A plasmid generally consists of 3–20 kilobase pairs of DNA, rounding up to a relative molecular mass of 13×10^6 Da, with the hydrodynamic radius larger than 100 nm. Apart from proteins and RNA, other isoforms of pDNA—namely, open circular, linear and denatured isoform—must be eliminated for the preparation of therapeutic DNA vaccines, and only the compact supercoiled isoform must be captured.^[223] The macropores of cryogels allow for the passage of large pDNA molecules through internal spaces at a high flow rate with low pressure drops. Good accessibility to surface ligands and practically unhindered internal mass transfer are the attributes of cryogels which make them suitable for pDNA adsorption.^[224]

DNA molecules bear high negative charge, so obviously the typical choice for pDNA purification becomes anion exchange chromatography, wherein phosphates on DNA and positively charged ligands, e.g. amines, interact on the column electrostatically.^[225] Hanora *et al.* demonstrated that cation-grafted affinity cryogel columns can capture plasmid DNA from the alkaline lysate of *E. coli* cells.^[226] Also, Cimen *et al.* demonstrated high pDNA selectivity of poly (hydroxyethyl methacrylate)-Cibacron Blue F3GA cryogel discs with 90% recovery.^[224] In addition, amino acids such as arginine and histidine have shown high specificity and selectivity in recognizing the supercoiled pDNA. Arginine-based cryogel affinity chromatography was reported by Almeida *et al.*^[227] Percin *et al.* also demonstrated the use of poly(hydroxyethyl methacrylate) for pDNA purification based on histidine affinity chromatography with 90% recovery.^[228]

3.9. Virus purification

Viruses stand as attractive gene delivery vehicles for a wide range of applications. Candidates include retroviruses, herpes simplex, adenoviruses, vaccinia, and even several plant viruses, e.g. Tomato mosaic virus.^[229] Bacteriophages, i.e. viruses infecting bacteria, have the potential to be used as either an alternative or a supplement to antibiotic treatments.^[230] Large-scale production of viruses is required for viral vaccines as well as for the use of viruses as gene delivery vehicles.

Historical procedures for virus purification involved clarification with organic solvents as a first step followed by differential centrifugation, membrane filtration, and density gradient centrifugation. Unlike liquid chromatography, these methods were lengthy and unspecific, and they resulted in lower turnover time. Then, researchers switched to liquid chromatography, which ensured high purity and better productivity.^[229, 231] Several attempts were made to develop adsorbents with improved flow and less resistance to fluid movement while maintaining specificity and productivity. Most notable are adsorbents with large pores and monolithic polymeric columns derived from synthetic organic or inorganic material.^[232] There are also reports on the use of heparin-affinity chromatography for retroviruses, which are popular gene delivery vectors.^[233] The use of monolithic columns revolutionized the purification process,^[234] reducing it from 5 days to 2 hours with higher viral purity and improving the recovery percentage to 90 at the chromatographic purification step.^[229]

Moloney Murine Leukaemia Virus, a replication-incompetent retrovirus, is often preferred as gene delivery vector. Williams *et al.* employed affinity capture as a fast, single step separation/purification technique for retroviruses using macroporous monolithic support.^[235] Noppe *et al.* developed an alternative for the classical biopanning with the use of cryogel as a chromatographic column as displayed in **Figure 14**.^[236] In contrast to classical biopanning, the selection, infection, amplification steps used by Noppe's team could be combined inside the column, and the total time needed for phage selection was reduced by 4–8-fold.^[236]

3.10. Separation and capture of microbial cells

The separation of microbial cells from a mixed population can be achieved in a single step using cryogel supports. Cryogel-based cell immobilized columns exhibit extended operational stability for months, as against Ca-alginate and k-carrageenan gels, which have been used traditionally as immobilization matrices. When an aqueous solution of PVA undergoes repeated freeze–thaw cycles with suspended cells, the process results in the entrapment of the cells within the pores, which are 100–1000 µm diameter.^[237] The cells can be entrapped inside the pores of cryogel

or immobilized within pore walls. For microbial cells and other particulate biomolecules separation chromatographic fractionation based on ion-exchange, affinity, or hydrophobic interactions using macroporous gels might also be effective.^[176]

The report by Arvidsson *et al.* can be regarded as one of the early attempts toward the use of microporous cryogels for cell chromatography.^[49, 238] The research team showed that cryogel columns grafted with a proper ligand allowed for the selective adsorption of microbial cells with elution efficiency up to 80% and further projected their applicability for the fractionation of cells from a mixed population based on the ligands' surface properties.^[239] Ligands of different affinities have been reported to result in a high level of purity for the separation of microbial cells.^[17] Also reported is the efficient isolation of bacterial cells of 3 types: wild type *Escherichia coli*, His-tagged *Escherichia coli*, and *Bacillus halodurans* using Cu²⁺- IDA. Dainiak *et al.* demonstrated perfect separation of *Saccharomyces cerevisiae* and *Escherichia coli* using Concanavalin-A immobilized cryogel columns.^[240] Evtyugin *et al.* grafted aliphatic chains of varying lengths within agarose cryogels for the separation of vegetative cells from a 60 day old culture.^[241] Thus, cryogel chromatographic columns can be used for separating or sorting different cell types from a mixed population. Further, this technique can be employed as immobilized cell biocatalyst.

3.11. Use of cryogel columns as immobilized cell biocatalysts

Immobilized cell preparations for biotechnological processes have multiple advantages: higher productivity, refined product, easier recovery and conservation of immobilized biocatalysts, along with the possibility to develop a continuous process. Also, immobilization shields the cells from environmental stress such as adverse pH or the presence of toxic compounds and also lowers the contamination risk, thereby increasing cells' overall longevity.^[237]

Various microorganisms, including gram-positive and gram-negative bacteria, yeasts, and also filamentous fungi, do retain viability and high metabolic activity in immobilized form within PVA cryogels even after 18–24 months' storage at -18°C. This finding indicated the potential of

cryogels to serve as robust immobilized bioreactor systems for the production of different microbial products.^[242] Agarose or PVA cryogels are generally used during the immobilization of microbial cells. Martynenko *et al.* used cryogels of PVA with immobilized champagne yeasts for wine champagnization. The process prevented the leaching out of cells from matrix thus maintaining the transparency and chemical as well as organoleptic properties.^[243] Lusta *et al.* utilized filamentous fungi-immobilized macroporous cryogel columns for extracellular enzyme production. They reported the longest durability to be 85 days.^[30] Hristov *et al.* employed *Rhodococcus wratislawiensis*-immobilized Cryogel for simultaneous biodegradation of phenol and n-Hexadecane.^[33] Furthermore, PVA cryogels have been applied in diverse areas such as biotransformation, fermentation, degradation, amino acids, and enzymes synthesis.^[34, 244] For example, Martin *et al.* developed combined immobilized bioreactor system with entrapped *Bacillus agaradhaerens* for β -cyclodextrin production. The PVA-cryogel column separated β -cyclodextrin based on the absorption principle.^[245] All of these examples suggest that cryogel columns could yield superior products of high purity while retaining their activity, making the purification process faster and more economical.

4. Cryogels for cell culture and tissue engineering

Due to the high porosity and mechanical integrity of cryogel based scaffolds, there is a growing body of literature demonstrating their application in tissue and cell engineering fields. Previously, biological research has been hindered by the inadequacy of two-dimensional cultures grown on surface cultures in mimicking *in vivo* cell-cell and cell-extracellular matrix interactions. Differences in microenvironment chemical gradients,^[246] as well as cell adhesion and mechanotransduction^[247] between 2D and 3D scaffolds, underlie this phenomenon. Advocates of cryogels as suitable 3D tissue engineering scaffolds have emphasized their ability to mimic the ECM^[248] and their superior biophysical properties.^[152, 249] Researchers comparing cryogel and hydrogel based tissue engineered scaffolds have found that cryogels consistently exhibit superior mechanical

strength and swelling ability than their hydrogel counterparts independent of the polymers used.^[160]

Though cryogels have been prominently used as bone, cartilage, and skin engineering scaffolds (cryogel scaffolds, as discussed in a later section), cryogels have also been used in the engineering of cardiovascular, intervertebral disc, neural, and skeletal muscle tissue.^[250] The ability of cryogels to regenerate tissue is so profound that loading the scaffold with cells may not even be necessary, as success in tissue regeneration *in vivo* is possible using cryogels loaded only with growth factors.^[251] Cryogels can not only promote tissue regeneration *in vivo*; they also have a differentiating effect on progenitor cells *in vitro*, implicating the use of cryogels in stem cell therapy.^[252] Cells that infiltrate cryogels *in vivo* can also manifest differential gene expression depending on the type of cryogel, allowing for customization options in tissues cultured in cryogels.^[111] Bioreactors, i.e. devices that can produce biological molecules, have found applications not only in biochemical engineering, but in the clinic as well. Further, cryogels could also be used in the construction of bioreactors, as the relevant biomolecule-producing agents—be they microbes or animal cells—must be hosted in a conducive environment. Cryogel bioreactors can be used for delivery of biologics in detoxified plasma,^[253] and they can also be loaded with hybridomas and used for monoclonal antibody production with a greater degree of efficiency than conventional flasks.^[254] Owing to their malleable shape, their durability, and their ability to mimic tissue in the parameter of sound conduction, cryogels have also found applications *in vitro* as magnetic resonance and ultrasound imaging “phantoms” which can replace animal models when appropriate.^[255] In addition to being shown to be appropriate tissue mimics *in vitro*, cryogels can act as tissue mimetics *in vivo*; for example, cryogel tricuspid valve mimics have been synthesized.^[256]

4.1. Bone

Bone constitutes one of the most important organs of the human body. It is highly vascularized and dynamic, remodeling itself continuously during the life of each individual.^[257] Not only is it crucial to protecting internal organs or ensuring locomotion by providing mechanical support for the

body, the bone structure is also involved in several biological functions including homeostasis and hematopoiesis.^[258] Thus, bone-related diseases represent a key clinical challenge worldwide, especially because they constitute 50 per cent of all chronic conditions in people over the age of 50.^[259] Although bone has the ability to regenerate and repair itself, large bone defects caused by severe trauma, bone tumor resection, cancer, infection, or congenital diseases can only be repaired by bone grafts.^[260] However, the use of bone grafting strategies is severely hampered: autografts are limited both by the short supply and the considerable donor site morbidity,^[261] while allografts can induce disease transmission or immune rejection.^[262] To solve this human health and social challenge, the bone regenerative engineering field has developed several promising strategies to circumvent limitations associated with the conventional treatments.^[263] In particular, several studies have focused on using cryogel scaffolds, due to their unique physical properties and their ability to withstand external stimulus, as well as their macroporous structure which supports bone cells attachment and proliferation in 3D.^[250] Bolgen *et al.* first showed that HEMA-lactate-dextran cryogels injected with stem cell suspension could induce stable bone restoration of cranial bone defects in rats while promoting the formation of new blood vessels to support new bone formation.^[264] Similarly, Liao *et al.* investigated the ability of fabricated gelatin-based cryogel loaded with adipose-derived stem cells (ADSC) to regenerate bone defects (Figure 15).^[106] In addition to allowing osteogenic differentiation of ADSC and the expression of bone-specific proteins, the work of Liao *et al.* further demonstrated the ability of cryogels to support the bone regeneration of calvarial critical size defects in rabbits.

However, one of the key challenges in bone engineering involves recreating the bone ECM composed of collagen (type 1 collagen) and hydroxyapatite (HA) crystals (**Figure 15C**).^[265] Indeed, ECM plays a critical role in maintaining cell function and structure, tissue morphogenesis, cell-to-cell signaling^[266] as well as cell interaction.^[266, 267] Thus, various studies have focused on reproducing the natural bone ECM using cryogels. For instance, Hixon *et al.* developed a chitosan-gelatin cryogels containing different forms of HA crystals.^[268] These scaffolds exhibited good porosity, interconnectivity, swelling potential and other physical properties, while allowing an excellent degree

of cell attachment and increased mineralization suitable to support bone regeneration. In a related report, Salgado *et al.* evaluated the interaction of various collagen/nanohydroxyapatite cryogels (Coll/nanoHA) with human bone marrow stromal cells (HBMSC) as well as their biodegradation.^[269] Coll/nanoHA cryogels were found to allow cell survival and proliferation for 21 days *in vitro*, and *in vivo* evaluation after subcutaneous and bone implantation highlighted the biocompatibility of such scaffolds due to the absence of any adverse reactions. Additionally, their work demonstrated cryogels' potential to repair bone defects, as the coll/nanoHA of ratio 70:30 promoted tissue regeneration and induced osteoconduction. More recently, Shalumon *et al.* reported the fabrication of a gelatin/nanohydroxyapatite cryogel embedded with poly(lactic-*co*-glycolic acid)/nanohydroxyapatite microspheres with both load-bearing and bone-regenerative capabilities.^[270] This scaffold, loaded with rabbit bone marrow-derived stem cells (rBMSCs), demonstrated an increase of Young's modulus and relative mRNA expression of specified osteogenic markers/scaffold over 28 days of culture, correlated with an increase of mineral deposition and bone regeneration. Furthermore, this construct exhibited the ability to repair a mid-daphyseal tibia defect in rabbit, confirming the potential of cryogels as biomaterials suitable to repair bone defects.

The utilization of biocomposite-based scaffolds is also another alternative under investigation for bone regeneration.^[271-273] Misha *et al.* developed inorganic/organic biocomposite cryogels of polyvinyl alcohol–tetraethylorthosilicate–alginate–calcium oxide (PTAC), scaffolds with high porosity and osteoblast biocompatibility.^[271] Once implanted in Winstar rats suffering from critical-size cranial bone defects, these scaffolds showed an increased bone regeneration at the implanted site over a period of 4 weeks while also supporting osteoclastic differentiation.^[272]

4.2. Cartilage

Cartilage is very highly specialized tissue involved in many biological functions, including the appropriate functioning of joints, smooth sliding (with minimal friction), the protection of bone ends from shear forces, and the load-bearing capacity to withstand standard repetitive loads.^[274, 275]

Cartilage injuries are frequent and mainly caused by trauma, aging, congenital diseases, or cancer removal, and they represent one of the most challenging problem of modern medicine, as cartilage deteriorates in the very common type of arthritis, osteoarthritis (OA).^[276] This issue can cause tremendously disruption in the patient's livelihood and day-to-day activities, with over millions of cases reported among Americans.^[277, 278] Currently, OA is the most prevalent joint disorder in the United States^[279, 280] with estimated medical expenses totaling billions of dollars annually.^[279, 281] In the osteoarthritic subject, due to the absence of vasculature and the presence of only a sparse population of chondrocyte, cartilage possesses poor intrinsic repair capacity.^[282] Current methodology employed in repairing cartilage includes autographs^[283, 284] and microfracture,^[285] as well as autologous chondrocyte implantation.^[286] These methods have their advantages, but they also have challenges, such as donor-site morbidity, lack of integration, and unmatched properties of the repaired regions, which still limit the use of these methods.^[283, 287] Alternatives using biodegradable scaffolds containing chondrocytes are under persistent investigation, as is the utilization of cryogels in engineering cartilage due to their unique biophysical and biomechanical properties.

To develop cryogels suitable for cartilage applications, not only is the porous structure of the scaffold important to allow chondrocyte infiltration and proliferation within the construct: also, the material composition must mimic native cartilage ECM while having mechanical properties that support those of the original cartilage (i.e. the mechanical properties to withstand the loading conditions of the joints).^[277, 288] Specifically, Han *et al.* developed a highly porous ECM-based cryogel fabricated from either methacrylated chondroitin sulfate (MeCS) or methacrylated hyaluronic acid (MeHA) and cross-linked with PEGDA (**Figure 16A**).^[111] The resulting scaffolds exhibited a highly interconnected macroporous structure (**Figure 16B**) with large pore size and about 75% porosity (**Figure 16C**). Moreover, the team's work showed that the addition of MeHA and MeCS to the PEGDA significantly enhanced the mechanical properties of the acellular cryogels (**Figure 16B**), while allowing adequate chondrocyte infiltration and homogeneous distribution throughout the cryogels (**Figure 16D**). The fabricated cryogel was also found to stimulate the expression of cartilage-

related genes, followed by the accumulation of respective proteins, suggesting that ECM-based cryogels may be viable for cartilage tissue engineering by promoting specific ECM secretion. Bölgem *et al.* also demonstrated the biocompatibility of a 2-hydroxyl methacrylate-lactate-dextran (HEMA-LLA-D)-based cryogels against cartilage cells, showing that chondrocytes both attached, infiltrated, and laid down their own natural ECM, recreating a cartilage-like microenvironment within the scaffolds.^[289] Their work further showed that ~73% cells were viable after 15 days, confirming the relative biocompatibility of such scaffolds relative to previous approaches.

An alternative to increasing cartilage regeneration relies on delivering cell-derived bioactive molecules in order to stimulate chondrocyte proliferation. To this end, Gupta *et al.* fabricated chitosan-agarose-gelatin cryogel scaffolds loaded with growth factor- β 1.^[274] Although growth factor- β 1 alone led to a significant cartilage regeneration after 3 weeks in a New Zealand rabbit model of subchondral cartilage defects, their work clearly demonstrated that the combination of this factor with chondrocyte-seeded cryogels further enhanced the cartilage repair, confirming the potential of cryogels as versatile tools for cartilage tissue engineering.

4.3. Skin

The skin, one of the largest organs of the body, comprised of three distinct layers, is primarily involved as a protective barrier against the external environment with immunologic and sensorial functions; it also serves the body's thermoregulation.^[290, 291] Extensive skin loss due to burns, traumatic accidents, or chronic wounds is therefore a crucial threat to patients' health and has been an intensive area of research over the last decade.^[292] The current standard treatments employed include wound dressing, autografts, and allografts, but their efficiency is limited.^[291, 293] Lately, the development of skin substitutes has gained momentum as an approach to restoring and healing skin injuries,^[294] but many challenges still remain to be addressed, such as low adherence to wound bed, patients' morbidity, insufficient vascularization, and high manufacturing costs,^[291] limiting their clinical application for skin regeneration. Therefore, there is a need to enhance tissue-engineered

constructs to facilitate healing while avoiding infection and ensuring a long shelf life. With their macroporous structure enhancing cell migration and their sponge-like structure that could prevent liquid accumulation in the wound, cryogels appeared as a promising solution to create enhanced skin substitutes.^[295], 361, 397–398]

Wang *et al.* first developed a novel porous scaffold of hyaluronic acid, collagen, and gelatin for wound healing.^[296] They demonstrated suitable biochemical and biophysical properties for skin repair *in vitro*, with high water absorption capacity, biodegradability, and reorganization of keratinocytes, melanocytes, and fibroblasts seeded for 7 days in the scaffold mimicking native human dermis and epidermis structures. Additionally, *in vivo* implantation of the scaffolds in rats helped the wound to close faster with no further inflammation or side effects. For example, Priya *et al.* investigated the potential for bilayer cryogels to mimic the various layers of skins.^[297] They combined a layer of polyvinylpyrrolidone-iodine (PVP-1) cryogel-bearing antiseptic properties with a layer of gelatin cryogel to confer regenerative properties. The layers constituting the scaffolds possessed similar structural networks, interconnected macropores, and mechanical stability; the resulting cryogels showed antimicrobial effects against skin pathogens and an increase of keratinocyte and fibroblast attachment and proliferation. Their work also demonstrated that once implanted in rabbits, the cryogels promoted better and faster wound healing compared to untreated rabbits, and a complete skin regeneration occurred after 4 weeks with no sign of an inflammatory response.

4.4. Other models

4.4.1. *Neuronal*

Nerve injuries, both of the peripheral nervous system and the central nervous system, affect millions of people worldwide, causing permanent cognitive, motor, or psychotic repercussions and dramatically decreasing patients' quality of life.^[298] Nerve grafts have been extensively investigated for their potential to enhance patient outcomes, but autologous grafts have limitations, including morbidity, neuroma formation, scarring, and sensory loss, while allogenic grafts induce pro-

inflammatory immune response, quickly disabling the transplanted cells.^[299] To overcome these challenges, researchers are investigating tissue engineering approaches based on biomaterials that enable nerve regeneration and tissue replacement at the site of injury.^[300] In particular, cryogels have appeared as promising biomaterials to support neural tissue regeneration and transplantation to living organisms, thanks to their high porosity and physical properties that mimic native ECM and provide support and guidance for neural cells.

Jurga *et al.* first designed dextran or gelatin-based cryogels linked to laminin, the main component of brain ECM, to confer neurogenic properties to cryogels.^[301] Their study demonstrated the capability of such cryogels to promote the formation of artificial neural tissue *in vitro* by inducing human cord blood-derived stem cell differentiation. Additionally, they showed that these cryogels could be transplanted into a rat brain without inducing inflammation or glial scarring while promoting the host's neuroblasts infiltration. The implantation of large and complex solid grafts into the brain can lead to further tissue damage rather than the desired reconstruction, so Béduer *et al.* developed injectable alginate and carboxymethyl-cellulose cryogels for minimally invasive delivery *in vivo*.^[302] These cryogels possessed native laminin, allowing neural adhesion and neurite development, while having both a high local Young's modulus (protecting the neuronal architecture during injection) and a low macroscopic Young's modulus (allowing for the scaffolds' integration in soft tissues such as the brain). In another study, Newland *et al.* also addressed the delivery issues of neuronal cells, preparing microscale spherical macroporous cryogels made of starPEG and heparin.^[303] These cryogels could be injected through a 27G needle without either destruction of the scaffolds or alteration of cell viability. Their work also demonstrated the benefits of loading both glial line-derived neurotrophic factor (GDNF) and nerve growth factor (NGF) within cryogels to support bone marrow-derived stem cell (MSC) and PC12 cell differentiation, growth, and neurite production (**Figure 17**). Cryogels can also be designed to be conducive to supporting the development of such electrically excitable tissues. In a study, Humpolicek *et al.* fabricated biocompatible polyaniline cryogels with

intrinsic electrical conductivity that allowed the formation of beating foci within spontaneous differentiating embryonic stem cells, as well as the adhesion and growth of neural progenitors.^[75]

4.4.2. *Cardiovascular*

Cardiovascular disease (CVD) is the leading cause of death worldwide,^[304] characterized by injured and damaged blood vessels, valves, and cardiac tissue.^[305] Significant advances in the medical management of patients suffering from CVD and prosthetic implant development have recently been made. However, vascular or valve grafts, with heart transplants, remain the only definitive treatments for end-stage CVD, despite the dramatic lack of donors. Additionally, several complications are associated with these treatments, such as calcification, infection, poor durability, and pro-inflammatory immune response leading to graft rejection.^[306] Thus, cardiovascular tissue engineering has gained momentum to develop an unlimited source of non-immunogenic functional tissues, and researchers have keenly investigated the utilization of cryogels due to their promising physical properties.^[307]

Indeed, Vrana *et al.* designed PVA cryogels able to support abrupt and ramped disturbed shear stress conditions.^[308] They functionalized these cryogels with gelatin to promote endothelial cells' adhesion and proliferation. Their study showed that shear stress dramatically increases endothelial cell proliferation and facilitates neo-endothelialization, making cryogels particularly suitable for developing artificial arterial grafts. Similarly, Conconi *et al.* used PVA cryogels coated with lyophilized decellularized vascular matrix (DVM) to enhance the adhesion of human umbilical vein endothelial cells (HUVEC).^[309] After *in vivo* transplantation of PVA-DVM cryogels, they observed the generation of a highly thrombogenic surface, leading to the mortality of all animals after few days. However, their study showed that rats implanted with plain PVA cryogels survived for 12 months, and that these scaffolds displayed a suitable endothelial tissue formation without reduction of the inner diameter—making them promising for the fabrication of artificial vessels. In another study, Jiang *et al.* used PVA-cryogels to fabricate tri-leaflet heart valve prostheses.^[256] PVA-cryogel heart

valves were able to open and close following cyclic flow, and they were able to compress temporarily into a small ball to facilitate implantation into the chest cavity without alteration of their integrity.

4.4.3. Intervertebral disc

Degenerative disc disease (DDD) is the major cause of low back pain and develops gradually with age.^[310] DDD is caused by long-term compressive loading of intervertebral disk (IVD), inducing a decrease of vascularization and alterations of the ECM composition leading to IVD degeneration and degradation.^[311] Ultimately, DDD induces pinching of nerves and severe back pain, requiring an extremely invasive spinal fusion surgery which is costly and only a temporary solution. An alternative is whole IVD replacement, by which cryogels are engineered as entire discs substitutes that could be inserted into the joint space.

In their work, Wang *et al.* assessed the mechanical stability of PVA cryogels and determined that PVA cryogels that are freeze-dried 3 times more accurately mimic the human IVD in compression, stress relaxation and creep.^[312] Similarly, Temofeew *et al.* fabricated hybrid gelatin and poloxamer 407 (P407) cryogels to increase water retention and pore size of cryogels to facilitate cell infiltration while maintaining mechanical stability over 28 days.^[311] To improve implant integration and confer regeneration compatibilities to cryogel-based IVD, Neo *et al.* functionalized PVA cryogels with silk fibroin (SF).^[130] These cryogels possessed improved cell-hosting abilities, compressive moduli, and hoop stress values, leading to the creation of cellularized IVD cryogels suitable for IVD replacement. However, implantation of such scaffolds can remain complicated; thus, Zeng *et al.* investigated the development of injectable microcryogels to allow for the minimally invasive delivery of mesenchymal stromal cells within IVD for improving regeneration.^[313, 314] Their team encapsulated MSCs within PGEDA microcryogels reinforced with alginate and demonstrated that this system allowed a better MSC differentiation in nucleus pulposus cells, as well as an alleviation of IVD degeneration in a canine model, while preventing any cellular leakage outside of the scaffolds.

4.4.4. Skeletal muscle

Although minor skeletal muscle injuries can naturally regenerate, more severe damage occurring from trauma or myopathies will lead to the irreversible loss of muscle mass and function as well as the formation of scar tissues.^[315] Cell therapies have been extensively investigated as promising treatments for these severe injuries. However, the poor survival of delivered cells led to the development of biomaterials-based strategies to improve cells' viability by mimicking key biochemical and biophysical features of the native muscular tissue. Thus, cryogels have become a target of interest for researchers investigating various skeletal muscle regeneration applications.

Singh *et al.* first demonstrated that PHEMA-gelatin cryogels could be used to culture myoskeletal cells (C2C12), leading to their proliferation in 3D as well as the formation of tubular structure and the alignment of cells during tubule formation.^[316] To develop a strategy based only on autologous materials for medical applications, Elowsson *et al.* evaluated the utilization of blood and plasma to create macroporous cryogels to support C2C12 cultivation and transplantation *in vivo*.^[317] They demonstrated that C2C12 cells can attach to, proliferate within, and migrate through the cryogels, that they can undergo myogenic differentiation, and that they express typical markers of myoblasts. Moreover, the transplanted cell-laden scaffolds in mouse quadriceps degraded over time and were replaced with regenerated skeletal muscles. Pumberger *et al.* proposed another approach, which relied on the utilization of alginate-based cryogels seeded with MSCs to promote muscle regeneration by secreting bioactive molecules.^[318] They showed that alginate cryogels enhanced MSCs' adhesion and spreading and the secretion of IGF-1 and VEGF, and further that the transplantation of this synthetic niche *in vivo* in rats improved muscle fiber regeneration. Qazi *et al.* have further characterized this system and have demonstrated that cryogel-enhanced MSC paracrine secretion leads to a better regeneration of muscle fibers compared to conventional nanoporous hydrogels.^[319] This finding can be attributed to cryogels' unique macroporous structure, which favorizes cell-cell interaction during culture, strengthening the suitability of cryogels for such applications.

4.5. Cryogels as bioreactors

With the advances occurring within the tissue engineering field, bioreactors have gained momentum, as they can allow mammalian cells to grow within a well-defined and controlled environment while promising the possibility of scaling up to an industrial level.^[320] Providing a suitable biochemical and physical environment is crucial in order to help the *in vitro* proliferation and differentiation of cells, the neo-synthesis of ECM, or the production of signaling molecules.^[321] Recently, cryogels have played significant roles in developing new bioreactors systems, specifically for the production and isolation of various therapeutic molecules. Kumar *et al.* used the unique interconnected macroporous structure of cryogels to allow both cell growth and protein separation in order to develop an automated bioreactor with a high protein capture (yield of 80%) and high selectivity (purification factor of 27).^[188, 322] They synthesized pAAm cryogels, functionalized either with (i) covalently coupled gelatin (gelatin-pAAm) to allow human fibrosarcoma HT1080 or human colon cancer HCT116 growth and urokinase secretion, or with (ii) Cu(II)–iminodiacetic acid (Cu(II)–IDA)-ligands (Cu(II)–IDA–pAAm cryogel) for the capture of urokinase from the media (**Figure 18**). In another study, Nilsang *et al.* investigated the capability of cryogel-based bioreactors to support functionally active monoclonal antibody (mAb) production by mouse hybridoma cells (M2139).^[323] They showed that gelatin-pAAm cryogel bioreactors operating continuously for 55 days allowed mAb production, similarly to a commercially available flask-based system (CL-1000), but with a higher yield (3 times greater) while retaining their functionality *in vivo* in the context of mice arthritis induction. In further studies, Jain *et al.* investigated the capability of cryogel-based bioreactors to support monoclonal antibody (mAb) production by various hybridoma cells in static cultures.^[324, 325] They first demonstrated that polyacrylamide–chitosan (PAAC) cryogels allowed a high mAb production by hybridoma cells and promoted an enhancement of cell growth while removing animal-derived polymers (such as gelatin or collagen).^[324] Three different bioreactor formats were also designed, and the researchers' results demonstrated the crucial impact of cryogel geometry—as

monolith bioreactors performed more efficiently, allowing a four-fold higher mAb production compared to t-flask culture over a 60-day continuous run. Similarly, they also demonstrated that semi-interpenetrating PAAm-chitosan cryogels can be used for therapeutic protein production, highlighting the versatility, low cost, and high efficiency of cryogels-based bioreactors for small-scale therapeutic development and initial clinical trials.

Cryogels' ability to withstand repetitive compression via their unique physical and shape memory properties revolutionized the development of bone-related bioreactors. Bolgen *et al.* first demonstrated that 2-hydroxyethyl methacrylate (HEMA)-lactate-dextran cryogels allowed osteoblast-like cells (MG-63) to grow in dynamic conditions (perfusion), and that repetitive compression of the scaffolds had a positive effect on MG-63 proliferation and maturation, ECM synthesis, and alkaline phosphatase (ALP) activity.^[326] This finding was further confirmed by Chen *et al.*, who showed that the cyclic dynamic compression of gelatin/chondroitin-6-sulfate/hyaluronan/chitosan cryogels seeded with porcine chondrocytes and porcine adipose-derived stem cells induced neo-ECM synthesis throughout the scaffolds, chondrocyte gene expression, and a significant generation of ectopic neo-cartilage tissue following subcutaneous injection.^[327] Similarly, Xu *et al.* also demonstrated that the dynamic compression of small intestinal submucosa cryogels seeded with primary rat nucleus pulposus cells promotes matrix synthesis by maintaining N-CDH expression and PI3K/Akt pathway activity compared to static compression.^[328] Beyond tissue modeling, cryogels have also shown great potential as bioreactors for the preparation of bioartificial organs in three dimensions, in which capacity they would provide a bridge to patients waiting for organ transplant. For example, in the context of liver failure, Jain *et al.* demonstrated that interpenetrated polymer networks (IPN) of chitosan and PNIPAm (PNIPAm)-chitosan) were able to promote the growth and function of fibroblasts (COS-7) and human liver cells (HepG2) *in vitro*.^[329] Additionally, poly(NiPAAm)-chitosan cryogels demonstrated a high bio- and hemocompatibility while preserving the ability of cells seeded within cryogels to purify plasma, making cryogel-based bioreactors suitable as bioartificial livers (BALs) by supporting liver functions such as detoxification

and synthesis of crucial metabolites. In other studies, Damania *et al.* optimized a poly(NiPAAm)-chitosan cryogel-based BAL system by designing a hybrid bioreactor that integrates hepatic cell-loaded cryogels and activated carbon cloth to overcome the plasma's toxicity effect on cells.^[330, 331] They first demonstrated *in vitro* that this bioreactor can maintain its functionality regarding albumin and urea synthesis after intermittent exposure to a patient's plasma, suggesting the possibility that this system could be put to use as a reusable BAL.^[331] This cryogel-based bioreactor was also connected extracorporeally to rats suffering from acute liver failure for 3 hours, and it demonstrated a high efficiency by decreasing bilirubin and aspartate transaminase by 20–60%, and also by allowing an increase of urea by 40% and a decrease in ammonia by 18%.^[330] Damania *et al.* also demonstrated that decellularized liver matrices can be used to coat poly(NiPAAm)-chitosan, not only improving the viability and functionality of hepatocytes *in vitro*, but also extending cellular functionality *in vivo*.^[331]

5. Other applications of cryogels

The macroporous, interconnected architecture of cryogels makes them highly suitable to be used as scaffolds in a wide range of biomedical applications. As described above, their similarity to the structure of the ECM has led to the utilization of cryogels in tissue engineering and more recently as microenvironmental mimics of disease states. Furthermore, combining the idea that cryogels are suitable as both cell immobilizers and drug delivery vehicles has resulted in the fabrication of antibody-producing stem cell-loaded cryogels^[332] and immunostimulatory protein-loaded cryogels^[89] as cancer immunotherapy agents. Additionally, the intricate and three-dimensional nature of cryogels can allow for controlled drug release. Higher sustained delivery by cryogels relative to corresponding hydrogels can occur and is related to the superior mechanical strength^[333] and swelling ability^[334] of the former.

5.1. Cryogels as tumor microenvironment mimics

Besides (re)generation of healthy tissues, there is a need for suitable 3D cell culture systems to better mimic natural tumor formation. For several decades, anti-cancer drugs have been tested on monolayer cultures of cancer cell lines. Although these 2D approaches have been essential for our current understanding of cancer biology, it is becoming increasingly clear that 2D *in vitro* assays poorly predict the clinical benefit of novel drugs.^[335] Instead, both scaffold-free and scaffold-based 3D cell culture methods are increasingly being used.^[336] Scaffold-free 3D culture systems, such as hanging drop cultures, allow for the *in vitro* formation of multicellular aggregates, or spheroids, that better reflect drug responses found *in vivo*.^[337] However, scaffold-free approaches are difficult to standardize for high throughput cancer drug screening, and they are not applicable for all cell types.^[338, 339] Instead, scaffold-based 3D culture methods allow for more control over the cellular environment. Since the tumor microenvironment and ECM provide important signals that greatly affect cancer cells, scaffolds should mimic natural 3D tumor micro-architecture as closely as possible to accurately study proliferation and drug responses of tumors *in vitro*.^[340, 341] Scaffolds derived from biological tissues, such as Matrigel, have been used extensively for tumor cell culture. However, their composition and properties are difficult to adjust and standardize. Due to their interconnected macroporous structure and tunable tissue-resembling elasticity, cryogels are particularly well-suited for this purpose.^[120] Because of this suitability, cryogels made from different materials have been applied in various studies to form tumor spheroids that bridge the gap between *in vitro* and *in vivo* cancer cell behavior (**Figure 19**).

Cryogels can be further optimized as *in vitro* tumor models by tuning scaffold elasticity, porosity, and presentation of chemical cues to better mimic the tumor microenvironment ECM. Studies with different formulations of cryogels composed of alginate, gelatin, and PEGDA have demonstrated the influence of these scaffold characteristics on prostate cancer cell growth. High elasticity and porosity were found to result in strong proliferation of different prostate cancer cell lines, while the presence of chemical ligands, such as cell-adhesive RGD peptides, was not essential

for optimal cell growth.^[120, 342] In addition, prostate cancer cells only responded to androgens when cultured on cryogels with high porosity and high elasticity that contained RGD.^[120] The elasticity of PEGDA cryogels can also be optimized by varying PEGDA molecular weight. Prostate cancer cells cultured on these elasticity-optimized PEGDA cryogels also showed increased proliferation and high expression of androgen response genes compared to 2D and scaffold-free 3D culture methods.^[343] Similarly, prostate cancer spheroids have been grown on cryogels consisting of silk fibroin blended with gelatin, collagen, chitosan, and the spider silk protein spidroin.^[344] In particular, high levels of proliferation and spheroid formation were observed when cells were cultured on the remarkably porous silk fibroin-chitosan gels.^[344] For breast cancer cells, the effect of different functional ligands on spheroid formation has also been determined, which was done in transparent hyaluronic acid cryogels. When RGD-functionalized cryogels were used, breast cancer cells showed a similar morphology to cells cultured in 2D. Alternatively, spheroid formation could be induced by replacing RGD peptides with a laminin 1-mimetic IKVAV peptide.^[345] In polyacrylamide-based cryogels, spheroid formation was demonstrated to be RGD-dependent for both colon cancer and leukemia cells.^[346] This finding further highlights that for each 3D cryogel culture system, the material characteristics need to be tailored to the specific cell types intended.

In particular, spheroid formation in chitosan-alginate complex cryogel (CA) scaffolds was demonstrated for several cancer cell types.^[280, 347, 348] CA scaffolds are biodegradable, non-immunogenic, and can be degraded using mild conditions, which allows for straightforward retrieval of cultured cells. The behavior of human glioma cells seeded into these CA scaffolds more closely resembled the behavior and morphology of tumors *in vivo* compared to cells cultured in 2D or Matrigel. In addition, glioma cells cultured on CA scaffolds showed a more malignant phenotype *in vivo* due to an increased expression of (angiogenic) growth factors.^[280] Similarly, hepatocellular carcinoma (HCC) cells grown on CA scaffolds formed multicellular spheroids and showed an increased expression of malignancy markers. HCC cells cultured in the cryostructured CA scaffolds were markedly more resistant to doxorubicin treatment compared to 2D or Matrigel-cultured cells.^[347]

Nanoparticle-mediated prostate cancer gene therapy applied in these cryogels could also better predict *in vivo* responses than other *in vitro* culture systems.^[348] Furthermore, CA scaffolds have been applied as *in vitro* ECM mimics to study interactions of tumors with other cells, such as immune cells, which showed that CA-based prostate and breast tumor models can support interactions between 3D tumor spheroids, T cells, and fibroblasts.^[349, 350] This way, a more clinically relevant platform was provided for *in vitro* validation of cancer immunotherapies.^[350, 351] Interactions of breast cancer cells with carcinoma-associated fibroblasts have also been investigated using gelatin cryogels; these investigations demonstrated that fibroblasts promote metastasis of breast cancer cells.^[352] Significantly, CA-based cryogels also promote the proliferation and enrichment of glioblastoma, breast, prostate and liver cancer stem cells. As these cells are notoriously difficult to propagate under 2D conditions, 3D cancer stem cell culture could allow for a better understanding of their biology and could be a valuable tool for developing therapies that target cancer stem cells.^[353] Similarly, cryostructured macroporous gels composed of a mixture of chitosan and hyaluronic acid have also been used to mimic the microenvironment of glioblastomas, because hyaluronic acid is an important component of brain ECM. These scaffolds can also support the growth of cancer stem cells harvested from glioblastoma tumors. Cells cultured in these scaffolds also show more resistance to a variety of anti-cancer drugs.^[340]

Because cryogel-based *in vitro* tumor models better reflect *in vivo* behavior of cancer cells, these models can be used to predict *in vivo* cancer drug responses in high throughput systems. For this purpose, cancer drugs have been screened on colon cancer and leukemia cells grown in RGD- or collagen-functionalized polyacrylamide cryogels in a 96-wells format. In these gels, cancer cells showed lower sensitivity to both cisplatin and cytosine 1-β-D-arabinofuranoside.^[346] When cultured in gelatin cryogels in a similar 96-well-based system, breast and lung cancer cells showed increased resistance to tamoxifen and paclitaxel compared to cells cultured in 2D. Drug resistance was increased even more in the presence of poly *N*-isopropylacrylamide, a thermoresponsive polymer that aids spheroid formation.^[354] To further advance translation of spheroid cultures for high throughput tests,

generating gelatin cryogels in off-the-shelf microarray chips that can be used in benchtop equipment in 96-well and 384-well format can be advantageous.^[338, 355] Similarly to other 3D culture methods, these micro-3D-tumor arrays predicted *in vivo* drug responses to doxorubicin, gemcitabine, and vinorelbine more accurately than 2D cancer cell cultures. Using this platform, cell lines, patient-derived xenografts, and patient biopsies have been tested for their sensitivity to a wide variety of anti-cancer drugs.^[355] Taken together, ECM-mimicking cryogels have great potential for 3D tumor culture that is more reflective of *in vivo* tumor behavior than other approaches. Application of cryogels in high throughput equipment may greatly benefit the translation of novel anti-cancer drugs to clinical practice.

5.2. Cryogels in anti-cancer vaccination strategies

In addition to providing an *in vitro* 3D environment for cell culture, cryogels can be used to deliver cells and/or therapeutics for cancer immunotherapy. Over the past decades, immunotherapy, by which the patient's immune system is directed to attack cancer cells, has emerged as a promising approach for the treatment of advanced cancers. These therapies generally rely on the activation of specific T cells by tumor antigen-presenting dendritic cells. Strategies that use *ex vivo* activated T cells or *ex vivo* antigen-loaded dendritic cells have shown some success.^[356] Clinical effectiveness is often limited due to insufficient survival and localization of transferred cells, which can be improved by the transplantation of immune cells within macroporous hydrogels.^[357, 358] Nonetheless, the application of cell-based therapies remains challenging due to the need for cumbersome and expensive personalized cell culture. Therefore, different platforms have been engineered to efficiently attract, activate, and load dendritic cells with antigen *in vivo* in an off-the-shelf approach. An implantable PLGA scaffold vaccine has shown promising results in pre-clinical tumor models for melanoma and glioma^[359] and is currently undergoing phase I clinical trials for application in metastatic melanoma. Similar vaccines have also been developed using cryogels as an injectable alternative to the implantable PLGA scaffold.

As a first step, researchers encapsulated GM-CSF into cryogels to attract immune cells.^[52] *In vivo* injection of GM-CSF-containing gelatin cryogels resulted in infiltration of large amounts of cells into these gels.^[360] To develop immune cell-attracting gels into cancer vaccines, alginate cryogels were generated, containing GM-CSF and TLR agonist (CpG ODN) to attract and activate dendritic cells. Transplantation of irradiated tumor cells within injectable GM-CSF- and CpG ODN-loaded alginate cryogels into tumor-bearing mice generated potent and durable anti-tumor immune responses. These immune responses were induced by attracting large numbers of dendritic cells, which were activated by CpG ODN while being in close contact with tumor antigens within the alginate cryogels.^[108] Furthermore, transplanting breast cancer cells into mice using tough, better-injectable cryogels loaded with GM-CSF and CpG led to the production of high levels of protective antitumor antibodies. Instead of whole tumor cells, these cryogels were also loaded with model tumor antigens to provoke potent anti-tumor immune responses (**Figure 20**).^[361]

Sustained *in vivo* production of anti-tumor antibodies has also been achieved through the transplantation of gene-modified stromal cells. Cryogels formed from star-shaped PEG and heparin were used to transplant immunotherapeutic organoids containing mesenchymal stromal cells capable of producing anti-CD33/CD3-bispecific antibodies into tumor-bearing mice. The generated antibodies were able to direct T cells toward CD33⁺ acute myeloid leukemia cells, which resulted in effective anti-tumor responses.^[362] In a similar approach, these organoids were used to produce target modules *in vivo* that could link tumor cells to an engineered chimeric antigen receptor (CAR) on T cells. This approach resulted in specific killing of CD19⁺ tumor cells by retargeted CAR T cells.^[363] Thus, cryogels provide a promising platform for minimally invasive (and possibly off-the-shelf) anti-cancer vaccines.

5.3. Cryogels for sustained delivery of cells and drugs

In addition to their applications in cancer immunotherapies, cell-based therapies hold great promise for the regeneration of damaged or diseased tissues. However, because cells are often

damaged during injection and do not stay localized to the diseased tissue, cell-based therapies often do not reach their full therapeutic potential.^[364, 365] Scaffolds can be used to overcome these problems by ensuring local delivery while protecting cells from injection damage and harmful microenvironments *in vivo*.^[366] In tissue engineering, efficient cell delivery has been achieved using a variety of implantable materials, including cryogels. For example, implanting gelatin-dextran cryogels containing genetically modified chondrocytes, researchers were able to heal cartilage defects in rabbits,^[367] and also used gelatin-hyaluronic acid cryogels to transplant adipose-derived stem cells for soft tissue engineering.^[368] Furthermore, Borg *et al.* implanted starPEG-heparin cryogels loaded with both mesenchymal stromal cells and pancreatic islets into mice to improve islet survival.^[369] In these approaches, cryogel scaffolds are mainly used as mechanical supports for transplanted cells. However, scaffold implantation requires invasive surgical procedures and can be challenging for some applications, such as neuronal cell therapy.^[303]

5.3.1. Therapeutic cell delivery with injectable scaffolds

To avoid surgery-induced tissue damage during implantation, several novel strategies focus on minimally invasive scaffold introduction *in vivo* through injection. For this reason, several scaffolds that spontaneously assemble after injection are currently under development for transplantation of cells and as therapeutics. For example, researchers have used polymers that are able to both spontaneously self-assemble into porous scaffolds upon injection and induce anti-tumor immune responses in mouse models.^[357, 370] However, these hydrogels are highly dependent on *in situ* gelling conditions that are difficult to control, such as gelation time and polymer concentrations after injection. Furthermore, cargo and liquid precursors that should be incorporated into the injected scaffolds might leak from the injection site, which may lead to toxicity and limited control over the scaffold macrostructure.^[52, 371] Self-healing shear-thinning injectable hydrogels have been used to avoid these issues, but application of these scaffolds is limited by their weak cross-linking interactions.^[372] Instead, cryogels have a more defined, interconnected, and macroporous architecture

with shape memory properties and can withstand large amounts of stress, allowing them to be injected. To investigate their value for cell-based therapies, researchers demonstrated that cryogels promote localization and retention of bioluminescent reporter cells after subcutaneous injection into mice.^[52]

In addition to the immunotherapeutic strategies described above, injectable cryogels can be used for a variety of cell therapies. As such, alginate and carboxymethyl-cellulose cryogels have been used as injectable neural engineering scaffolds that protect cells during injection. Due to their compressibility, these scaffolds were used in tests for injection of large neural networks, which may allow for a minimally invasive repair of brain tissue damage.^[302] Furthermore, heparin-functionalized gelatin cryogels have been used as a fibroblast carrier to induce neovascularization in an ischemic hindlimb ischemia model. After excision of femoral arteries, cryogel-based fibroblast injection in the damaged area resulted in significantly increased recovery of blood flow and reduced necrosis. Injectability of these gelatin/heparin cryogels was better for gels with a lower gelatin content.^[373] Cryogel mechanical properties can be further optimized by incorporating ionic cross-links into methacrylate-alginate cryogels. These ionic cross-links are dynamic and can reversibly break during injection, which enhances the toughness of the gel and allows for injection through smaller needles. As discussed above, these tough cryogels were applied as anti-cancer vaccines.^[361]

Intact cryogel injection through thinner needles can also be achieved by using formulations of multiple microcryogels. Macroporous, micro-sized cryogels have been generated both by micromolding on chips and by using water-in-oil emulsion methods.^[303, 374] In contrast to bulk cryogels, microgels do not have a large pre-formed macrostructure that is necessary for some tissue engineering applications. Nonetheless, the smaller gels are injectable through fine-size needles while maintaining survival of transferred cells.^[374] Hence, microcryogels have been studied for applications in a variety of cell therapies. On-chip-fabricated alginate-loaded PEG-based cryogels were used to efficiently inject fibroblasts to increase site-directed angiogenesis.^[374] Microchip-generated gelatin microgels have also been used to improve survival and retention of mesenchymal stem cells after *in*

vivo injection. These cryogel-based cell injections improved angiogenesis, enhanced blood perfusion, and reduced muscle degeneration in ischemic hindlimbs.^[365] Furthermore, researchers developed alginate/PEG based microcryogels for treatment of intervertebral disc degeneration, a cause of lower back and neck pain. Since cryogels can bear large mechanical loads, they are particularly suited for intervertebral discs, as discussed earlier. For this application, the gels were loaded with mesenchymal stromal cells that could be preconditioned inside these gels.^[314] Injection of pre-conditioned stromal cells within cryogels prevented cell leakage, and cryogel delivery of these cells into canine intervertebral discs alleviated degeneration better than scaffold-free application.^[313] Gelatin microcryogels, generated on microchips using a similar method, were also successfully used for the delivery of human adipose-derived stem cells to enhance wound healing in mice.^[375] Microcryogels fabricated via an oil-in-water emulsion method have also been applied for the delivery of human adipose-derived stem cells *in vivo*. Inside the porous gels, stem cells were highly viable, showed potent adipogenic differentiation, and formed extensive cell-cell contacts, which resulted in effective adipose tissue formation.^[376] Injectable microgels, fabricated via a similar emulsion method, have also been developed for the injection of neuronal cells. Using these gels, neurons and stem cells were injected through small needles without a loss of viability.^[303] Taken together, cryogels can be used to improve injectable cell-based therapies by protecting cells during injection, localizing cells at the injected site, preventing cell death due to lack of attachment after injection, and allowing tissue regeneration due to their elastic macroporous structure.

5.3.2. Cryogels for controlled drug release

The interconnected, porous structure of cryogels is essential for efficient infiltration or delivery of cells. However, this architecture can be problematic for controlled drug delivery, as the porous structure may result in too-rapid release and limited loading capacity for some molecules. Several approaches exist for the controlled release of drugs and proteins (**Figure 21**). Proteins and drugs encapsulated in cryogels generally show an initial rapid burst release.^[90, 377] Alternatively,

proteins entrapped in densely packed cryogel walls may only be released upon degradation of the scaffold, as appears to occur for injectable biodegradable alginate cryogels.^[52] This process can be aided by incorporation of protease-cleavable cross-links in cryogels, which leads to increased scaffold degradation after cell infiltration.^[360] For small molecules, control over release properties has been achieved through optimization of cryogel formulations. In these cases, drug release is generally controlled by the swelling behavior of the polymers.^[81] Several studies have demonstrated control over this swelling behavior and drug release by adding polymers, such as cellulose or PNIPAm, that reduce the pore size or provide charged surfaces.^[81, 378] Additional control over release profiles can be gained by making use of responsive materials. For example, cryogels that are responsive to temperature, pH, and local salt concentrations have been developed to controllably release diclofenac sodium.^[379]

Gelatin is a popular scaffold material for cryogels, because processing and modification of gelatin alters its electrostatic properties. Because of this property, differently-charged molecules may be released depending on gelatin modification. Extensive cross-linking of gelatin cryogels has also been used to control sustained drug delivery.^[380] Drug release has been controlled more specifically by incorporating polymers with specific drug binding sites into cryogels using molecular imprinting technology. Using this method, cryogels have been developed that bind drugs via metal chelators, ionic interactions, and specific protein interactions.^[381] For example, controlled release of the cationic chemotherapeutic agent doxorubicin was achieved using PEG-based cryogels that were cross-linked together with glutamic acid-containing polymers, which also allowed for pH-responsive drug delivery.^[382]

Similarly, controlled delivery of specific growth factors and chemokines is possible by incorporating heparin into cryogels. For example, injecting vascular endothelial growth factor (VEGF)-loaded heparin-functionalized gelatin cryogels into ischemic hindlimbs of mice, which induced angiogenesis through controlled release of VEGF.^[373] However, *in vivo* controlled release of VEGF has also been achieved using gelatin-based cryogels without heparin functionalization to treat

bone defects in rabbits.^[251] Similarly, neuronal growth factors have been loaded in heparin-containing starPEG microcryogels to promote neuron survival.^[303]

Delivery of drugs from cryogels may also be further controlled by creating composites with particles. For example, pre-adsorbing proteins to negatively charged Laponite nanoplatelets has been used to prevent burst release and provide sustained protein release from alginate cryogels, which could be tuned by altering the Laponite content within the gels.^[90] Similarly, the release of the broad-range antibiotic ciprofloxacin from gelatin cryogels could be tuned by incorporating the drug in calcium carbonate microspheres.^[377] Particles have also been generated from materials approved for clinical use, such as PLGA, to modify protein release. For example, Chang *et al.* developed cryogels containing PLGA microspheres and loaded with bone morphogenetic protein-2 for bone integration of implants.^[383] When applied in a rat model for dental implants, these composites were able to effectively induce osteogenesis *in vivo*. Thus, in addition to their application as cell delivery vehicles, cryogels have been developed into injectable depots for local drug delivery. Release kinetics may be controlled by modifying the cryogel structure or incorporating other drug delivery modalities into the scaffold.

6. Conclusion

Cryogels clearly have great potential for many emerging biomedical applications, as detailed in this review. However, despite many technological advances, much work remains for their broader translation to the market. One of the major advantages cryogel-based materials offer is their unique properties, which attract researchers from various fields. Simply by controlling fabrication parameters (e.g. polymer choice, temperature, solute concentration and cooling rate), scientists are able to generate cryogels with highly tunable physico-chemical properties and large interconnected pores. Given these properties, cryogels were commercially developed as monoliths in bioseparation processes including fractionation of molecules (e.g., proteins, nucleic acids) and/or microorganisms

(cells, viruses, bacteria). The macroporous network of cryogels supported superior mass flow rates at the cost of lowered binding capacity that researchers addressed with molecular imprinting and affinity chromatography strategies. More recently, this class of macroporous hydrogels has drawn great interest in the biomaterial community for tissue engineering and bioreactor applications. Their unique macroporous architecture, physical properties recapitulative of native tissues, and shape memory properties make cryogels exemplary substitutes for 3D tissue constructs. An additional advantage is that cryogels are readily amenable to various functionalization chemistries that could confer novel biological functions. Furthermore, some cryogels can be formulated to be injectable, making them great candidates for minimally invasive delivery for both tissue engineering and spatiotemporal controlled delivery of therapeutics and cells. Most recently, cryogels have been developed as advanced cancer immunotherapy vehicles.

However, to further advance cryogel technologies in the clinic, key questions need to be addressed, including the impact of how cryogels' physical properties affect cell behavior. Detailed examinations focusing on how pore size, volume and interconnectivity, as well as cryogel bulk and local mechanical properties, influence cell physiology and differentiation need to be carried out. Similarly, how cryogels' properties affect molecular diffusions (e.g. diffusion of nutrients, oxygen, waste removal or drugs released) require further investigation. Once these and similar studies are complete, challenges in the scale-up potential of cryogels must be addressed, especially in cases when extremely well-controlled and reproducible freezing conditions are required to obtain functional cryogels. For example, comparative scrutiny of cryogels might be necessary to determine key parameters crucial for the design of cryogel-based biomaterials specific for each application. In conclusion, cryogels are extremely versatile biomaterials that can be utilized in a wide range of biomedical applications, spanning from bioseparation to immunoengineering, that require further consideration to reach their full commercial potential.

Acknowledgements

This work was supported by Northeastern University (Boston, MA, USA) Seed Grant/Proof of Concept Tier 1 Research Grant and startup funds provided by the Department of Chemical Engineering. Burroughs Wellcome Fund (BWF) and Thomas Jefferson/Face foundations awards, Deanship of Scientific Research, and Center of Nanotechnology at King Abdulaziz University, are also acknowledged.

Received: ((will be filled in by the editorial staff))

Revised: ((will be filled in by the editorial staff))

Published online: ((will be filled in by the editorial staff))

References

[1] R. G. Jones, *Compendium of Polymer Terminology and Nomenclature: IUPAC Recommendations*, 2008, Royal Society of Chemistry Cambridge, 2009.

[2] E. M. Ahmed, Journal of advanced research 2015, 6, 105.

[3] A. D. McNaught, A. D. McNaught, *Compendium of chemical terminology*, Vol. 1669, Blackwell Science Oxford, 1997.

[4] Z. Gu, L. Chen, Y. Xu, Y. Liu, Z. Zhao, C. Zhao, W. Lei, Q. Rong, R. Fang, T. Zhao, ACS applied materials & interfaces 2018, 10, 4161; A. K. Gaharwar, N. A. Peppas, A. Khademhosseini, Biotechnology and bioengineering 2014, 111, 441; A. Memic, H. A. Alhadrami, M. A. Hussain, M. Aldhahri, F. Al Nowaiser, F. Al-Hazmi, R. Oklu, A. Khademhosseini, Biomedical materials 2015, 11, 014104.

[5] R. Pathak, S. Lochab, N. Raghuram, M. Moo-Young, *Comprehensive biotechnology*, Elsevier, Oxford, 2011.

[6] S. B. Lee, Y. H. Kim, M. S. Chong, S. H. Hong, Y. M. Lee, Biomaterials 2005, 26, 1961.

[7] H. Tokuyama, A. Kanehara, Langmuir 2007, 23, 11246.

[8] P. Liu, W. Chen, S. Bai, Q. Wang, W. Duan, Composites Part A: Applied Science and Manufacturing 2018, 107, 675.

[9] S. J. Bryant, J. L. Cuy, K. D. Hauch, B. D. Ratner, Biomaterials 2007, 28, 2978.

[10] T. M. Henderson, K. Ladewig, D. N. Haylock, K. M. McLean, A. J. O'Connor, Journal of Materials Chemistry B 2013, 1, 2682.

[11] R. G. Jones, E. S. Wilks, W. V. Metanomski, J. Kahovec, M. Hess, R. Stepto, T. Kitayama, *Compendium of Polymer Terminology and Nomenclature*, Royal Society of Chemistry, London 2009.

[12] V. I. Lozinsky, Russian Chemical Reviews 1998, 67, 573.

[13] V. I. Lozinsky, in *Polymeric Cryogels: Macroporous Gels with Remarkable Properties*, (Ed: O. Okay), Springer, Berlin/Heidelberg 2014, 1.

[14] F. Plieva, X. Huiting, I. Galaev, B. Bergenstähl, B. Mattiasson, J. Mater. Chem. 2006, 16, 4065.

[15] V. I. Lozinsky, I. Galaev, F. M. Plieva, I. N. Savina, H. Jungvid, B. Mattiasson, Trends in Biotechnology 2003, 21, 445.

[16] A. Kumar, D. B. Raina, in *Supermacroporous Cryogels: Biomedical and Biotechnological applications*, (Ed: A. Kumar), C.R.C., Boca Raton 2016, 3.

[17] A. Kumar, *Supermacroporous Cryogels: Biomedical and Biotechnological Applications*, CRC Press, 2016.

[18] E. Caló, V. V. Khutoryanskiy, European Polymer Journal 2015, 65, 252.

[19] N. Y. Chirani, L.; Gritsch, L.; Motta, F.L.; Chirani, S.; Fare, S., J Biomedical Sci 2015, 4, 2.

[20] S. A. Bencherif, T. M. Braschler, P. Renaud, Journal of Periodontal & Implant Science 2013, 43, 251.

[21] T. M. A. Henderson, K. Ladewig, D. N. Haylock, K. M. McLean, A. J. O'Connor, Journal of Materials Chemistry B 2013, 1, 2682.

[22] F. M. Plieva, H. Kirsebom, B. Mattiasson, Journal of Separation Science 2011, 34, 2164.

[23] R. Üzek, L. Uzun, S. Şenel, A. Denizli, Colloids Surf B Biointerfaces 2013, 102, 243.

[24] B. Nasri-Nasrabadi, A. Kaynak, Z. K. Nia, A. Kouzani, Cellulose 2018, 25, 549.

[25] B. Yetiskin, C. Akinci, O. Okay, Polymer 2017, 128, 47.

[26] J. Van Rie, H. Declercq, J. Van Hoorick, M. Dierick, L. Van Hoorebeke, R. Cornelissen, H. Thienpont, P. Dubrule, S. Van Vlierberghe, Journal of Materials Science: Materials in Medicine 2015, 26, 123.

[27] H. R. Oxley, P. H. Corkhill, J. H. Fitton, B. J. Tighe, Biomaterials 1993, 14, 1064; N. Sultana, M. Hassan, M. Lim, N. Sultana, M. Hassan, M. Lim, *Composite Synthetic Scaffolds for Tissue Engineering and Regenerative Medicine*, 2015.

[28] K. J. De France, F. Xu, T. Hoare, *Adv Healthc Mater* 2018, 7.

[29] Y. Nam, T. Park, *Journal of Biomedical Materials Research* 1999, 47, 8; A. N. Stachowiak, A. Bershteyn, E. Tzatzalos, D. J. Irvine, *Advanced Materials* 2005, 17, 399; M. C. Ford, J. P. Bertram, S. Hynes, M. Michaud, Q. Li, M. Young, S. S. Segal, J. A. Madri, E. B. Lavik, *Proceedings of the National Academy of Sciences of the United States of America* 2006, 103, 2512; Y. Gong, Z. Ma, C. Gao, W. Wang, J. Shen, *Journal of Applied Polymer Science* 2006, 101, 3336.

[30] Q. Liu, E. L. Hedberg, Z. Liu, R. Bahulekar, R. K. Meszlenyi, A. G. Mikos, *Biomaterials* 2000, 21, 2163.

[31] E. Behravesh, S. Jo, K. Zygourakis, A. G. Mikos, *Biomacromolecules* 2002, 3, 374; E. Behravesh, M. D. Timmer, J. J. Lemoine, M. A. Liebschner, A. G. Mikos, *Biomacromolecules* 2002, 3, 1263.

[32] L. Draghi, S. Resta, M. G. Pirozzolo, M. C. Tanzi, *Journal of Materials Science: Materials in Medicine* 2005, 16, 1093.

[33] K. Huh, N. Baek, K. Park, *Journal of Bioactive and Compatible Polymers* 2005, 20, 231.

[34] Y. Nam, J. Yoon, T. Park, *Journal of Biomedical Materials Research* 2000, 53, 1.

[35] A. Salerno, S. Iannace, P. A. Netti, *Macromolecular Bioscience* 2008, 8, 655.

[36] X. Zhu, L. Lee, J. Jackson, Y. Tong, C. H. Wang, *Biotechnology and Bioengineering* 2008, 100, 998.

[37] A. Barbetta, A. Gumiero, R. Pecci, R. Bedini, M. Dentini, *Biomacromolecules* 2009, 10, 3188.

[38] A. Barbetta, G. Rizzitelli, R. Bedini, R. Pecci, M. Dentini, *Soft Matter* 2010, 6, 1785.

[39] F. Dehghani, N. Annabi, *Current Opinion in Biotechnology* 2011, 22, 661.

[40] C. Ji, N. Annabi, A. Khademhosseini, F. Dehghani, *Acta Biomaterialia* 2011, 7, 1653.

[41] L. Serex, T. Braschler, A. Filippova, A. Rochat, A. Béduer, A. Bertsch, P. Renaud, *Advanced Materials Technologies* 2018, 3, 1700340.

[42] M. Nadgorny, J. Collins, Z. Xiao, P. J. Scales, L. A. Connal, *Polymer Chemistry* 2017, 9, 1684.

[43] A. Forte, C. Parisi, D. Dini, L. Silvio, Z. Tan, *Scientific Reports* 2017, 7, 16293; K. R. Hixon, A. M. Melvin, A. Y. Lin, A. F. Hall, S. A. Sell, *Journal of Biomaterials Applications* 2017, 32, 598.

[44] J. Tao, Y. Hu, S. Wang, J. Zhang, X. Liu, Z. Gou, H. Cheng, Q. Liu, Q. Zhang, S. You, M. Gou, *Scientific Reports* 2017, 7, 46038.

[45] C. Wang, Q. Zhao, M. Wang, *Biofabrication* 2017, 9, 25031.

[46] H. Kim, E. Bae, I. Kwon, R. Pal, J. Nam, D. Lee, *Biomaterials* 2004, 25, 2319; H. Zhang, I. Hussain, M. Brust, M. F. Butler, S. P. Rannard, A. I. Cooper, *Nature Materials* 2005, 4, 787.

[47] M. K. Smith, M. C. Peters, T. P. Richardson, J. C. Garbern, D. J. Mooney, *Tissue engineering* 2004, 10, 63; A. Feaver, S. Sepehri, P. Shamberger, A. Stowe, T. Autrey, G. Cao, *The Journal of Physical Chemistry B* 2007, 111, 7469; H. Zhang, A. I. Cooper, *Advanced Materials* 2007, 19, 1529.

[48] V. I. Lozinsky, A. L. Zubov, E. F. Titova, *Enzyme and Microbial Technology* 1996, 18, 561; V. I. Lozinsky, F. M. Plieva, I. Y. Galaev, B. Mattiasson, *Bioseparation* 2001, 10, 163; E. Behravesh, A. G. Mikos, *Journal of Biomedical Materials Research Part A* 2003, 66A, 698; A. Kumar, F. M. Plieva, I. Galaev, B. Mattiasson, *J Immunol Methods* 2003, 283, 185; R. G. J. C. Heijkants, R. V. Calck, J. H. Groot, A. J. Pennings, A. J. Schouten, T. G. van Tienen, N. Ramrattan, P. Buma, R. P. H. Veth, *J Mater Sci Mater Med* 2004, 15, 423; F. M. Plieva, J. Andersson, I. Galaev, B. Mattiasson, *J Sep Sci* 2004, 27, 828; F. M. Plieva, M. Karlsson, M. R. Aguilar, D. Gomez, S. Mikhalkovsky, I. Galaev, B. Mattiasson, *Journal of Applied Polymer Science* 2006, 100, 1057; D. Ceylan, O. Okay, *Macromolecules* 2007, 40, 8742; V. M. Dinu, M. M. Ozmen, S. E. Dragan, O. Okay, *Polymer* 2007, 48, 195; F. M. Plieva, I. Galaev, B. Mattiasson, *J Sep Sci* 2007, 30, 1657; N. Bölgens, Y. Yang, P. Korkusuz, E. Güzel, A. J. Haj, E. Pişkin, *Tissue Engineering Part*

A 2008, 14, 1743; M. B. Dainiak, I. N. Savina, I. Musolino, A. Kumar, B. Mattiasson, I. Y. Galaev, *Biotechnology Progress* 2008, 24, 1373.

[49] P. Arvidsson, F. M. Plieva, V. I. Lozinsky, I. Galaev, B. Mattiasson, *J Chromatogr A* 2003, 986, 275.

[50] F. J. O'Brien, Harley, I. V. Yannas, L. J. Gibson, *Biomaterials* 2005, 26, 433.

[51] D. Demir, N. Bölgön, *International Journal of Polymeric Materials and Polymeric Biomaterials* 2017, 66, 686.

[52] S. A. Bencherif, W. R. Sands, D. Bhatta, P. Arany, C. S. Verbeke, D. A. Edwards, D. J. Mooney, *Proc Natl Acad Sci U S A* 2012, 109, 19590.

[53] N. Annabi, J. W. Nichol, X. Zhong, C. Ji, S. Koshy, A. Khademhosseini, F. Dehghani, *Tissue engineering. Part B, Reviews* 2010, 16, 371.

[54] J. Park, D. Woo, B. Sun, H.-M. Chung, S. Im, Y. Choi, K. Park, K. Huh, K.-H. Park, *Journal of Controlled Release* 2007, 124, 51.

[55] J. Kim, S. Lee, S. Kim, Y. Lee, *Polymer* 2002, 43, 7549.

[56] D. Horák, H. Hlídková, J. Hradil, M. Lapčíková, M. Šlouf, *Polymer* 2008, 49, 2046.

[57] J. T. Delaney, A. R. Liberski, J. Perelaer, U. S. Schubert, *Soft Matter* 2010, 6, 866.

[58] C. Hwang, S. Sant, M. Masaeli, N. N. Kachouie, B. Zamanian, S.-H. Lee, A. Khademhosseini, *Biofabrication* 2010, 2, 35003.

[59] V. Shastri, P. Hildgen, R. Langer, *Biomaterials* 2003, 24, 3133.

[60] N. Annabi, S. M. Mithieux, A. S. Weiss, F. Dehghani, *Biomaterials* 2010, 31, 1655.

[61] J. Barry, M. Silva, V. K. Popov, K. M. Shakesheff, S. M. Howdle, *Philosophical transactions. Series A, Mathematical, physical, and engineering sciences* 2006, 364, 249.

[62] A. Fathi, S. M. Mithieux, H. Wei, W. Chrzanowski, P. Valtchev, A. S. Weiss, F. Dehghani, *Biomaterials* 2014, 35, 5425.

[63] X. Wu, Y. Liu, X. Li, P. Wen, Y. Zhang, Y. Long, X. Wang, Y. Guo, F. Xing, J. Gao, *Acta Biomaterialia* 2010, 6, 1167.

[64] Z. Peng, F. Chen, *Journal of Macromolecular Science, Part B* 2011, 50, 340; A. Autissier, C. Visage, C. Pouzet, F. Chaubet, D. Letourneur, *Acta Biomaterialia* 2010, 6, 3640.

[65] C. M. Brougham, T. J. Levingstone, N. Shen, G. M. Cooney, S. Jockenhoevel, T. C. Flanagan, F. J. O'Brien, *Advanced Healthcare Materials* 2017, 6, 1700598.

[66] A. Barros, S. Quraishi, M. Martins, P. Gurikov, R. Subrahmanyam, I. Smirnova, A. C. Duarte, R. L. Reis, *Chemie Ingenieur Technik* 2016, 88, 1770.

[67] S. Kwon, H. Kim, H. Jin, *Advanced Materials Research* 2008, 47-50, 1105.

[68] B. Newland, P. B. Welzel, H. Newland, C. Renneberg, P. Kolar, M. Tsurkan, A. Rosser, U. Freudenberg, C. Werner, *Small* 2015, 11, 5047.

[69] L. Qian, H. Zhang, *Journal of Chemical Technology and Biotechnology* 2011, 86, 172.

[70] W. Liu, Y. Li, Y. Zeng, X. Zhang, J. Wang, L. Xie, X. Li, Y. Du, *Acta Biomaterialia* 2014, 10, 1864.

[71] H. Nishihara, S. R. Mukai, D. Yamashita, H. Tamon, *Chemistry of Materials* 2005, 17, 683.

[72] X. Wu, L. Black, G. Santacana - Laffitte, C. W. Patrick, *Journal of Biomedical Materials Research Part A* 2007, 81A, 59.

[73] S. Stokols, M. H. Tuszyński, *Biomaterials* 2004, 25, 5839.

[74] V. I. Lozinsky, E. S. Vainerman, G. F. Korotaeva, S. V. Rogozhin, *Colloid & Polymer Science* 1984, 262, 617.

[75] P. Humpolicek, K. A. Radaszkiewicz, Z. Capakova, J. Pachernik, P. Bober, V. Kasparkova, P. Rejmontova, M. Lehocky, P. Ponizil, J. Stejskal, *Sci Rep* 2018, 8, 135.

[76] J. Kumari, A. A. Karande, A. Kumar, *ACS Applied Materials & Interfaces* 2016, 8, 264.

[77] N. E. Vrana, A. O'Grady, E. Kay, P. A. Cahill, G. B. McGuinness, *Journal of Tissue Engineering and Regenerative Medicine* 2009, 3, 567; N. E. Vrana, K. Matsumura, S. H. Hyon, L. M. Geever, J. E. Kennedy, J. G. Lyons, C. L. Higginbotham, P. A. Cahill, G. B. McGuinness, *Journal of Tissue Engineering and Regenerative Medicine* 2012, 6, 280.

[78] J. Kumari, A. Kumar, *Scientific Reports* 2017, 7, 41551.

[79] J. Wang, H. Yang, *Scientific Reports* 2018, 8, 7155.

[80] T. Y. Shih, S. O. Blacklow, A. W. Li, B. R. Freedman, S. Bencherif, S. T. Koshy, M. C. Darnell, D. J. Mooney, *Advanced Healthcare Materials* 2018, 7, 1701469.

[81] D. Ciolacu, C. Rudaz, M. Vasilescu, T. Budtova, *Carbohydrate Polymers* 2016, 151, 392.

[82] R. Parhi, *Adv Pharm Bull* 2017, 7, 515.

[83] Y. Zhang, C. Wang, G. Han, W. Jiang, W. Zuo, *Scientific Reports* 2017, 7, 1.

[84] G. S. Offeddu, I. Mela, P. Jeggle, R. M. Henderson, S. K. Smoukov, M. L. Oyen, *Scientific Reports* 2017, 7, 42948.

[85] N. Bhattacharai, J. Gunn, M. Zhang, *Advanced Drug Delivery Reviews* 2010, 62, 83.

[86] A. Z. C. Editors Kelly, *Comprehensive Composite Materials*, 2000.

[87] C. Oelschlaeger, F. Bossler, N. Willenbacher, *Biomacromolecules* 2016, 17, 580.

[88] L. Cheng, K. Ji, T.-Y. Shih, A. Haddad, G. Giatsidis, D. J. Mooney, D. P. Orgill, C. S. Nabzdyk, *Tissue Engineering Part A* 2016, 23, 243.

[89] S. T. Koshy, T. C. Ferrante, S. A. Lewin, D. J. Mooney, *Biomaterials* 2014, 35, 2477.

[90] S. T. Koshy, D. K. Y. Zhang, J. M. Grolman, A. G. Stafford, D. J. Mooney, *Acta Biomater* 2018, 65, 36.

[91] L. S. Nair, *Injectable Hydrogels for Regenerative Engineering*, 2016.

[92] M. F. Akhtar, M. Hanif, N. M. Ranjha, *Saudi pharmaceutical journal* 2016, 24, 554.

[93] M. Ozmen, Q. Fu, J. Kim, G. G. Qiao, *Chemical Communications* 2015, 51, 17479.

[94] M. U. Kahveci, Z. Beyazkilic, Y. Yagci, *Journal of Polymer Science Part A: Polymer Chemistry* 2010, 48, 4989.

[95] M. J. E. Fischer, *Methods in Molecular Biology* 2010, 627, 55.

[96] I. Kim, S. S. Lee, S. Bae, H. Lee, N. S. Hwang, *Biomacromolecules* 2018.

[97] T. Henderson, K. Ladewig, D. N. Haylock, K. M. McLean, A. J. O'Connor, *Journal of Biomaterials Science, Polymer Edition* 2015, 26, 881.

[98] D. M. Lynn, R. Langer, *Journal of the American Chemical Society* 2000, 122, 10761; B. D. Mather, K. Viswanathan, K. M. Miller, T. E. Long, *Progress in Polymer Science* 2006, 31, 487; D. P. Nair, M. Podgórski, S. Chatani, T. Gong, W. Xi, C. R. Fenoli, C. N. Bowman, *Chemistry of Materials* 2013, 26, 724.

[99] C. Hoffmann, M. C. Stuparu, A. Daugaard, A. Khan, *Journal of Polymer Science Part A: Polymer Chemistry* 2015, 53, 745.

[100] V. I. Lozinsky, *Russ Chem Rev* 2002, 71, 489.

[101] B. D. Ulery, L. S. Nair, C. T. Laurencin, *Journal of polymer science. Part B, Polymer physics* 2011, 49, 832.

[102] R. L. Reis, N. M. Neves, J. F. Mano, M. E. Gomes, A. P. Marques, H. S. Azevedo, *Natural-Based Polymers for Biomedical Applications*, 2008.

[103] S. G. Kumbar, C. T. Laurencin, M. Dend, *Natural and Synthetic Biomedical Polymers*, 2014.

[104] D. P. Biswas, P. A. Tran, C. Tallon, A. J. O'Connor, *J Biomater Sci Polym Ed* 2016, 28, 207.

[105] V. S. Vlierberghe, P. Dubrule, E. Lippens, M. Cornelissen, E. Schacht, *Journal of Biomaterials Science, Polymer Edition* 2009, 20, 1417; X. Zhao, J. Kim, C. A. Cezar, N. Huebsch, K. Lee, K. Bouhadir, D. J. Mooney, *Proceedings of the National Academy of Sciences* 2011, 108, 67.

[106] H.-T. Liao, K. T. Shalumon, K.-H. Chang, C. Sheu, J.-P. Chen, *Journal of Materials Chemistry B* 2016, 4, 1827.

[107] S. Partap, I. Rehman, J. R. Jones, J. A. Darr, *Advanced Materials* 2006, 18, 501; A. Barbetta, E. Barigelli, M. Dentini, *Biomacromolecules* 2009, 10, 2328; A. Béduer, T. Braschler, O. Peric, G. E. Fantner, S. Mosser, P. C. Fraering, S. Benchérif, D. J. Mooney, P. Renaud, *Advanced*

Healthcare Materials 2015, 4, 301; K. R. Hixon, T. Lu, M. N. Carletta, S. H. McBride - Gagyi, B. E. Janowiak, S. A. Sell, *J Biomed Mater Res B Appl Biomater* 2017, 106, 1918.

[108] S. A. Bencherif, W. R. Sands, O. A. Ali, W. A. Li, S. A. Lewin, T. M. Braschler, T.-Y. Shih, C. S. Verbeke, D. Bhatta, G. Dranoff, D. J. Mooney, *Nat Commun* 2015, 6, 7556.

[109] S. C. Owen, S. A. Fisher, R. Y. Tam, C. M. Nimmo, M. S. Shoichet, *Langmuir* 2013, 29, 7393.

[110] A. Ström, A. Larsson, O. Okay, *Journal of Applied Polymer Science* 2015, 132, 42194.

[111] M.-E. Han, S.-H. Kim, H. D. Kim, H.-G. Yim, S. A. Bencherif, T.-I. Kim, N. S. Hwang, *International Journal of Biological Macromolecules* 2016, 93, 1410.

[112] D. B. Raina, Isaksson, H., Teotia, A.K., Lidgren ,L., Tägil, M., and Kumar, A. , *J Control Release* 2016, 235, 365.

[113] F. Ak, Z. Oztoprak, I. Karakutuk, O. Okay, *Biomacromolecules* 2013, 14, 719; P. U. Kadakia, E. Jain, K. R. Hixon, C. T. Eberlin, S. A. Sell, *Materials Research Express* 2016, 3, 55401; B. Yetiskin, C. Akinci, O. Okay, *Polymer* 2017, 128, 47.

[114] E. Bellas, T. J. Lo, E. P. Fournier, J. E. Brown, R. D. Abbott, E. S. Gil, K. G. Marra, P. J. Rubin, G. G. Leisk, D. L. Kaplan, *Advanced Healthcare Materials* 2015, 4, 452.

[115] B. Yetiskin, O. Okay, *Polymer* 2017, 112, 61.

[116] L. P. Bagri, J. Bajpai, A. K. Bajpai, *Bulletin of Materials Science* 2011, 34, 1739.

[117] L. K. Lazzari, V. B. Zampieri, M. Zanini, A. J. Zattera, C. Baldasso, *Cellulose* 2017, 24, 3421; J. Štefelová, V. Slovák, *Journal of Thermal Analysis and Calorimetry* 2015, 119, 359; E. Larsson, A. Boujemaoui, E. Malmström, A. Carlmark, *RSC Advances* 2015, 5, 77643.

[118] Z. Oztoprak, T. Hekimoglu, I. Karakutuk, D. C. Tuncaboylu, O. Okay, *Polymer Bulletin* 2014, 71, 1983.

[119] R. Akbarzadeh, A. M. Yousefi, *Journal of Biomedical Materials Research Part B: Applied Biomaterials* 2014, 102, 1304.

[120] A. Backer, B. Goppert, S. Sturm, P. Abaffy, T. Sollich, F. J. Gruhl, *SpringerPlus* 2016, 5, 902.

[121] J.-W. Jeong, G. Shin, S. Park, K. Yu, L. Xu, J. A. Rogers, *Neuron* 2015, 86, 175.

[122] G. Conoscenti, T. Schneider, K. Stoelzel, F. Pavia, V. Brucato, C. Goegele, V. Carrubba, G. Schulze-Tanzil, *Materials Science and Engineering: C* 2017, 80, 449.

[123] G. C. Ingavle, L. Baillie, Y. Zheng, E. K. Lis, I. N. Savina, C. A. Howell, S. V. Mikhalkovsky, S. R. Sandeman, *Biomaterials* 2015, 50, 140.

[124] W. Wan, A. D. Bannerman, L. Yang, M.-H. Cryogels, *Polymeric Cryogels* 2014.

[125] E. Caló, J. Barros, L. Ballamy, V. V. Khutoryanskiy, *RSC Advances* 2016, 6, 105487.

[126] S. Ceylan, D. Göktürk, N. Bölgön, *Bio-Medical Materials and Engineering* 2016, 27, 327.

[127] A. Golunova, J. Jaroš, V. Jurtíková, I. Kotelníkov, J. Kotek, H. Hlídková, L. Streit, A. Hampl, F. Rypáček, V. Proks, *Physiological research* 2015, 64 Suppl 1, 27.

[128] A. Wartenberg, J. Weisser, S. Thein, H.-P. Suso, R. Schmidt, M. Schnabelrauch, *Journal of Medical Materials and Technologies* 2017, 1, 26.

[129] Y. Liu, K. Xu, Q. Chang, M. Darabi, B. Lin, W. Zhong, M. Xing, *Advanced Materials* 2016, 28, 7758.

[130] P. Neo, P. Shi, J. Goh, S. Toh, *Biomed Mater* 2014, 9, 065002.

[131] L. Su, L. Miao, S. Tanemura, *Materials Science Forum* 2010, 663-665, 1242; A. Karimi, W. Daud, *JOM* 2017, 69, 1213; A. M. Atta, H. A. Al - Lohedan, A. M. Tawfeek, M. A. Ahmed, *Polymer International* 2018, 67, 925; H. Kirsebom, D. Topgaard, I. Galaev, B. Mattiasson, *Langmuir* 2010, 26, 16129; T. Laochai, M. Mooltongchun, S. Teepoo, *Energy Procedia* 2016, 89, 248; N. Sahiner, S. Demirci, M. Sahiner, S. Yilmaz, *Journal of Applied Polymer Science* 2016, 133, 43438.

[132] A. Chaturvedi, A. K. Bajpai, J. Bajpai, A. Sharma, *Designed Monomers and Polymers* 2015, 18, 385.

[133] M. Rezaeeyazdi, T. Colombani, A. Memic, S. A. Bencherif, *Materials* 2018, 11, 1374.

[134] S. Bhat, A. Tripathi, A. Kumar, *Journal of The Royal Society Interface* 2011, 8, 540.

[135] X. Zhang, C. Li, Y. Luo, *Langmuir* 2011, 27, 1915.

[136] L. Wang, J. Jiang, W. Hua, A. Darabi, X. Song, C. Song, W. Zhong, M. M. Q. Xing, X. Qiu, *Advanced Functional Materials* 2016, 26, 4293.

[137] B. Tian, J. Liu, T. Dvir, L. Jin, J. H. Tsui, Q. Qing, Z. Suo, R. Langer, D. S. Kohane, C. M. Lieber, *Nature Materials* 2012, 11, 986.

[138] N. Sahiner, S. Demirci, N. Aktas, *Journal of Polymer Research* 2017, 24, 126.

[139] Z. Deng, Y. Guo, P. X. Ma, B. Guo, *Journal of Colloid and Interface Science* 2018.

[140] T. Boyaci, N. Orakdogen, *European Polymer Journal* 2017.

[141] N. Bölgön, M. Aguilar, M. del Fernández, S. Gonzalo-Flores, S. Villar-Rodil, J. Román, E. Pişkin, *Artificial Cells, Nanomedicine, and Biotechnology* 2013, 43, 40; A. Srivastava, A. Kumar, *Journal of Materials Science: Materials in Medicine* 2010, 21, 2937.

[142] O. Okay, *Polymeric Cryogels*, Springer International Publishing, Switzerland 2014.

[143] P. B. Welzel, J. Friedrichs, M. Grimmer, S. Vogler, U. Freudenberg, C. Werner, *Advanced healthcare materials* 2014, 3, 1849.

[144] D. Singh, V. Nayak, A. Kumar, *International journal of biological sciences* 2010, 6, 371.

[145] A. Srivastava, E. Jain, A. Kumar, *Materials Science and Engineering: A* 2007, 464, 93; N. Orakdogen, T. Boyaci, *Reactive and Functional Polymers* 2016, 102, 82.

[146] X.-Z. Zhang, C.-C. Chu, *Chemical Communications* 2003, 1446; N. Orakdogen, B. Sanay, *Polymer Degradation and Stability* 2017, 144, 251.

[147] D. E. Discher, P. Janmey, Y.-l. Wang, *Science* 2005, 310, 1139; A. J. Engler, S. Sen, L. H. Sweeney, D. E. Discher, *Cell* 2006, 126, 677; A. J. Engler, F. Rehfeldt, S. Sen, D. E. Discher, *Part IV Mechanical Stimuli to Cells* 2007, 83, 521.

[148] X.-Z. Zhang, Y.-Y. Yang, T.-S. Chung, K.-X. Ma, *Langmuir* 2001, 17, 6094.

[149] J. D. Kaufman, G. J. Miller, E. F. Morgan, C. M. Klapperich, *Journal of Materials Research* 2008, 23, 1472.

[150] D. M. Ebenstein, L. A. Pruitt, *Journal of Biomedical Materials Research Part A* 2004, 69A, 222.

[151] B. Sun, Z. Wang, Q. He, W. Fan, S. Cai, *Soft Matter* 2017, 13, 6852; N. Bodenberger, D. Kubiczek, I. Abrosimova, A. Scharm, F. Kipper, P. Walther, F. Rosenau, *Biotechnology Reports* 2016, 12, 6.

[152] Y. Hwang, C. Zhang, S. Varghese, *Journal of Materials Chemistry* 2009, 20, 345.

[153] S. Lin, N. Sangaj, T. Razafiarison, C. Zhang, S. Varghese, *Pharmaceutical Research* 2011, 28, 1422.

[154] F. M. Plieva, M. Karlsson, M.-R. Aguilar, D. Gomez, S. Mikhalovsky, I. Galaev, *Soft Matter* 2005, 1, 303.

[155] J. Yao, S. L. Tao, M. J. Young, *Polymers* 2011, 3, 899; K. L. Christman, A. J. Vardanian, Q. Fang, R. E. Sievers, H. H. Fok, R. J. Lee, *Journal of the American College of Cardiology* 2004, 44, 654.

[156] B. Wang, W. Liu, D. Xing, Y. Li, R. Li, Y. Du, J. Lin, *Osteoarthritis and Cartilage* 2017, 25, S333 ; M. Liu, X. Zeng, C. Ma, H. Yi, Z. Ali, X. Mou, S. Li, Y. Deng, N. He, *Bone research* 2017, 5, 17014.

[157] M. Guvendiren, H. D. Lu, J. A. Burdick, *Soft Matter* 2012, 8, 260; E. A. Silva, D. J. Mooney, *Journal of Thrombosis and Haemostasis* 2007, 5, 590.

[158] V. M. Gun'ko, I. N. Savina, S. V. Mikhalovsky, *Advances in colloid and interface science* 2013, 187-188, 1.

[159] F. Svec, *Journal of chromatography. A* 2010, 1217, 902; I. N. Savina, G. C. Ingavle, A. B. Cundy, S. V. Mikhalovsky, *Scientific Reports* 2016, 6, 21154.

[160] K. R. Hixon, C. T. Eberlin, P. U. Kadakia, S. H. McBride-Gagyi, E. Jain, S. A. Sell, *Biomedical Physics & Engineering Express* 2016, 2, 35014.

[161] S. Amziane, P. Clermont-Ferrand, *Bio-aggregates based building materials: State-of-the-Art Report of the RILEM Technical Committee 236-BBM*, Springer Netherlands, 2017.

[162] J. Goworek, W. Stefaniak, *Thermochimica Acta* 1996, 286, 199.

[163] D. Liu, Z. Ma, Z. Wang, H. Tian, M. Gu, *Langmuir* 2014, 30, 9544.

[164] H. Zhang, X. Liu, M. Yang, L. Zhu, *Materials Science and Engineering: C* 2015, 55, 8.

[165] T. V. Burova, N. V. Grinberg, E. V. Kalinina, R. V. Ivanov, V. I. Lozinsky, C. Alvarez - Lorenzo, V. Y. Grinberg, *Macromolecular Chemistry and Physics* 2011, 212, 72.

[166] W. Camp, T. Dispinar, B. Dervaux, F. E. Prez, J. C. Martins, B. Fritzinger, *Macromolecular Rapid Communications* 2009, 30, 1328.

[167] Y. E. Shapiro, *Progress in Polymer Science* 2011, 36, 1184.

[168] P. Karacan, O. Okay, *Reactive and Functional Polymers* 2013, 73, 442.

[169] V. E. G., T. T. B., *Journal of Separation Science* 2007, 30, 2801.

[170] F. M. Plieva, E. D. Seta, I. Y. Galaev, B. Mattiasson, *Separation and Purification Technology* 2009, 65, 110.

[171] M. Rangan, H. D. S., *Journal of Separation Science* 2006, 29, 1686.

[172] G. Erturk, B. Mattiasson, *J Chromatogr A* 2014, 1357, 24.

[173] M. Andac, I. Y. Galaev, A. Denizli, *Journal of chromatography. B, Analytical technologies in the biomedical and life sciences* 2016, 1021, 69.

[174] V. I. Lozinsky, I. Y. Galaev, F. M. Plieva, I. N. Savina, H. Jungvid, B. Mattiasson, *Trends in biotechnology* 2003, 21, 445.

[175] F. Plieva, X. Huiting, I. Y. Galaev, B. Bergenstahl, B. Mattiasson, *Journal of Materials Chemistry* 2006, 16, 4065.

[176] F. M. Plieva, I. Galaev, B. Mattiasson, *J Sep Sci* 2007, 30, 1657.

[177] M. Erzengin, N. Unlu, M. Odabasi, *J Chromatogr A* 2011, 1218, 484.

[178] M. Uygun, B. Akduman, S. Akgol, A. Denizli, *Appl Biochem Biotechnol* 2013, 170, 1815.

[179] D. Nazan, T. Nalan, G. I. Yu, P. Erhan, D. Adil, *Journal of Applied Polymer Science* 2007, 105, 1808; A. Dogan, S. Ozkara, M. M. Sari, L. Uzun, A. Denizli, *Journal of chromatography. B, Analytical technologies in the biomedical and life sciences* 2012, 893-894, 69.

[180] M. Andac, G. Baydemir, H. Yavuz, A. Denizli, *J Mol Recognit* 2012, 25, 555.

[181] C. Babac, H. Yavuz, I. Y. Galaev, E. Pişkin, A. Denizli, *Reactive and Functional Polymers* 2006, 66, 1263.

[182] F. Svec, *Journal of chromatography. A* 2010, 1217, 902.

[183] I. Guven, O. Gezici, M. Bayrakci, M. Morbidelli, *J Chromatogr A* 2018, 1558, 59.

[184] F. M. Plieva, I. N. Savina, S. Deraz, J. Andersson, I. Y. Galaev, B. Mattiasson, *Journal of chromatography. B, Analytical technologies in the biomedical and life sciences* 2004, 807, 129.

[185] A. Jungbauer, R. Hahn, *J Chromatogr A* 2008, 1184, 62.

[186] J. M. Billakanti, C. J. Fee, *Biotechnol Bioeng* 2009, 103, 1155.

[187] B. M. Carvalho, L. M. Carvalho, W. F. Silva, Jr., L. A. Minim, A. M. Soares, G. G. Carvalho, S. L. da Silva, *Food chemistry* 2014, 154, 308; N. S. Bibi, N. K. Singh, R. N. Dsouza, M. Aasim, M. Fernandez-Lahore, *J Chromatogr A* 2013, 1272, 145; D. Ali, E. Bahar, P. Gözde, O. Mehmet, *Journal of Applied Polymer Science* 2008, 109, 2905; M. B. Dainiak, A. Kumar, F. M. Plieva, I. Y. Galaev, B. Mattiasson, *J Chromatogr A* 2004, 1045, 93; D. Cimen, A. Denizli, *Colloids Surf B Biointerfaces* 2012, 93, 29.

[188] A. Kumar, V. Bansal, J. Andersson, P. K. Roychoudhury, B. Mattiasson, *J Chromatogr A* 2006, 1103, 35.

[189] Ö. Acet, T. Baran, D. Erdönmez, N. H. Aksoy, İ. Alacabey, A. Menteş, M. Odabaşı, *J Chromatogr A* 2018, 1550, 21.

[190] N. K. Singh, R. N. Dsouza, M. Grasselli, M. Fernandez-Lahore, *J Chromatogr A* 2014, 1355, 143; I. Percin, R. Khalaf, B. Brand, M. Morbidelli, O. Gezici, *J Chromatogr A* 2015, 1386, 13; F. Chen, K. Yao, S. Shen, J. Yun, *Chemical Engineering Science* 2008, 63, 71; S. I. N., G. I.

Yu., M. Bo, Journal of Molecular Recognition 2006, 19, 313; S. P. Tao, J. Zheng, Y. Sun, J Chromatogr A 2015, 1389, 104.

- [191] I. N. Savina, I. Y. Galaev, B. Mattiasson, J Chromatogr A 2005, 1092, 199.
- [192] F. M. Plieva, P. Ekstrom, I. Y. Galaev, B. Mattiasson, Soft Matter 2008, 4, 2418.
- [193] K. Yao, J. Yun, S. Shen, L. Wang, X. He, X. Yu, J Chromatogr A 2006, 1109, 103; S. P. Tao, C. Wang, Y. Sun, J Chromatogr A 2014, 1359, 76; S. Sun, Y. Tang, Q. Fu, X. Liu, L. Guo, Y. Zhao, C. Chang, Int J Biol Macromol 2012, 50, 1002; G. Baydemir, E. A. Turkoglu, M. Andac, I. Percin, A. Denizli, Biotechnology and applied biochemistry 2015, 62, 200.
- [194] H. Solmaz, M. Bo, K. Harald, Macromolecular Materials and Engineering 2014, 299, 631.
- [195] a. P Cuatrecasas, C. B. Anfinsen, Annual Review of Biochemistry 1971, 40, 259.
- [196] W. Noppe, F. M. Plieva, K. Vanhoorelbeke, H. Deckmyn, M. Tuncel, A. Tuncel, I. Y. Galaev, B. Mattiasson, Journal of biotechnology 2007, 131, 293.
- [197] V. I. Muronetz, T. Korpela, Journal of chromatography. B, Analytical technologies in the biomedical and life sciences 2003, 790, 53.
- [198] H. Alkan, N. Bereli, Z. Baysal, A. Denizli, Biochemical Engineering Journal 2009, 45, 201.
- [199] G. Erturk, N. Bereli, M. A. Tumer, R. Say, A. Denizli, J Mol Recognit 2013, 26, 633.
- [200] K. Mosbach, Ramstr, O. m, *The Emerging Technique of Molecular Imprinting and Its Future Impact on Biotechnology*, Vol. 14, 1996.
- [201] K. Flavin, M. Resmini, *Imprinted nanomaterials: A new class of synthetic receptors*, Vol. 393, 2008; Y.-P. Huang, Z.-S. Liu, C. Zheng, R.-Y. Gao, 2009, 30, 155; C. Baggiani, G. Giraudi, C. Giovannoli, F. Trotta, A. Vanni, Journal of Chromatography A 2000, 883, 119; N. M. Maier, W. Lindner, Analytical and bioanalytical chemistry 2007, 389, 377.
- [202] M. Rabieizadeh, S. M. R. Kashefi Mofrad, F. Naeimpoor, *Monolithic Molecularly Imprinted Cryogel for Lysozyme Recognition*, Vol. 37, 2014.
- [203] M. Andaç, A. Denizli, RSC Advances 2014, 4, 31130.
- [204] S. Asliyuce, L. Uzun, A. Y. Rad, S. Unal, R. Say, A. Denizli, Journal of chromatography. B, Analytical technologies in the biomedical and life sciences 2012, 889-890, 95.
- [205] S. Hajizadeh, K. Kettisen, M. Gram, L. Bülow, L. Ye, Journal of Chromatography A 2018, 1534, 22.
- [206] A. Kumar, I. Galaev, B. Mattiasson, T. Aarvak, *Cell separation : fundamentals, analytical and preparative methods*, Springer, Berlin ; 2007; M. J. Tomlinson, S. Tomlinson, X. B. Yang, J. Kirkham, Journal of Tissue Engineering 2013, 4, 2041731412472690.
- [207] A. Kumar, A. Srivastava, Nature protocols 2010, 5, 1737.
- [208] A. Kumar, A. Rodríguez - Caballero, F. M. Plieva, I. Galaev, K. Nandakumar, M. Kamihira, R. Holmdahl, A. Orfao, B. Mattiasson, J Mol Recognit 2005, 18, 84.
- [209] A. Kumar, F. M. Plieva, I. Y. Galaev, B. Mattiasson, J Immunol Methods 2003, 283, 185.
- [210] A. Kumar, A. Srivastava, Nature Protocols 2010, 5, 1737.
- [211] W. P. Blackstock, M. P. Weir, Trends in biotechnology 1999, 17, 121.
- [212] M. Andaç, A. Denizli, RSC Advances 2014, 4, 31130.
- [213] R. S. Tirumalai, K. C. Chan, D. A. Prieto, H. J. Issaq, T. P. Conrads, T. D. Veenstra, Molecular & cellular proteomics : MCP 2003, 2, 1096.
- [214] C. Yang, Y. R. Liu, Y. Zhang, J. Wang, L. L. Tian, Y. N. Yan, W. Q. Cao, Y. Y. Wang, Proteomics 2017, 17, 1600284.
- [215] G. Baydemir, M. Odabaşı, Artificial Cells, Nanomedicine, and Biotechnology 2013, 41, 319; D. Ali, B. Gözde, A. Müge, S. Rıdvan, G. I. Yu, D. Adil, Macromolecular Chemistry and Physics 2010, 211, 657; N. Bereli, G. Şener, E. B. Altıntaş, H. Yavuz, A. Denizli, Materials Science and Engineering: C 2010, 30, 323; L. Uzun, C. Armutcu, O. Bicen, A. Ersoz, R. Say, A. Denizli, Colloids Surf B Biointerfaces 2013, 112, 1; G. Baydemir, M. Andac, I. Percin, A. Derazshamshir, A. Denizli, J Mol Recognit 2014, 27, 528.
- [216] F. Bonini, S. Piletsky, A. P. Turner, A. Speghini, A. Bossi, Biosensors & bioelectronics 2007, 22, 2322.

[217] Z. Zhang, X. Yang, X. Chen, M. Zhang, L. Luo, M. Peng, S. Yao, *Analytical and bioanalytical chemistry* 2011, 401, 2855.

[218] A. Fatoni, A. Numnuam, P. Kanatharana, W. Limbut, P. Thavarungkul, *The Analyst* 2014, 139, 6160.

[219] M. P. McTaggart, C. P. Price, R. G. Pinnock, P. E. Stevens, R. G. Newall, E. J. Lamb, *American Journal of Kidney Diseases* 2012, 60, 787.

[220] A. Zöchling, R. Hahn, K. Ahrer, J. Urthaler, A. Jungbauer, *Journal of Separation Science* 2004, 27, 819.

[221] J. Urthaler, R. Schlegl, A. Podgornik, A. Strancar, A. Jungbauer, R. Necina, *Journal of Chromatography A* 2005, 1065, 93.

[222] M. Benčina, A. Podgornik, A. Štrancar, *Journal of Separation Science* 2004, 27, 801.

[223] F. Sousa, D. M. Prazeres, J. A. Queiroz, *Biomed Chromatogr* 2007, 21, 993; A. Sousa, A. M. Almeida, U. Cernigoj, F. Sousa, J. A. Queiroz, *J Chromatogr A* 2014, 1355, 125.

[224] D. Cimen, F. Yilmaz, I. Percin, D. Turkmen, A. Denizli, *Mater Sci Eng C Mater Biol Appl* 2015, 56, 318.

[225] S. Cardoso, U. Černigoj, N. Lendero Krajnc, A. Štrancar, *Separation and Purification Technology* 2015, 147, 139.

[226] A. Hanora, I. Savina, F. M. Plieva, V. A. Izumrudov, B. Mattiasson, I. Y. Galaev, *Journal of biotechnology* 2006, 123, 343.

[227] A. M. Almeida, J. A. Queiroz, F. Sousa, A. Sousa, *Journal of chromatography. B, Analytical technologies in the biomedical and life sciences* 2015, 978-979, 145.

[228] I. Percin, E. Saglar, H. Yavuz, E. Aksoz, A. Denizli, *Int J Biol Macromol* 2011, 48, 577.

[229] P. Kramberger, M. Peterka, J. Boben, M. Ravník, A. Strancar, *J Chromatogr A* 2007, 1144, 143.

[230] D. M. Lin, B. Koskella, H. C. Lin, *World J Gastrointest Pharmacol Ther* 2017, 8, 162.

[231] T. Rodrigues, M. J. Carondo, P. M. Alves, P. E. Cruz, *Journal of biotechnology* 2007, 127, 520.

[232] K. Branovic, D. Forcic, J. Ivancic, A. Strancar, M. Barut, T. Kosutic-Gulija, R. Zgorelec, R. Mazuran, *Journal of Virological Methods* 2003, 110, 163.

[233] M. M. Segura, A. Kamen, P. Trudel, A. Garnier, *Biotechnol Bioeng* 2005, 90, 391.

[234] F. Smrekar, M. Ciringer, M. Peterka, A. Podgornik, A. Strancar, *Journal of chromatography. B, Analytical technologies in the biomedical and life sciences* 2008, 861, 177.

[235] S. L. Williams, M. E. Eccleston, N. K. Slater, *Biotechnol Bioeng* 2005, 89, 783.

[236] W. Noppe, F. Plieva, I. Y. Galaev, H. Pottel, H. Deckmyn, B. Mattiasson, *BMC Biotechnol* 2009, 9, 21.

[237] F. M. Plieva, I. Y. Galaev, W. Noppe, B. Mattiasson, *Trends Microbiol* 2008, 16, 543.

[238] P. Arvidsson, F. M. Plieva, I. N. Savina, V. I. Lozinsky, S. Fexby, L. Bülow, I. Y. Galaev, B. Mattiasson, *Journal of Chromatography A* 2002, 977, 27.

[239] S. J. Shirbin, S. J. Lam, N. Chan, M. Ozmen, Q. Fu, N. O'Brien-Simpson, E. C. Reynolds, G. G. Qiao, *ACS Macro Letters* 2016, 5, 552.

[240] M. B. Dainiak, I. Y. Galaev, B. Mattiasson, *J Chromatogr A* 2006, 1123, 145.

[241] V. G. Evtyugin, A. B. Margulis, L. G. Damshkalin, V. I. Lozinsky, A. I. Kolpakov, O. N. Ilinskaya, *Microbiology* 2009, 78, 603.

[242] E. N. Efremenko, N. Y. Tatarinova, *Microbiology* 2007, 76, 336; F. M. Plieva, A. Oknianska, E. Degerman, B. Mattiasson, *Biotechnol J* 2008, 3, 410.

[243] A. Al - Abboodi, J. Fu, P. M. Doran, P. P. Chan, *Biotechnology and bioengineering* 2013, 110, 318.

[244] E. Efremenko, O. Spiricheva, S. Varfolomeyev, V. Lozinsky, *Appl Microbiol Biotechnol* 2006, 72, 480.

[245] R. F. Martins, F. M. Plieva, A. Santos, R. Hatti-Kaul, *Biotechnology Letters* 2003, 25, 1537.

[246] S. P. Grogan, S. F. Duffy, C. Pauli, M. K. Lotz, D. D. D'Lima, *J Orthop Res* 2018, 36, 1947.

[247] M. L. Upton, C. L. Gilchrist, F. Guilak, L. A. Setton, *Biophysical Journal* 2008, 95, 2116.

[248] C.-Y. Kuo, C.-H. Chen, C.-Y. Hsiao, J.-P. Chen, *Carbohydrate Polymers* 2015, 117, 722.

[249] R. Reddy, A. Srivastava, A. Kumar, *PLoS One* 2013, 8, e77861.

[250] K. R. Hixon, T. Lu, S. A. Sell, *Acta Biomaterialia* 2017, 62, 29.

[251] B. Ozturk, I. Inci, S. Egri, A. Ozturk, H. Yetkin, G. Goktas, C. Elmas, E. Piskin, D. Erdogan, *Eur J Orthop Surg Traumatol* 2013, 23, 767.

[252] R. Mishra, D. Raina, M. Pelkonen, L. Lidgren, M. Tägil, A. Kumar, *International Journal of Biological Sciences* 2015, 11, 1325.

[253] A. Damania, M. Hassan, N. Shirakigawa, H. Mizumoto, A. Kumar, S. K. Sarin, H. Ijima, M. Kamihira, A. Kumar, *Scientific Reports* 2017, 7, 40323.

[254] E. Jain, A. Kumar, *Nature Protocols* 2013, 8, 821.

[255] K. J. M. Surry, H. J. B. Austin, A. Fenster, T. M. Peters, *Physics in Medicine and Biology* 2004, 49, 5529.

[256] H. Jiang, G. Campbell, D. Boughner, W.-K. Wan, M. Quantz, *Med Eng Phys* 2004, 26, 269.

[257] M. M. Stevens, *Materials today* 2008, 11, 18.

[258] L. Terranova, R. Mallet, R. Perrot, D. Chappard, *Acta biomaterialia* 2016, 29, 380; A. Maksimkin, F. Senatov, N. Y. Anisimova, M. Kiselevskiy, D. Y. Zalepuhin, I. Chernyshova, N. Tilkunova, S. Kaloshkin, *Materials Science and Engineering: C* 2017, 73, 366; H. Lu, Y. Liu, J. Guo, H. Wu, J. Wang, G. Wu, *International journal of molecular sciences* 2016, 17, 334.

[259] M. R. Brinker, D. P. O'connor, *J Bone Joint Surg Am* 2004, 86, 290; B. Baroli, *Journal of pharmaceutical sciences* 2009, 98, 1317.

[260] F. Yang, J. Wang, J. Hou, H. Guo, C. Liu, *Biomaterials* 2013, 34, 1514; C. Laurencin, Y. Khan, S. F. El-Amin, *Expert Rev Med Devices* 2006, 3, 49.

[261] J. S. Silber, D. G. Anderson, S. D. Daffner, B. T. Brislin, J. M. Leland, A. S. Hilibrand, A. R. Vaccaro, T. J. Albert, *Spine* 2003, 28, 134; C. Lord, M. Gebhardt, W. Tomford, H. Mankin, *The Journal of bone and joint surgery. American volume* 1988, 70, 369.

[262] D. L. Muscolo, M. A. Ayerza, L. A. Aponte-Tinao, *Orthopedic Clinics* 2006, 37, 65.

[263] X. Yu, X. Tang, S. V. Gohil, C. T. Laurencin, *Advanced healthcare materials* 2015, 4, 1268.

[264] N. Bolgen, Korkusuz, P., Vargel, I., Kilic, E., Guzel, E., Cavusoglu, T., Uckan, D. and Piskin, E., *Artif. Cells Nanomed. Biotechnol.* 2014, 42, 70.

[265] C. Frantz, Stewart, K.M. and Weaver, V.M., *J Cell Sci* 2010, 123, 4195; J. K. Kular, Basu, S. and Sharma, R.I. . *Journal of Tissue Engineering* 2014, 5, 1; E. A. Zimmermann, Busse, B. and Ritchie, R.O. , *Bonekey Rep.* 2015, 4, 1.

[266] R. A. a. D. Rossello, H. , *Commun Integr Biol* 2010, 3, 51.

[267] K. R. Hixon, T. Lu, S. A. Sell, *Acta Biomaterialia* 2017, 62, 29; R. G. Pearson, Bhandari, R., Quirk R.A. and Shakesheff, K.M. , *Commun Integr Biol* 2002, 12, 1; F. Rosso, Giordano, A., Barbarisi, M. and Barbarisi, A., *J. Cell Physiol* 2004, 199, 174.

[268] K. R. Hixon, Eberlin, C.T., Lu, T., Neal, S.M., Case, N.D., McBride-Gagyl, S.H. and Sell, S.A. , *Biomed Mater.* 2017, 12, 025005.

[269] C. L. Salgado, Grenho, L., Fernandes, M.H., Colaco, B.J. and Monteiro, F.J. , *J. Biomed. Mater. Res. A* 2016, 104, 57.

[270] K. T. Shalumon, Kuo, C-Y, Wong, C-B, Chien, Y-M, Chen, H-A and Chen, J-P. , *Polymers* 2018, 10, 1.

[271] R. Mishra, and Kumar, A. , *J. Biomater. Sci. Polym. Ed.* 2011, 22, 2107.

[272] R. Mishra, Goel, S.K., Gupta, K.C. and A. Kumar, *Tissue Eng. Part A* 2014, 20, 751.

[273] D. B. Raina, Isaksson, H., Teotia, A.K., Lidgren ,L., Tägil, M., and Kumar, A. , *J Control Release* 2016, 235, 365.

[274] A. Gupta, Bhat, S., Chaudhari, B.P., Gupta, K.C., Tägil, M., et.al., *J Tissue Eng Regen Med.* 2017, 11, 1689.

[275] G. S. Offeddu, I. Mela, P. Jeggle, R. M. Henderson, S. K. Smoukov, M. L. Oyen, *Scientific Reports* 2017, 7, 42948.

[276] L. Zhang, J. Hu, K. A. Athanasiou, Crit Rev Biomed Eng 2009, 37, 1.

[277] C. J. Little, Bawolin, N.K. and Chen, X. , Tissue Engineering: Part B., 2011, 17, 213.

[278] C. 2018, Vol. 2018, https://www.cdc.gov/arthritis/data_statistics/arthritis-related-stats.htm, Accessed on 06.30.2018 2018; R. C. Lawrence, Felson, D.T., Helmick, C.G., Arnold, L.M., Choi, H., Deyo, R.A., Gabriel, S., Hirsch, R., Hochberg, M.C., Hunder, G.G., Jordan, J.M., Katz, J.N., and Kremers, H.M. , Arthritis Rheum 2008, 58, 26.

[279] D. T. Felson, Lawrence, R.C., Dieppe, P.A., Hirsch, R.; Helmick, C.G.; Jordan, J.M.; Kington, R.S.; Lane, N.E.; Nevitt, M.C.; Zhang, Y.; Sowers, M.; McAlindon, T.; Spector, T.D.; Poole, A.R.; Yanovski, S.Z.; Ateshian, G.; Sharma, L.; Buckwalter, J.A.; Brandt, K.D.; Fries, J.F., Ann Intern Med 2000, 133, 635.

[280] F. M. Kievit, S. J. Florkzyk, M. Leung, O. Veiseh, J. O. Park, M. L. Disis, M. Zhang, Biomaterials 2010, 31, 5903.

[281] D. W. Jackson, Simon, T.M., and Aberman, H.M. , Clin Orthop Relat Res 2001, 391S; CDC, https://www.cdc.gov/arthritis/data_statistics/cost.htm The Cost of Arthritis in US Adults.

[282] G. Reinholtz, L. Lu, D. Saris, M. Yaszemski, S. O'driscoll, Biomaterials 2004, 25, 1511; J. C. Bernhard, G. Vunjak-Novakovic, Stem cell research & therapy 2016, 7, 56.

[283] M. K. Boushella, Hungb, C.T., Hunzikerc, E.B.; Strauss, E.J.; Lu, H.H., Connective Tissue Research 2017, 58, 393.

[284] F. I. P. Hangody L, J Bone Joint Surg Am 2003, 85, 25; W. Y.-w. a. W. Lee, B. , Journal of Orthopaedic Translation 2017, 2017, 76.

[285] C. V. Erggelet, P. , J Clin Orthop Trauma 2016, 7, 145.

[286] J. Zellner, Krutsch, W., Pfeifer, C., Koch, M., Nerlich, M. and Angele, P. , Orthopedic Research and Reviews 2015, 7, 149; L. A. Brittberg M, Nilsson A, Ohlsson C, Isaksson O, Peterson L. , N Engl J Med 1994, 331, 889.

[287] P.-G. C. Moran CJ, Chubinskaya S, Potter HG, Warren RF, Cole BJ, Rodeo SA, J Bone Joint Surg Am 2014, 96, 336; Y. Liu, Zhou, G. and Cao, Y. , Engineering 2017, 3, 28.

[288] Y. Hwang, Sangaj, N. and Varghese, S. , Tissue Eng. Part A 2010, 16, 3033; D. Singh, Tripathi, A., Nayak, V. and Kumar, A. , J. Biomater. Sci. Polym. Ed. 2011, 22, 1733.

[289] N. Bolgen, Yang, Y., Korkusuz, P., Guzel, E., El Haj, A.J. and Piskin, E. , J. Tissue Eng. Regen. Med. 2011, 5, 770.

[290] D. M. a. B. Supp, S.T. , Clin. Dermatol. 2005, 23, 403; A. D. a. F. Metcalfe, M.W. , J. R. Soc. Interface 2007, 4, 413.

[291] R. F. Pereira, Barrias, C.C., Granja, P.L. and Bartolo, P.J. , Nanomedicine 2013, 8, 603.

[292] A. A. Chaudhari, K. Vig, D. R. Baganizi, R. Sahu, S. Dixit, V. Dennis, S. R. Singh, S. R. Pillai, International journal of molecular sciences 2016, 17, 1974.

[293] T. N. Yildirimer L, Seifalian AM. , Trends in biotechnology 2012, 30, 638.

[294] M. Varkey, Ding, J. and Tredget, E.E. , J. Funct. Biomater 2015, 6, 547.

[295] L. Cheng, K. Ji, T.-Y. Shih, A. Haddad, G. Giatsidis, D. J. Mooney, D. P. Orgill, C. S. Nabzdyk, Tissue Engineering Part A 2017, 23, 243.

[296] H.-M. Wang, Chou, Y-T, et.al., PLoS One 2013, 8, e56330.

[297] S. G. Priya, Gupta, A., Jain, E et.al. , ACS Appl. Mater. Interfaces 2016, 8, 15145.

[298] X. Gu, Front Med 2015, 9, 401.

[299] P. Sensharma, G. Madhumathi, R. D. Jayant, A. K. Jaiswal, Mater Sci Eng C Mater Biol Appl 2017, 77, 1302.

[300] K. S. Straley, C. W. Foo, S. C. Heilshorn, J Neurotrauma 2010, 27, 1; R. Y. Tam, T. Fuehrmann, N. Mitrousis, M. S. Shoichet, Neuropsychopharmacology 2014, 39, 169.

[301] M. Jurga, M. B. Dainiak, A. Sarnowska, A. Jablonska, A. Tripathi, F. M. Plieva, I. N. Savina, L. Strojek, H. Jungvid, A. Kumar, B. Lukomska, K. Domanska-Janik, N. Forraz, C. P. McGuckin, Biomaterials 2011, 32, 3423.

[302] A. Beduer, T. Braschler, O. Peric, G. E. Fantner, S. Mosser, P. C. Fraering, S. Bencherif, D. J. Mooney, P. Renaud, Adv Healthc Mater 2015, 4, 301.

[303] B. Newland, P. B. Welzel, H. Newland, C. Renneberg, P. Kolar, M. Tsurkan, A. Rosser, U. Freudenberg, C. Werner, *Small* 2015, 11, 5047.

[304] E. S. Fioretta, L. von Boehmer, S. E. Motta, V. Lintas, S. P. Hoerstrup, M. Y. Emmert, *Exp Gerontol* 2018.

[305] G. A. Truskey, *F1000Res* 2016, 5, 1045.

[306] C. Best, E. Onwuka, V. Pepper, M. Sams, J. Breuer, C. Breuer, *Physiology (Bethesda)* 2016, 31, 7.

[307] M. Kharaziha, A. Memic, M. Akbari, D. A. Brafman, M. Nikkhah, *Adv Healthc Mater* 2016, 5, 1533.

[308] N. E. Vrana, P. A. Cahill, G. B. McGuinness, *J Biomed Mater Res A* 2010, 94, 1080.

[309] M. T. Conconi, L. Borgio, R. Di Liddo, L. Sartore, D. Dalzoppo, P. Amista, S. Lora, P. P. Parnigotto, C. Grandi, *Mol Med Rep* 2014, 10, 1329.

[310] Q. Yang, H. W. Xu, S. Hurday, B. S. Xu, *Orthop Surg* 2016, 8, 11.

[311] N. A. Temofeew, K. R. Hixon, S. H. McBride-Gagyi, S. A. Sell, *J Mater Sci Mater Med* 2017, 28, 36.

[312] B. H. Wang, G. Campbell, *Spine (Phila Pa 1976)* 2009, 34, 2745.

[313] Y. Zeng, C. Chen, W. Liu, Q. Fu, Z. Han, Y. Li, S. Feng, X. Li, C. Qi, J. Wu, D. Wang, C. Corbett, B. P. Chan, D. Ruan, Y. Du, *Biomaterials* 2015, 59, 53.

[314] Y. Zeng, S. Feng, W. Liu, Q. Fu, Y. Li, X. Li, C. Chen, C. Huang, Z. Ge, Y. Du, *J Biomed Mater Res B Appl Biomater* 2017, 105, 507.

[315] B. J. Kwee, D. J. Mooney, *Curr Opin Biotechnol* 2017, 47, 16.

[316] D. Singh, V. Nayak, A. Kumar, *Int J Biol Sci* 2010, 6, 371.

[317] L. Elowsson, H. Kirsebom, V. Carmignac, B. Mattiasson, M. Durbeej, *Biomaterials Science* 2013, 1, 402.

[318] M. Pumberger, T. H. Qazi, M. C. Ehrentraut, M. Textor, J. Kueper, G. Stoltenburg-Didinger, T. Winkler, P. von Roth, S. Reinke, C. Borselli, C. Perka, D. J. Mooney, G. N. Duda, S. Geissler, *Biomaterials* 2016, 99, 95.

[319] T. H. Qazi, D. J. Mooney, G. N. Duda, S. Geissler, *Biomaterials* 2017, 140, 103.

[320] N. Plunkett, F. J. O'Brien, *Technol Health Care* 2011, 19, 55.

[321] K. R. Hixon, T. Lu, S. A. Sell, *Acta Biomater* 2017, 62, 29.

[322] A. Kumar, V. Bansal, K. S. Nandakumar, I. Y. Galaev, P. K. Roychoudhury, R. Holmdahl, B. Mattiasson, *Biotechnol Bioeng* 2006, 93, 636.

[323] S. Nilsang, K. S. Nandakumar, I. Y. Galaev, S. K. Rakshit, R. Holmdahl, B. Mattiasson, A. Kumar, *Biotechnol Prog* 2007, 23, 932.

[324] E. Jain, A. A. Karande, A. Kumar, *Biotechnol Prog* 2011, 27, 170.

[325] E. Jain, A. Kumar, *Nature protocols* 2013, 8, 821.

[326] N. Bolgen, Y. Yang, P. Korkusuz, E. Guzel, A. J. El Haj, E. Piskin, *Tissue engineering. Part A* 2008, 14, 1743.

[327] C. H. Chen, C. Y. Kuo, J. P. Chen, *Int J Mol Sci* 2018, 19, 370.

[328] Y. Xu, H. Yao, P. Li, W. Xu, J. Zhang, L. Lv, H. Teng, Z. Guo, H. Zhao, G. Hou, *Cellular physiology and biochemistry : international journal of experimental cellular physiology, biochemistry, and pharmacology* 2018, 46, 482.

[329] E. Jain, A. Damania, A. K. Shakya, A. Kumar, S. K. Sarin, A. Kumar, *Colloids Surf B Biointerfaces* 2015, 136, 761.

[330] A. Damania, M. Hassan, N. Shirakigawa, H. Mizumoto, A. Kumar, S. K. Sarin, H. Ijima, M. Kamihira, A. Kumar, *Sci Rep* 2017, 7, 40323.

[331] A. Damania, A. Kumar, A. K. Teotia, H. Kimura, M. Kamihira, H. Ijima, S. K. Sarin, A. Kumar, *ACS Appl Mater Interfaces* 2018, 10, 114.

[332] R. Aliperta, P. B. Welzel, R. Bergmann, U. Freudenberg, N. Berndt, A. Feldmann, C. Arndt, S. Koristka, M. Stanzione, M. Cartellieri, A. Ehninger, G. Ehninger, C. Werner, J. Pietzsch, J. Steinbach, M. Bornhäuser, M. P. Bachmann, *Scientific Reports* 2017, 7, 42855.

[333] M. Dinu, M. Perju, E. Drăgan, *Reactive and Functional Polymers* 2011, 71, 881.

[334] D. Aydin, M. Arslan, A. Sanyal, R. Sanyal, *Bioconjugate Chemistry* 2017, 28, 1443.

[335] S. Breslin, L. O'Driscoll, *Drug discovery today* 2013, 18, 240.

[336] M. Rimann, U. Graf-Hausner, *Curr Opin Biotechnol* 2012, 23, 803.

[337] S. Nath, G. R. Devi, *Pharmacol Ther* 2016, 163, 94.

[338] X. Li, X. Zhang, S. Zhao, J. Wang, G. Liu, Y. Du, *Lab on a chip* 2014, 14, 471.

[339] T. Y. Tu, Z. Wang, J. Bai, W. Sun, W. K. Peng, R. Y. J. Huang, J. P. Thiery, R. D. Kamm, *Adv Healthc Mater* 2014, 3, 609.

[340] S. J. Florkzyk, K. Wang, S. Jana, D. L. Wood, S. K. Sytsma, J. Sham, F. M. Kievit, M. Zhang, *Biomaterials* 2013, 34, 10143.

[341] M. W. Tibbitt, K. S. Anseth, *Biotechnol Bioeng* 2009, 103, 655.

[342] A. Cecilia, A. Baecker, E. Hamann, A. Rack, T. van de Kamp, F. J. Gruhl, R. Hofmann, J. Moosmann, S. Hahn, J. Kashef, S. Bauer, T. Farago, L. Helfen, T. Baumbach, *Materials Science and Engineering: C* 2017, 71, 465.

[343] B. Göppert, T. Sollich, P. Abaffy, A. Cecilia, J. Heckmann, A. Neeb, A. Bäcker, T. Baumbach, F. J. Gruhl, A. C. B. Cato, *Small* 2016, 12, 3985.

[344] A. Backer, O. Erhardt, L. Wietbrock, N. Schel, B. Göppert, M. Dirschka, P. Abaffy, T. Sollich, A. Cecilia, F. J. Gruhl, *Biopolymers* 2017, 107, 70.

[345] R. Y. Tam, S. A. Fisher, A. E. G. Baker, M. S. Shoichet, *Chem. Mater.* 2016, 28, 3762.

[346] M. B. Dainiak, I. N. Savina, I. Musolino, A. Kumar, B. Mattiasson, I. Y. Galaev, *Biotechnol Prog* 2008, 24, 1373.

[347] M. Leung, F. M. Kievit, S. J. Florkzyk, O. Veiseh, J. Wu, J. O. Park, M. Zhang, *Pharm Res* 2010, 27, 1939.

[348] K. Wang, F. M. Kievit, S. J. Florkzyk, Z. R. Stephen, M. Zhang, *Biomacromolecules* 2015, 16, 3362.

[349] V. Phan-Lai, S. J. Florkzyk, F. M. Kievit, K. Wang, E. Gad, M. L. Disis, M. Zhang, *Biomacromolecules* 2013, 14, 1330.

[350] S. J. Florkzyk, G. Liu, F. M. Kievit, A. M. Lewis, J. D. Wu, M. Zhang, *Adv Healthc Mater* 2012, 1, 590.

[351] V. Phan-Lai, F. M. Kievit, S. J. Florkzyk, K. Wang, M. L. Disis, M. Zhang, *Anti-cancer agents in medicinal chemistry* 2014, 14, 204.

[352] G. Zhang, X. Song, J. Mei, G. Ye, L. Wang, L. Yu, X. Qiu, *RSC Advances* 2017, 7, 17208.

[353] S. J. Florkzyk, F. M. Kievit, K. Wang, A. E. Erickson, R. G. Ellenbogen, M. Zhang, *Journal of materials chemistry. B* 2016, 4, 6326; F. M. Kievit, S. J. Florkzyk, M. C. Leung, K. Wang, J. D. Wu, J. R. Silber, R. G. Ellenbogen, J. S. Lee, M. Zhang, *Biomaterials* 2014, 35, 9137.

[354] J. Sarkar, A. Kumar, *The Analyst* 2016, 141, 2553.

[355] X. Yan, L. Zhou, Z. Wu, X. Wang, X. Chen, F. Yang, Y. Guo, M. Wu, Y. Chen, W. Li, J. Wang, Y. Du, *Biomaterials* 2018.

[356] N. P. Restifo, M. E. Dudley, S. A. Rosenberg, *Nature reviews. Immunology* 2012, 12, 269; K. F. Bol, G. Schreibelt, W. R. Gerritsen, I. J. de Vries, C. G. Figdor, *Clinical cancer research : an official journal of the American Association for Cancer Research* 2016, 22, 1897.

[357] J. Weiden, J. Tel, C. G. Figdor, *Nature reviews. Immunology* 2018, 18, 212.

[358] V. Verma, Y. Kim, M. C. Lee, J. T. Lee, S. Cho, I. K. Park, J. J. Min, J. J. Lee, S. E. Lee, J. H. Rhee, *Oncotarget* 2016, 7, 39894.

[359] O. A. Ali, N. Huebsch, L. Cao, G. Dranoff, D. J. Mooney, *Nat Mater* 2009, 8, 151; O. A. Ali, D. Emerich, G. Dranoff, D. J. Mooney, *Sci Transl Med* 2009, 1, 8ra19; O. A. Ali, E. Doherty, W. J. Bell, T. Fradet, J. Hudak, M. T. Laliberte, D. J. Mooney, D. F. Emerich, *Pharm Res* 2011, 28, 1074.

[360] S. T. Koshy, T. C. Ferrante, S. A. Lewin, D. J. Mooney, *Biomaterials* 2014, 35, 2477.

[361] T. Y. Shih, S. O. Blacklow, A. W. Li, B. R. Freedman, S. Bencherif, S. T. Koshy, M. C. Darnell, D. J. Mooney, *Adv Healthc Mater* 2018, 7, e1701469.

[362] R. Aliperta, P. B. Welzel, R. Bergmann, U. Freudenberg, N. Berndt, A. Feldmann, C. Arndt, S. Koristka, M. Stanzione, M. Cartellieri, A. Ehninger, G. Ehninger, C. Werner, J. Pietzsch, J. Steinbach, M. Bornhäuser, M. P. Bachmann, *Sci Rep* 2017, 7, 42855.

[363] D. Bachmann, R. Aliperta, R. Bergmann, A. Feldmann, S. Koristka, C. Arndt, S. Loff, P. Welzel, S. Albert, A. Kegler, A. Ehninger, M. Cartellieri, G. Ehninger, M. Bornhäuser, M. von Bonin, C. Werner, J. Pietzsch, J. Steinbach, M. Bachmann, *Oncotarget* 2018, 9, 7487.

[364] M. H. Amer, L. J. White, K. M. Shakesheff, *J Pharm Pharmacol* 2015, 67, 640.

[365] Y. Li, W. Liu, F. Liu, Y. Zeng, S. Zuo, S. Feng, C. Qi, B. Wang, X. Yan, A. Khademhosseini, J. Bai, Y. Du, *Proc Natl Acad Sci U S A* 2014, 111, 13511.

[366] D. J. Mooney, H. Vandenburgh, *Cell stem cell* 2008, 2, 205; B. A. Aguado, W. Mulyasasmita, J. Su, K. J. Lampe, S. C. Heilshorn, *Tissue engineering. Part A* 2012, 18, 806.

[367] S. Odabas, G. A. Feichtinger, P. Korkusuz, I. Inci, E. Bilgic, A. S. Yar, T. Cavusoglu, S. Menevse, I. Vargel, E. Piskin, *J Tissue Eng Regen Med* 2013, 7, 831.

[368] K. H. Chang, H. T. Liao, J. P. Chen, *Acta Biomater* 2013, 9, 9012.

[369] D. J. Borg, P. B. Welzel, M. Grimmer, J. Friedrichs, M. Weigelt, C. Wilhelm, M. Prewitz, A. Stissel, A. Hommel, T. Kurth, U. Freudenberg, E. Bonifacio, C. Werner, *Acta Biomater* 2016, 44, 178.

[370] J. Kim, W. A. Li, Y. Choi, S. A. Lewin, C. S. Verbeke, G. Dranoff, D. J. Mooney, *Nature biotechnology* 2015, 33, 64.

[371] G. Vadala, G. Sowa, M. Hubert, L. G. Gilbertson, V. Denaro, J. D. Kang, *J Tissue Eng Regen Med* 2012, 6, 348.

[372] M. L. Guvendiren, Hoang D.; Burdick, Jason A., *Soft Matter* 2012, 8, 260.

[373] I. Kim, S. S. Lee, S. Bae, H. Lee, N. S. Hwang, *Biomacromolecules* 2018, 19, 2257.

[374] W. Liu, Y. Li, Y. Zeng, X. Zhang, J. Wang, L. Xie, X. Li, Y. Du, *Acta Biomater* 2014, 10, 1864.

[375] Y. Zeng, L. Zhu, Q. Han, W. Liu, X. Mao, Y. Li, N. Yu, S. Feng, Q. Fu, X. Wang, Y. Du, R. C. Zhao, *Acta Biomater* 2015, 25, 291.

[376] P. Xia, K. Zhang, Y. Gong, G. Li, S. Yan, J. Yin, *ACS Appl Mater Interfaces* 2017, 9, 34751.

[377] G. Pandey, N. Mittapelly, A. Pant, S. Sharma, P. Singh, V. T. Banala, R. Trivedi, P. K. Shukla, P. R. Mishra, *European journal of pharmaceutical sciences : official journal of the European Federation for Pharmaceutical Sciences* 2016, 91, 105.

[378] F. W. Zhang, Weibing; Zhang, Xiaodan; Meng, Xianzhi; Tong, Guolin; Deng Yulin;, *Cellulose* 2016, 23, 415.

[379] E. S. Dragan, A. I. Cocarta, *ACS Applied Materials & Interfaces* 2016, 8, 12018.

[380] S. Gorgieva, V. Kokol, *J Biomed Mater Res A* 2015, 103, 1119.

[381] K. Çetin, A. Denizli, *Colloids Surf B Biointerfaces* 2015, 126, 401; N. Bereli, M. Andac, G. Baydemir, R. Say, I. Y. Galaev, A. Denizli, *J Chromatogr A* 2008, 1190, 18; M. Bakhshpour, H. Yavuz, A. Denizli, *Artif Cells Nanomed Biotechnol* 2018, 46, 1.

[382] K. Çetin, H. Alkan, N. Bereli, A. Denizli, *Journal of Macromolecular Science, Part A* 2017, 54, 502.

[383] H. C. Chang, C. Yang, F. Feng, F. H. Lin, C. H. Wang, P. C. Chang, *Journal of the Formosan Medical Association = Taiwan yi zhi* 2017, 116, 973.

[384] T. Kim, J. Yoon, D. Lee, T. Park, *Biomaterials* 2006, 27, 152.

[385] J. Lee, M. Sultan, S. Kim, V. Kumar, Y. Yeon, O. Lee, C. Park, *International Journal of Molecular Sciences* 2017, 18, 1707.

Figures.

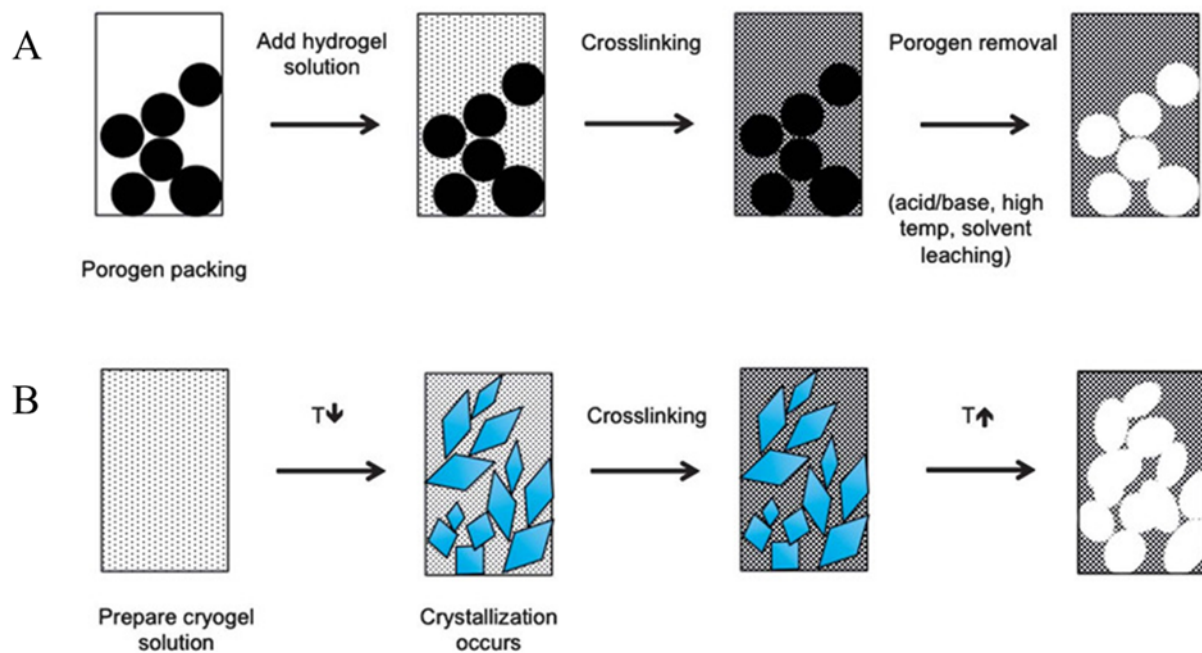


Figure 1. Macroporous hydrogel preparation. Schematic contrasting porogen-based methods (A) and cryogelation (B) for introducing pores in hydrogels. Reproduced with permission^[21], 2013, Royal Society of Chemistry (RSC).

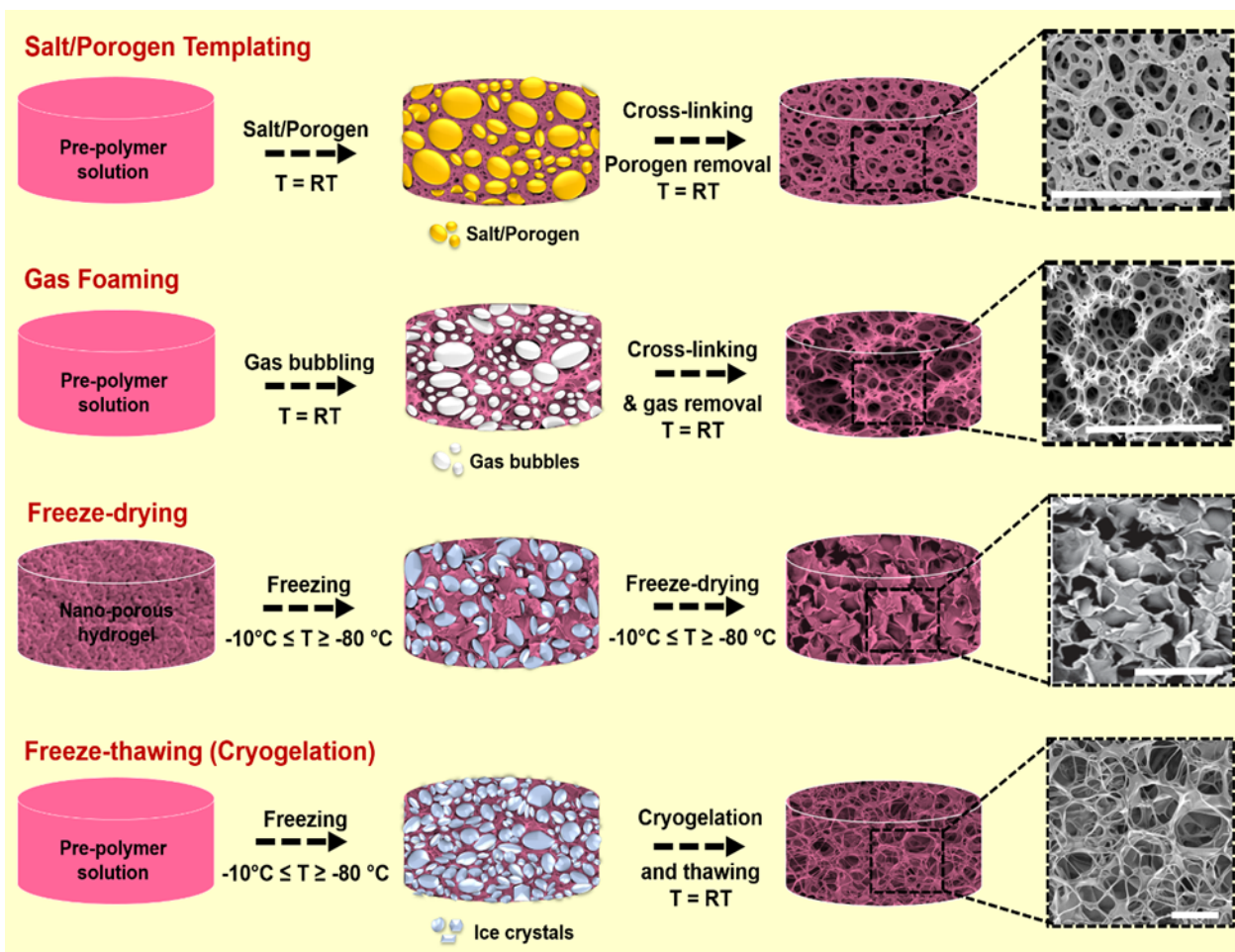


Figure 2. General steps in fabricating macroporous hydrogels via different techniques. SEM images for salt/porogen templating (reproduced with permission^[384], 2006, Elsevier), gas foaming (reproduced with permission^[38], 2010, RSC), freeze-drying (reproduced with permission^[317], 2013, RSC) and freeze-thawing (Reproduced under the terms of CC-BY 4.0 license,^[133], 2018, Rezaeeyazdi et al.) Scale bars are measured 100 μm .

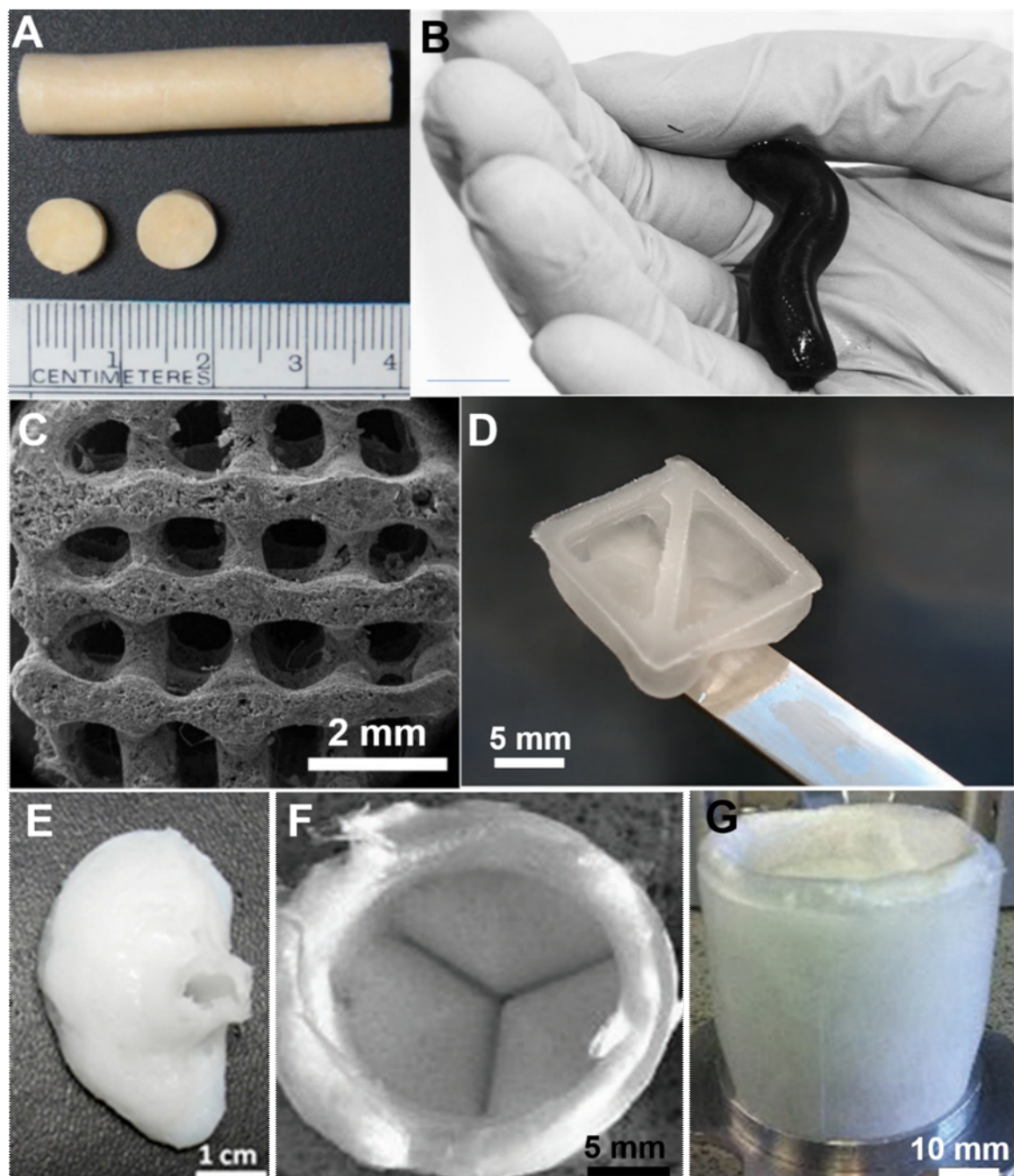


Figure 3. Cryogels can be fabricated in various shapes and sizes. (A) Digital image of a gelatin cryogel (Reproduced under the terms of CC-BY 4.0 license [78], 2017, Kumari et al.) (B) Polyaniline cryogel mimicking the properties of native tissue. Polyaniline is green in transparent thin films but appears black in thick layers or in powder form (reproduced under the terms of CC-BY 4.0 license [75], 2018, Humpolicek et al.) (C) SEM micrographs revealing the morphology of BPLLA scaffolds at low magnification (reproduced with permission [45], 2017, IOPScience) (D) A 3D printed cryogel.[41] (E) Back view of a PLA/SF ear-shaped cryogel.[385] F,G) ACG-HV scaffold with macro and microscopic homogeneity produced using the final mold.[65]

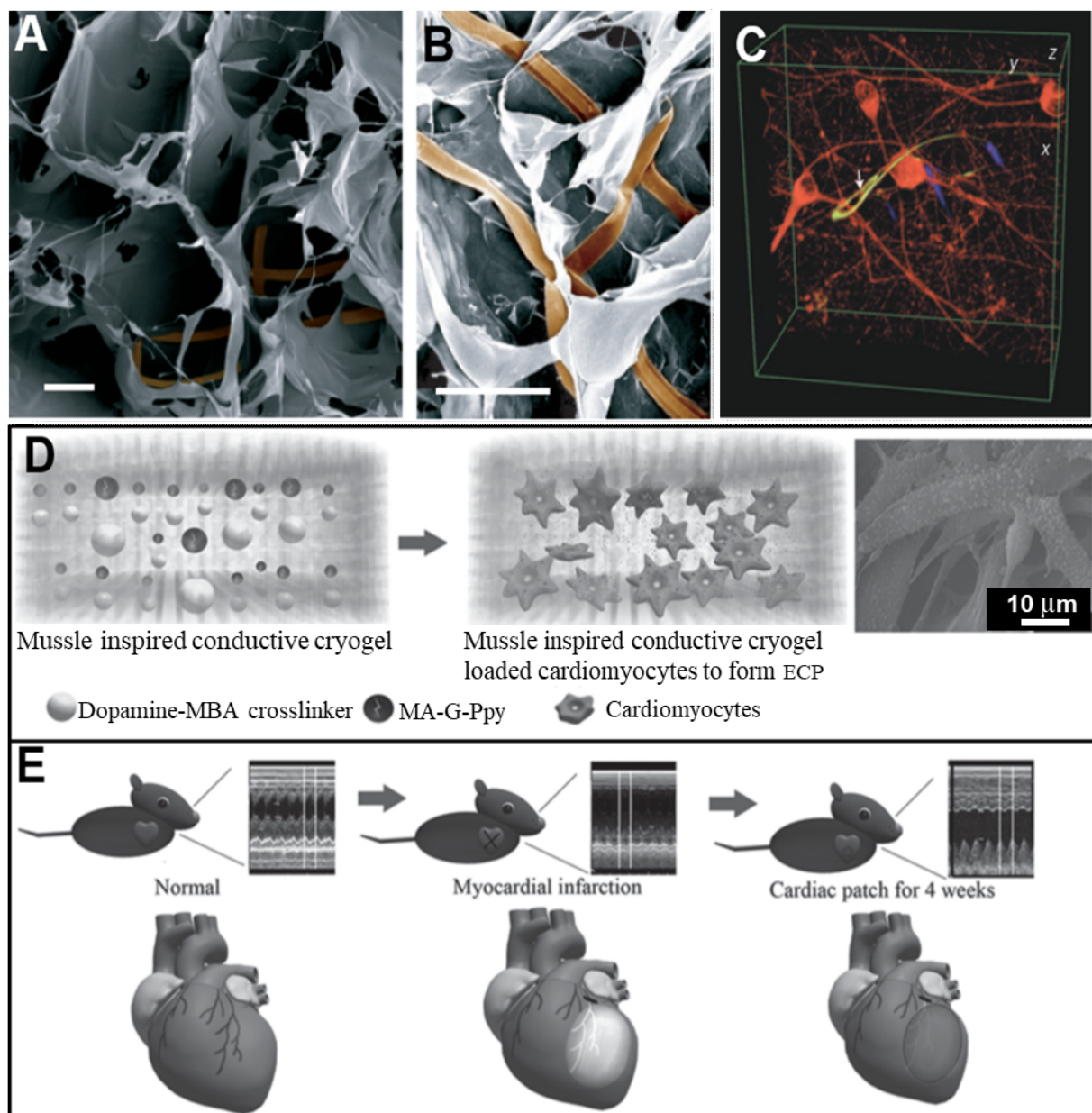


Figure 4. Conductive scaffolds used in biomedical applications. Scanning electron microscopy images of top (A) and side (B) views of a nanoES/alginate scaffold (reproduced with permission [137], 2012, Springer Nature). The nanoES ribbons are pseudo-colored in brown for better visualization. Scale bars, 200 μ m (A) and 100 μ m (B). (C) Confocal image of rat hippocampal neurons cultured in Matrigel containing reticular nanoES for two weeks. The metal ribbons are imaged in the reflected light mode and false-colored in blue (reproduced with permission [137], 2012, Springer Nature). (D) In vitro construction of conductive cryogels used as cardiac tissue patch.^[136] (E) *In vivo* implantation of the cardiac patch into the infarcted myocardium.^[136]

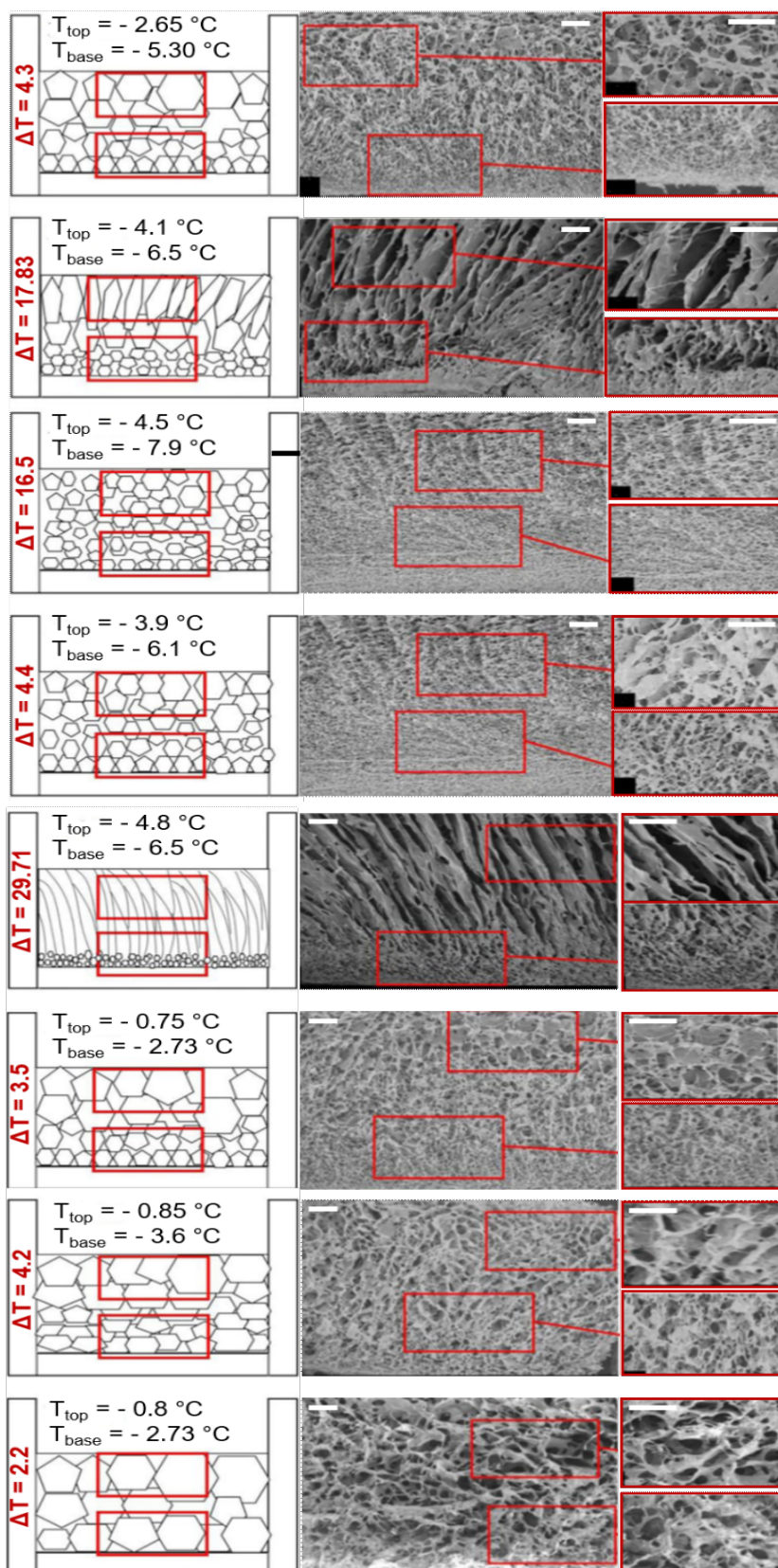


Figure 5. Effect of cryogelation temperature and cooling rate on pore structure of cryogels made of alginic acid cryogels cross-linked in calcium bath. Utilizing a stage cooling method to investigate the effect of cooling rate, pre-polymer temperature, and cryogelation time on pore architecture of alginic acid cryogels. Scale bars are measured 300 μm . Reproduced under the terms of CC-BY 4.0 license [83], 2017, Zhang et al.)

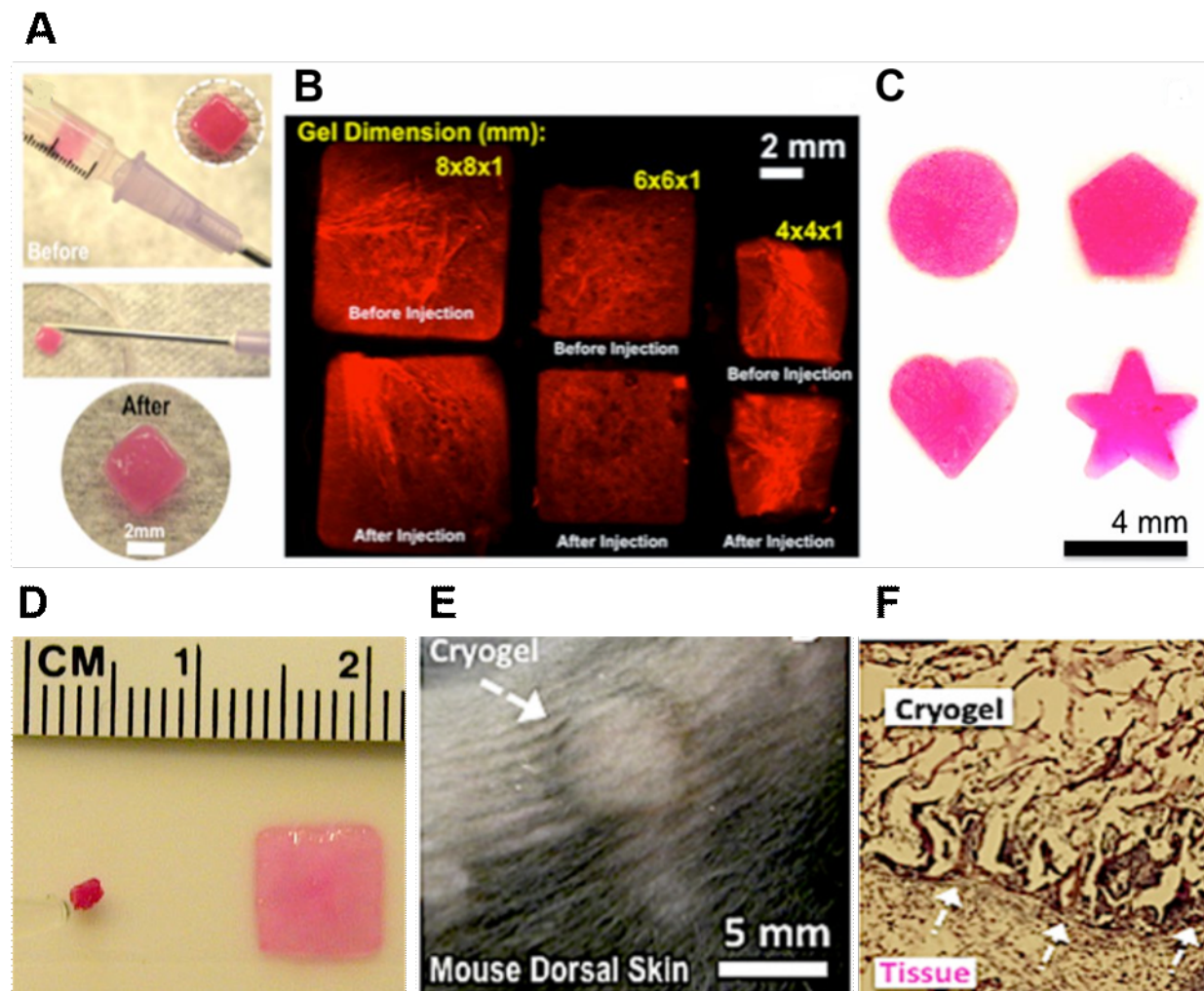


Figure 6. Injectable cryogels with shape memory features. (A) Images of MA-alginate cryogels before and after injection through 16-gauge needle. (B) Fluorescent microscopy images of MA-alginate cryogels with different sizes before and after injection through 16-gauge needle showing no change in macrostructure of the cryogels after injection. (C) Injectables cryogels can be fabricated in different sizes through cryopolymerization. (D) MA-alginate cryogel in dehydrated and swollen states showing the memory shape property of these cryogels. (E) Cryogel localization after subcutaneous injection of preformed MA-alginate cryogels ($4 \times 4 \times 1$ mm) in the subcutis of a mouse after 3 days. (F) Histological analysis (H&E stain) of explanted MA-alginate cryogel at day 3. The arrows indicate the interface between the subcutaneous connective tissue (lower left) and the cryogel matrix (upper right) (10 \times magnification). Reproduced with permission [52], 2012, Bencherif et al.)

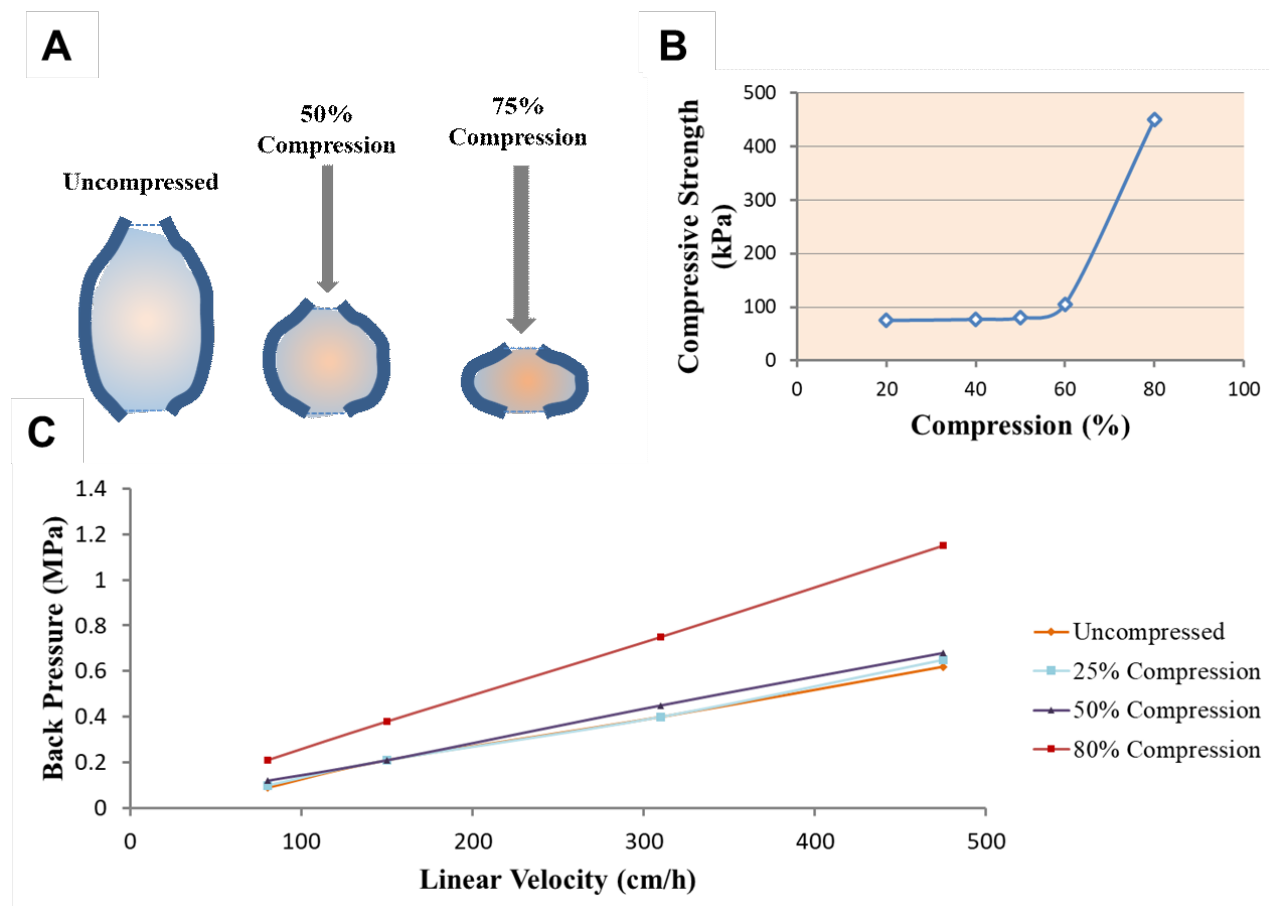


Figure 7. Flow, pressure and compression characteristics of polyacrylamide (pAAm) monoliths. (A) Impact of uniaxial compression on pAAm monolith pore structure. Significant deformation is observed at $\geq 60\%$ compression. (B) Impact of compression on pAAm monolith compressive strength. (C) Linear-velocity-backpressure curves for pAAm monoliths at different compression percentages. Reproduced with permission ^[170], 2009, Elsevier.

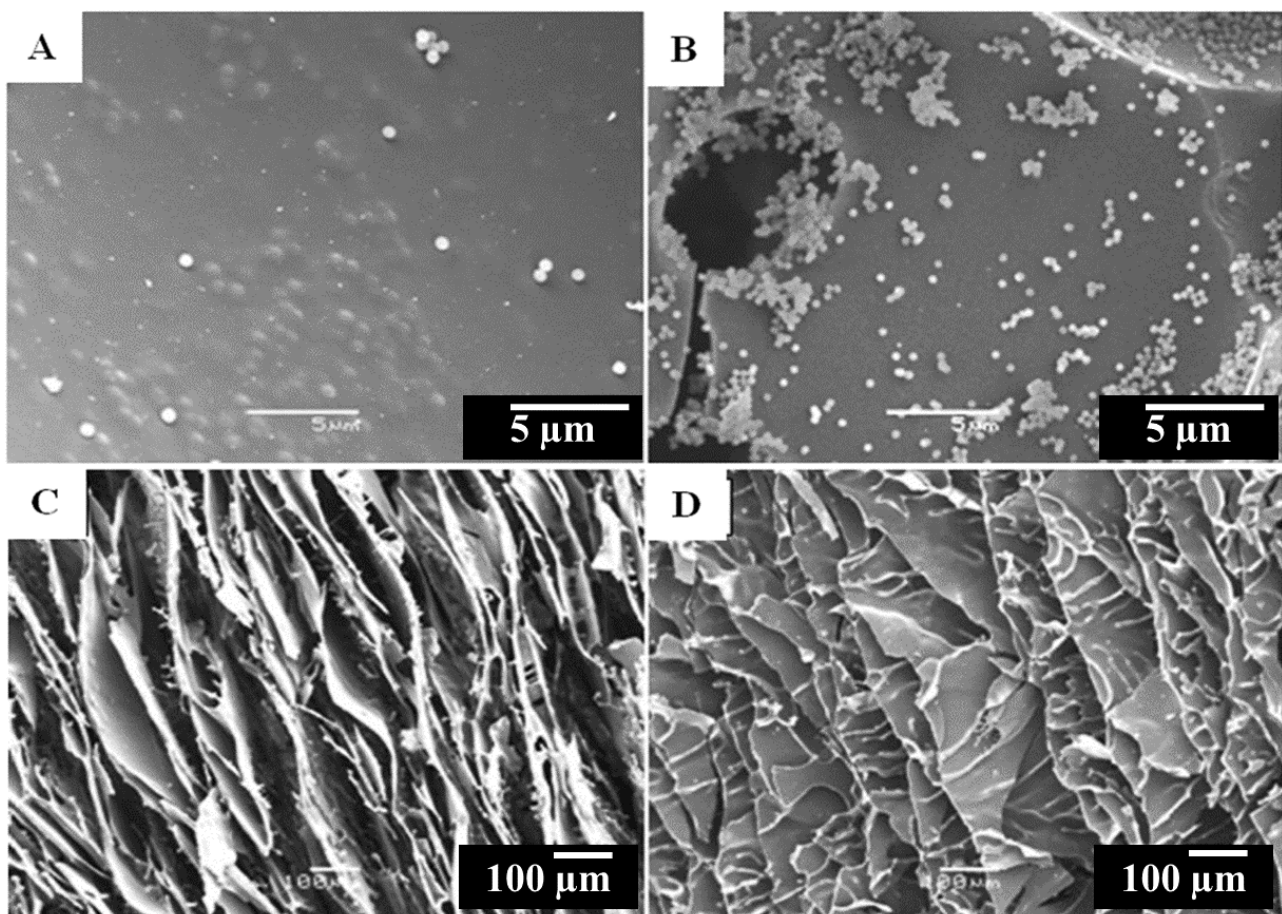


Figure 8. SEM images of poly(acrylamide-*co*- allyl glycidyl ether) poly(AAm-AGE) monoliths with immobilized or embedded particles. (A) SEM image of pAAm-AGE monoliths with amino-activated particles embedded during the cryogelation process. (B) SEM image of pAAm-AGE monoliths with amino-activated particles immobilized post-cryogelation and recirculated for 24 hours. (C) SEM image of pAAm-AGE monoliths embedded with amino-activated particles. (D) SEM image of pAAm-AGE monoliths embedded with epoxy-activated particles^[194].

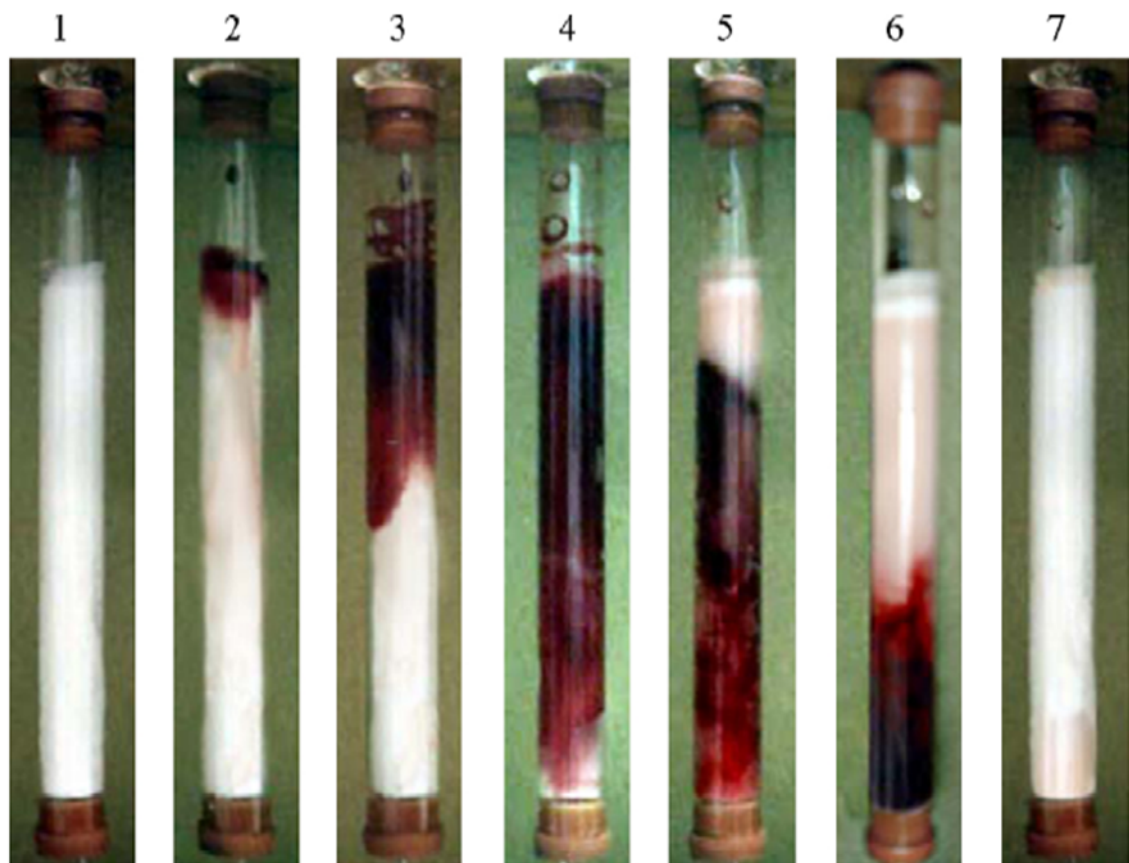


Figure 9. Whole blood applied to a protein A-poly (2-hydroxyethyl methacrylate) (A-PHEMA) monolith over time. Image 1 is the monolith before whole blood application. Image 2-6 is the monolith during whole blood application. Image 7 is the monolith after whole blood application. Reproduced with permission ^[198], 2009, Elsevier.

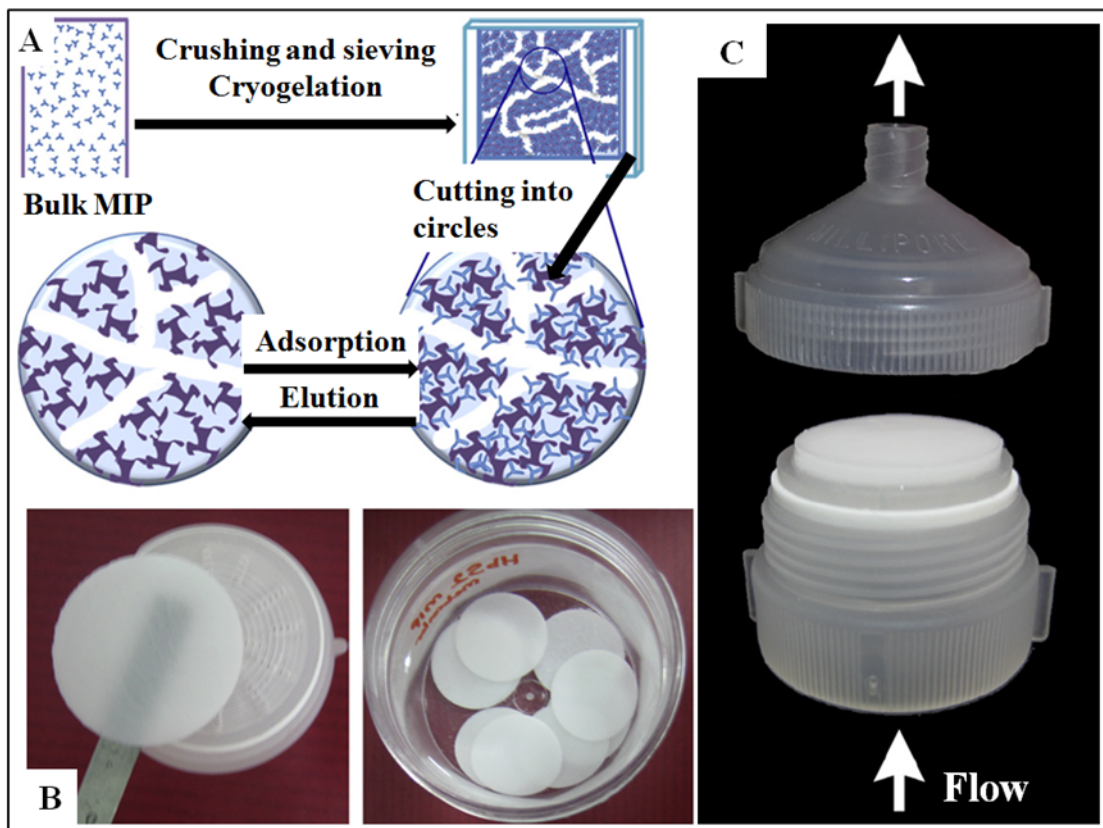


Figure 10. Anti-hepatitis B surface antibody (HBsAb)-imprinted composite cryogel. (A) Process for the formation of composite HBsAb-imprinted membranes. (B) Examples of the composite HBsAb-imprinted membranes. (C) The composite membranes are placed in plastic housing for continuous operation. Reproduced with permission [204], 2012, Elsevier.

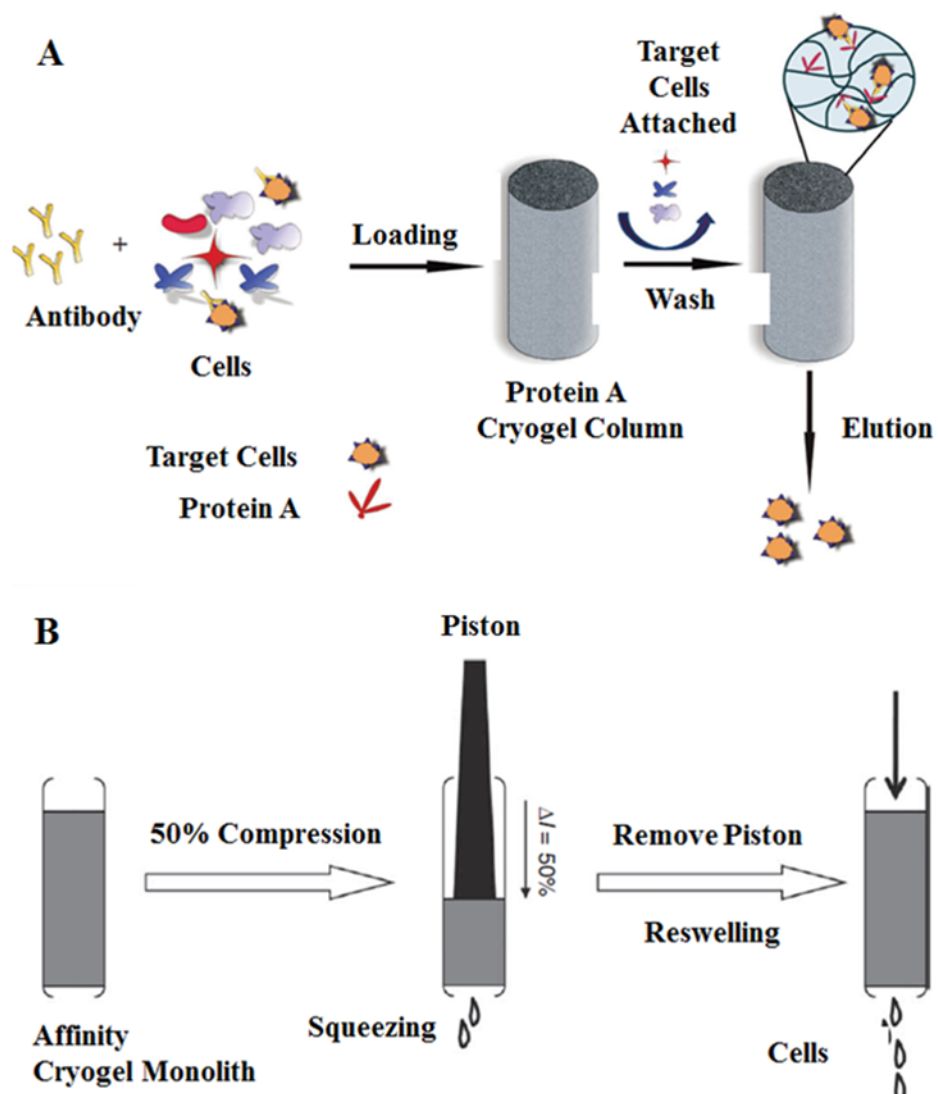


Figure 11. Polyacrylamide (pAAm)-based cryogel platform for cell separation. (A) Process for capturing hematopoietic stem cells from umbilical cord blood. IgG-labeled cells are introduced to a protein A-cryogel monolith, followed by a buffer wash to remove unbound cells. Elution of the target cells was achieved by mechanical squeezing; an alternative elution method is the introduction of immunoglobulin solution. (B) Mechanical squeezing of the cryogel monolith to elute target cells. A piston is used to compress the monolith 50%, eluting the liquid containing the target cells. Next, removal of the piston and buffer is used to regenerate the cryogel monolith to its original, non-compressed state. Reproduced with permission [207], 2010, Springer Nature.

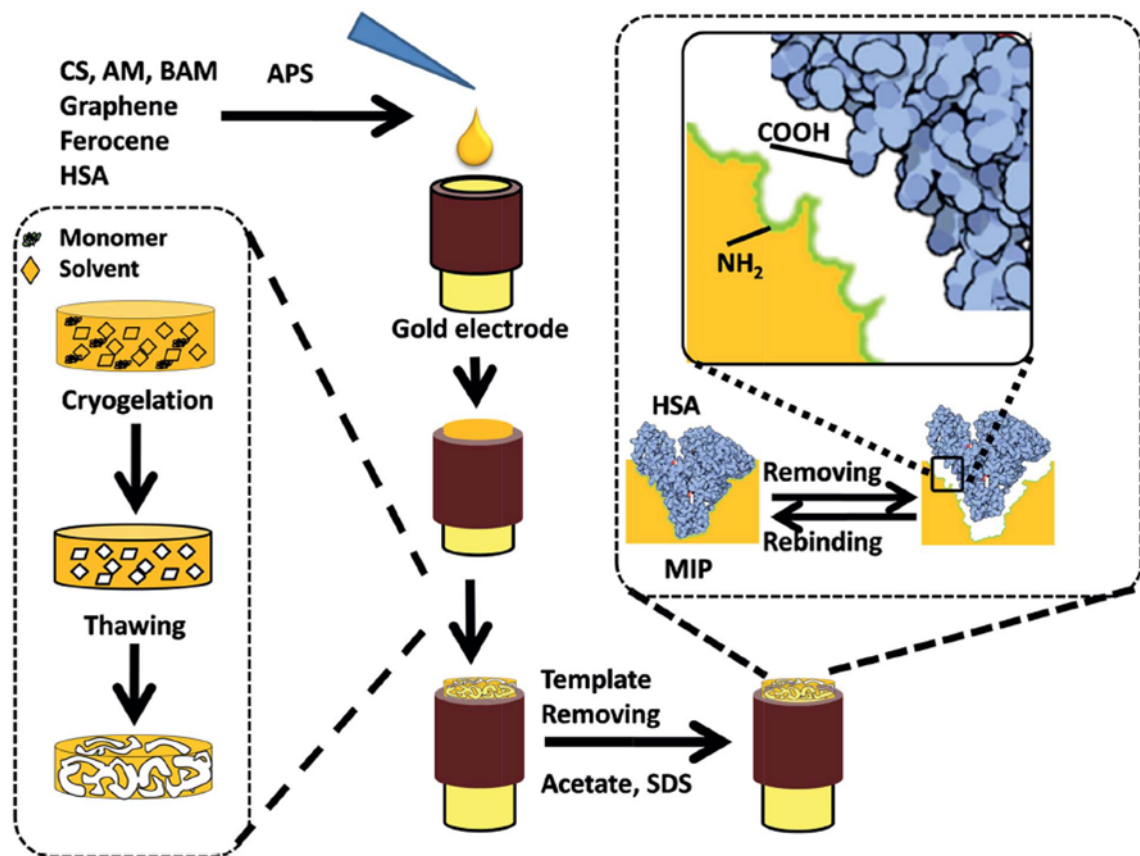


Figure 12. Process for the fabrication of a molecularly-imprinted composite polyacrylamide (pAAM) cryogel for the detection of human serum albumin (HSA. CS: chitosan; AM: polyacrylamide; BAM: N, N'-methylenebisacrylamide; APS: ammonium peroxodisulfate; HSA: human serum albumin; SDS: sodium dodecyl sulfate. Reproduced with permission [218], 2014, RSC.

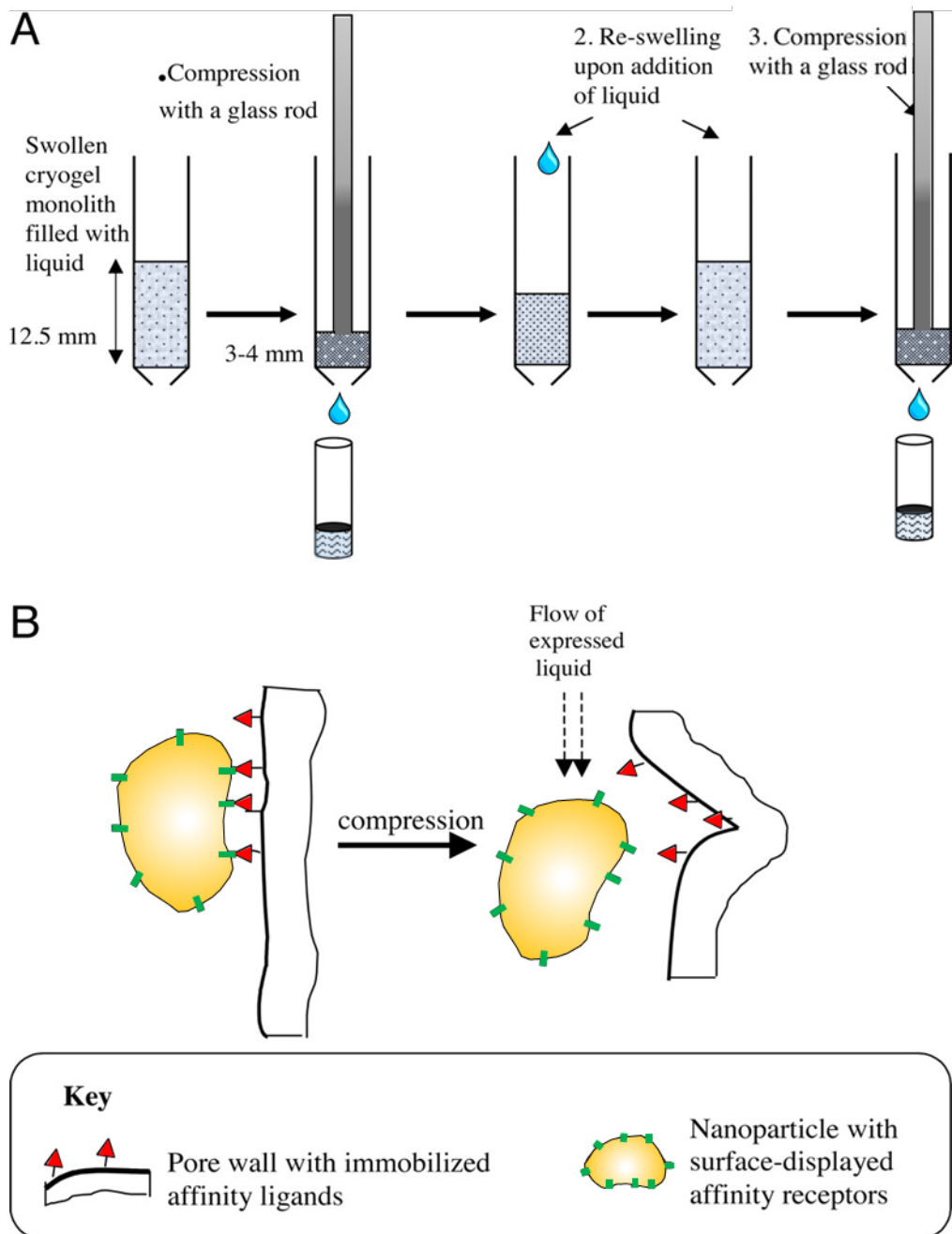


Figure 13. Efficient elution of bioparticles from cryogel-inserted columns. (A) Diagrammatic representation of reversible compression process used for elution of captured bioparticles from affinity cryogel column (B) Temporary physical distortion due to compression results in dislodging of bound particles. Reproduced with permission [240], 2006, Elsevier.

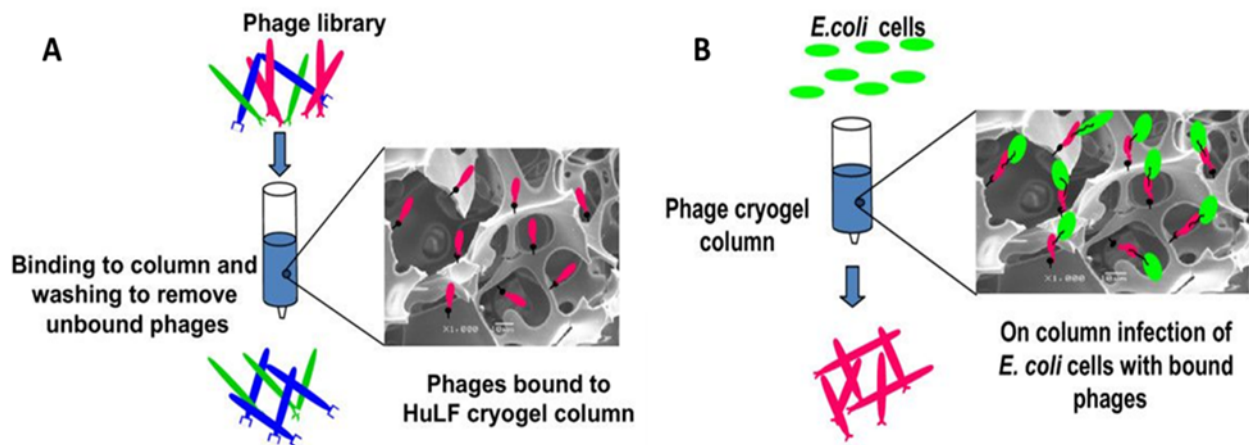


Figure 14. Combining bio-panning and selective bacteriophage multiplication inside cryogel column. (A) Bio panning within column- phages are selectively captured when the phage library is passed through the cryogel column containing covalently attached target protein (B) Phage multiplication- to the cryogel column containing bound phages, bacterial host cells are introduced. During the incubation, phages infect bacteria. These bound bacteria on elution, serve as reservoir of phage particles. Reproduced under the terms of CC-BY 4.0 license .^[236], 2009, Noppe et al.

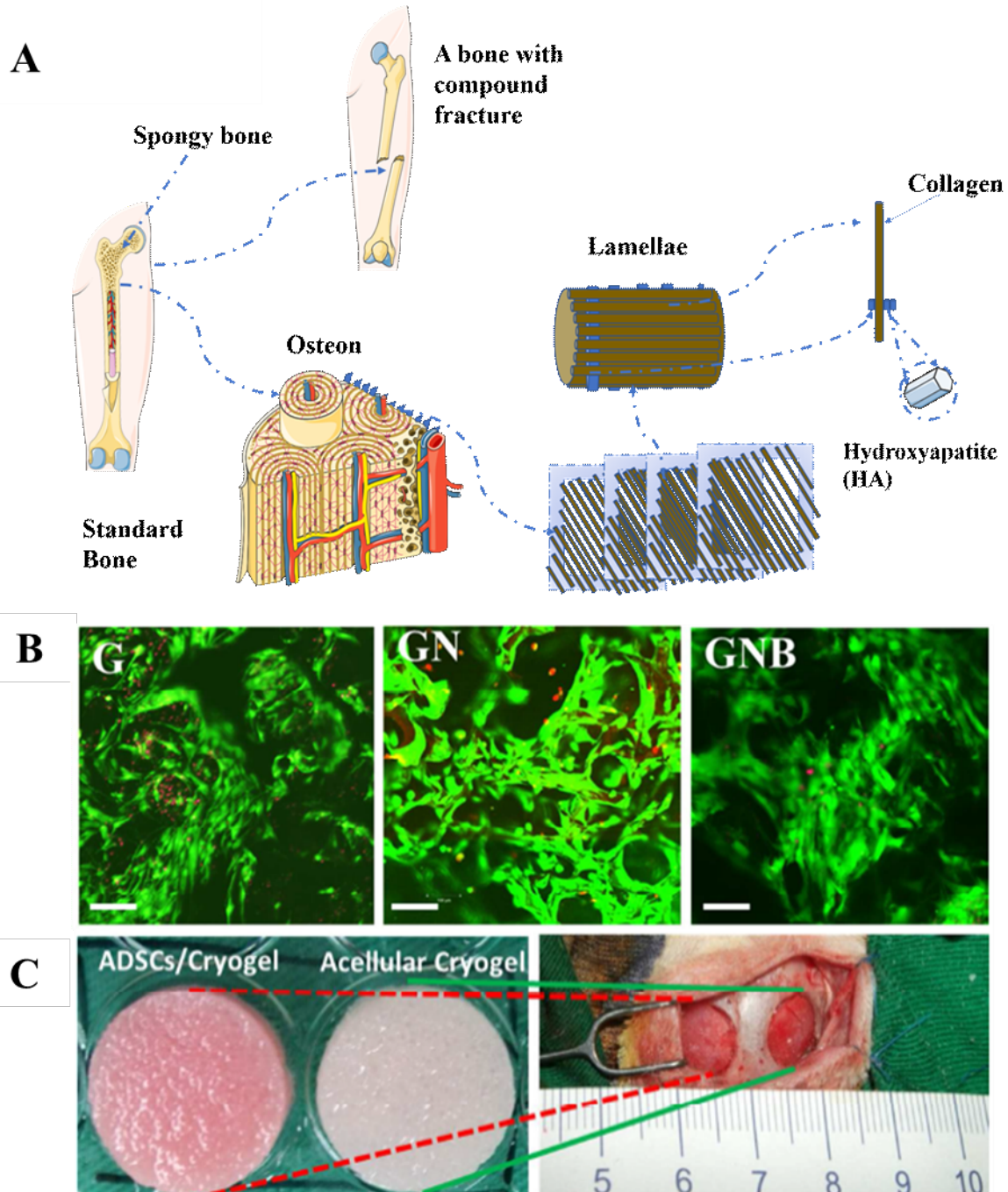


Figure 15. Cryogel design for bone tissue engineering. (A) Structural components of a full bone showing normal and fractured bone. (B) Effect of various fabricated cryogels on the viability of rabbit adipose-derived stem cells (ADSCs). Confocal microscopic images of fluorescently labelled cells confirm highly viable and well-spread ADSC cells 14 days after treatment with various cryogels. (C) A representative ADSCs cryogel versus acellular cryogel prior to implantation for bone regeneration of surgically-created critical cranial bone defect in a rabbit model (left) and representative image of the created bone defect to investigate the capability of the various cryogels (gelatin-based) for bone regeneration (right). Reproduced with permission ^[106], 2016, RSC.

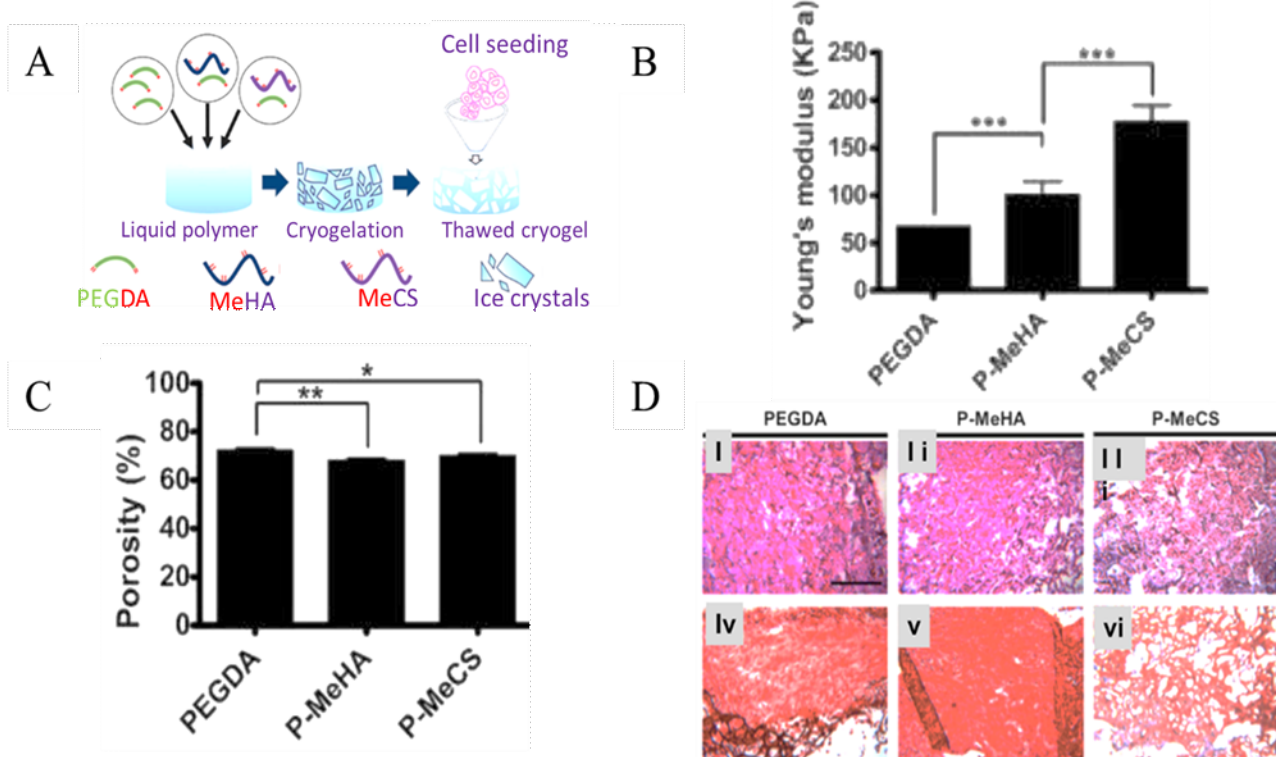


Figure 16. Cryogel design for cartilage tissue engineering. (A) Schematic representation of cryogel fabrication by free radical polymerization during cryogelation. (B) Mechanical properties of various cryogels (Young's modulus of acellular PEGDA, P-MeHA and P-MeCS) spread ADSCs cells 14 days after treatment with various cryogels. (C) Histological analysis of *in vivo* cellular response of chondrocytes in the tested cryogels showing homogeneous distribution of morphologically round cells within cryogel scaffolds (D, I-III) as well as the noticeable presence of proteoglycans (D, I-III) indicative of cartilage formation. Reproduced with permission ^[111], 2016, Elsevier.

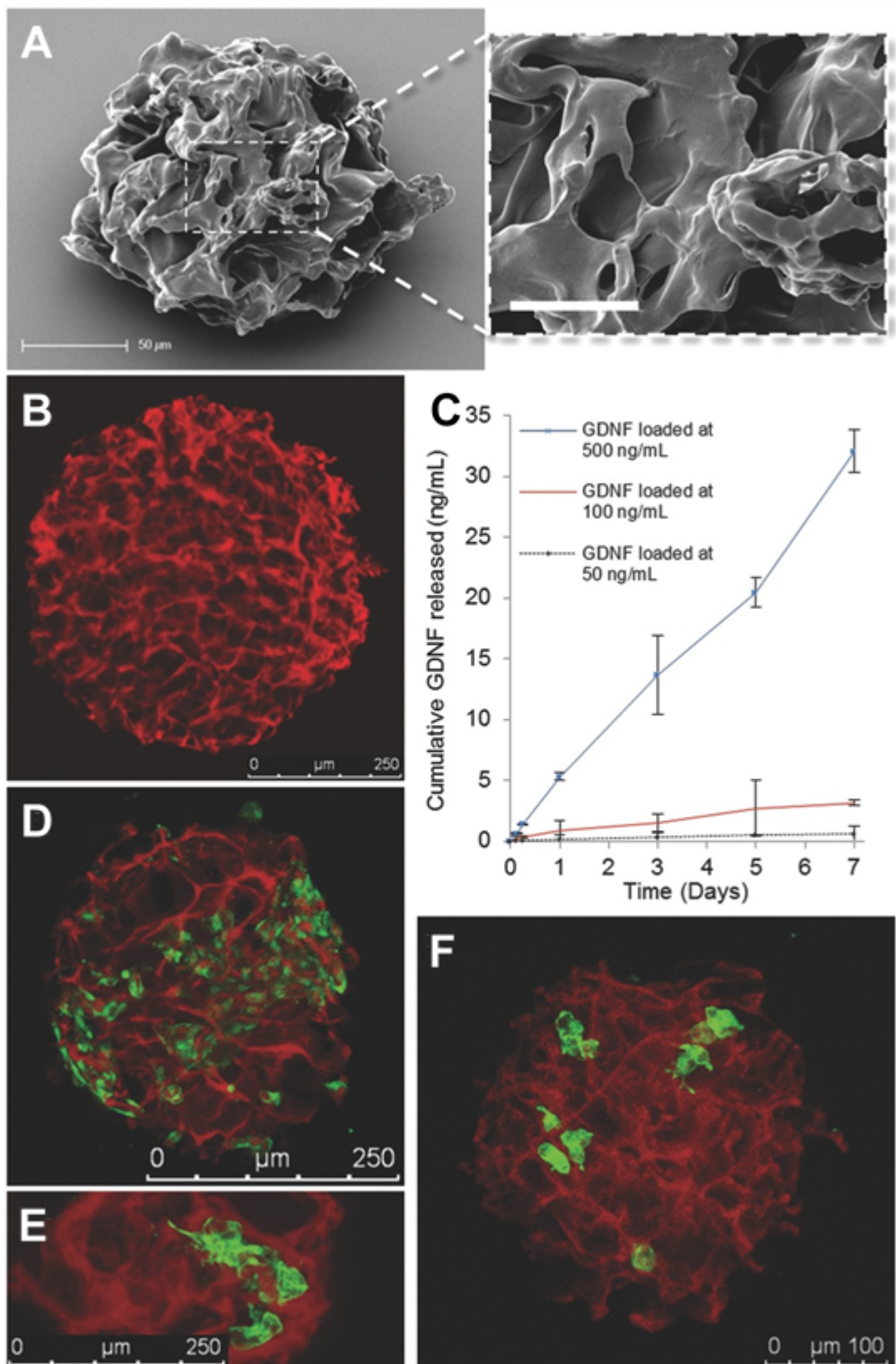


Figure 17. Microscale spherical cryogels characterization and cell growth. (A) SEM picture of the dry cryogel (scale bar: 50 and 20 μm). (B) CLSM fluorescence image of alexa 647-labeled cryogels (red). (C) GDNF released from the cryogels at various concentration. (D-F) CLSM pictures of GFP positive MSCs (D: green), or neurite projection from β III tubulin stained PC12 cells (E and F: green) cultured for seven days within cryogels.^[68]

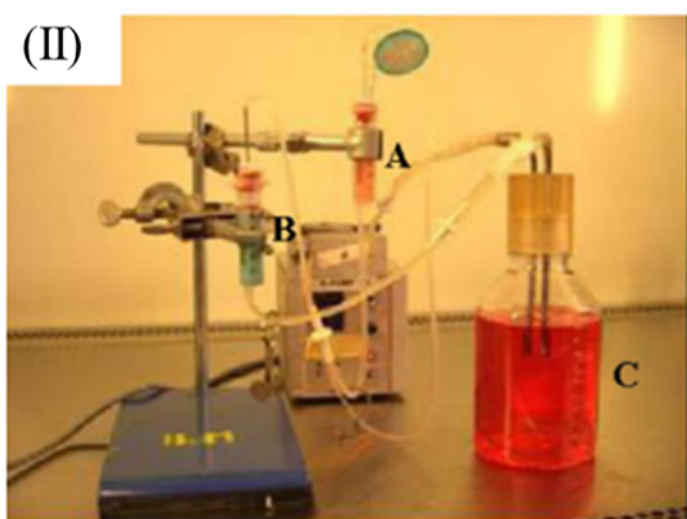
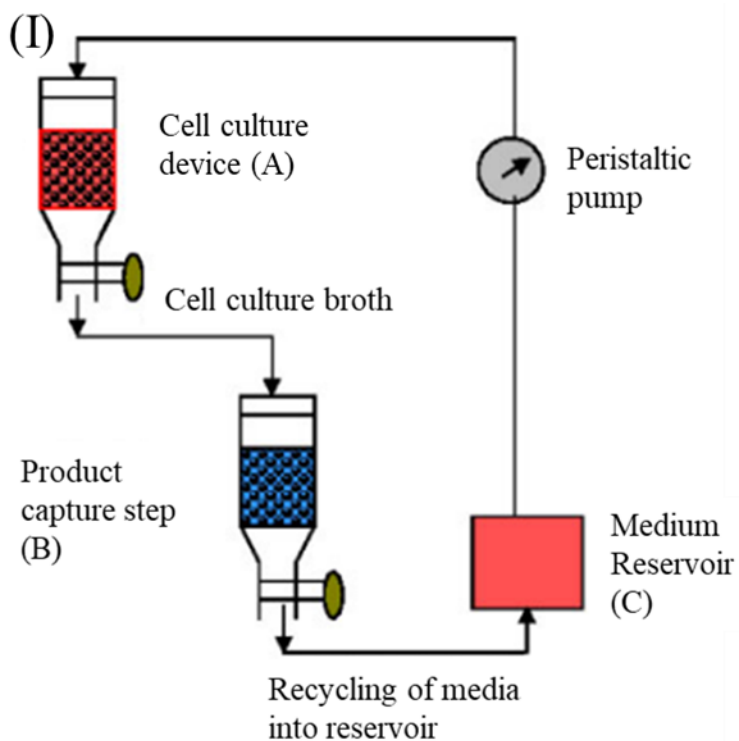


Figure 18. Urokinase production by a cryogel-based bioreactor. Schematic (I) and photograph (II) of the set-up. (A) HT1080 cells seeded in gelatin-pAAm cryogels column, (B) Cu(II)-pAAm cryogel column allowing capture of urokinase, and (C) medium reservoir coupled to a peristaltic pump for a continuous flow rate (0.2 mL/min).^[322]

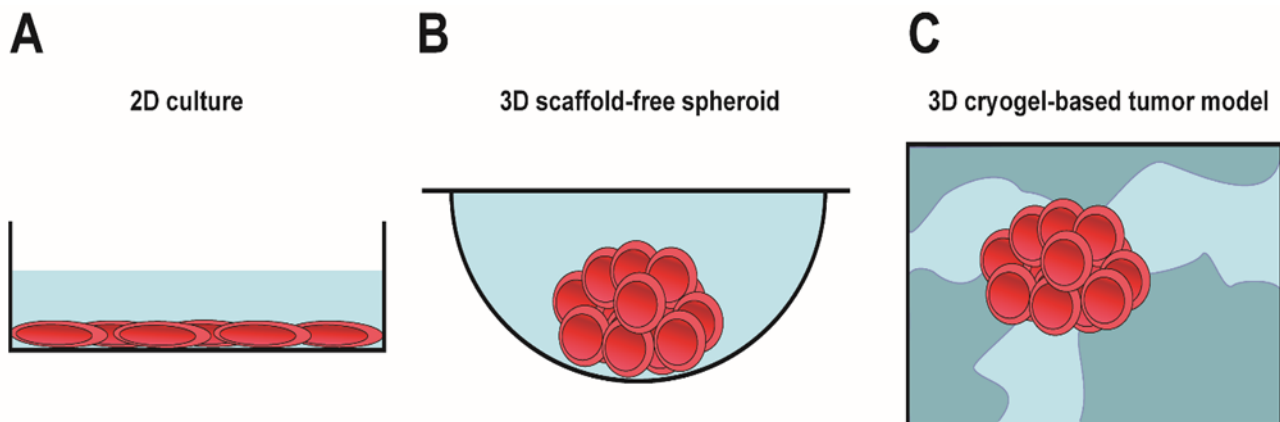
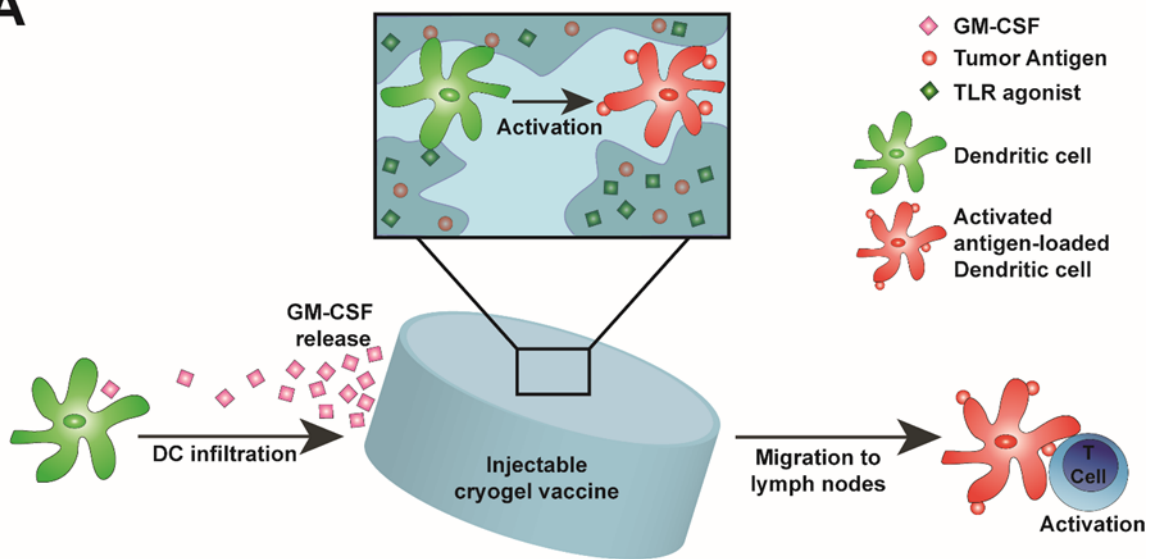


Figure 19. Cell culture methods and characteristics of *in vitro* tumor models. (A) 2D culture results in cells with flat and stretched morphology in a homogeneous population, protein expression patterns that do not resemble *in vivo* expression and increased sensitivity to cancer drugs. (B) Cell culture in 3D scaffold-free spheroids gives cells with a more natural cell shape, in a heterogeneous spheroid, with protein expression that is more similar to *in vivo* expression, and gives more resistance to cancer drugs. (C) Cell culture in cryogel-based tumor models provides a 3D culture system with tunable ECM properties, a controlled cellular environment that is applicable to a wider range of cancer cell types, and allows for straightforward standardization and high-throughput screening.

A



B

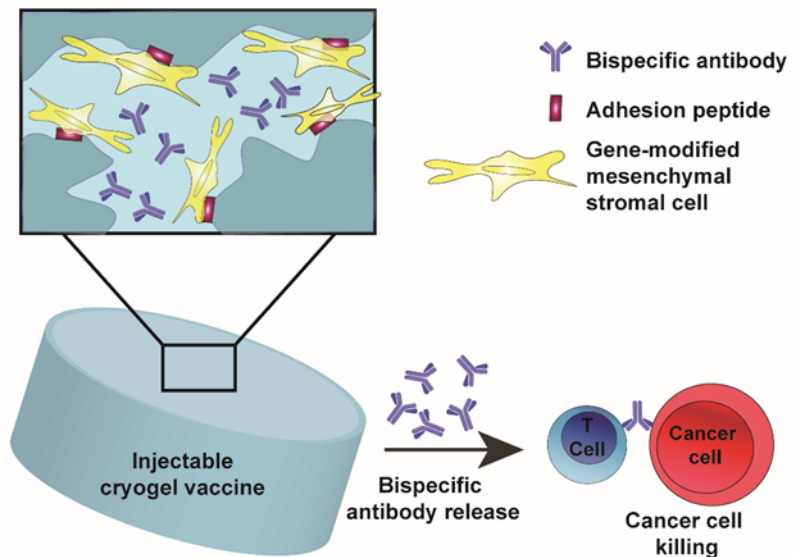


Figure 20. Immunostimulatory cryogel. (A) GM-CSF release recruits dendritic cells into the cryogel construct. Infiltrated dendritic cells take up tumor antigens and are activated with TLR agonists. Activated, tumor antigen-presenting dendritic cells migrate to lymph nodes to activate cancer-specific T cells. (B) Mesenchymal stromal cells are genetically engineered to release therapeutic antibodies. After loading the cells within cryogels, immunotherapeutic antibody factories are formed that allow survival and sustained release of bispecific antibodies that link T cells and cancer cells to induce tumor cell killing.

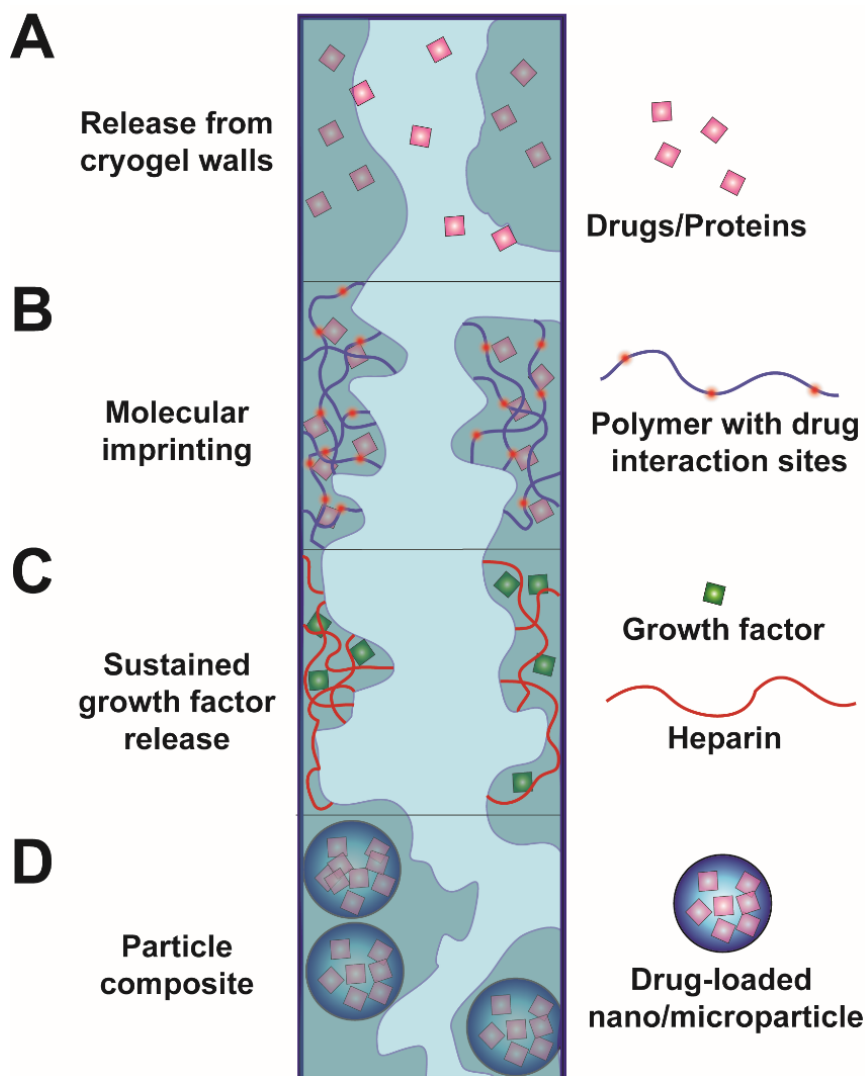


Figure 21. Different methods to control release of drugs and proteins from therapeutic cryogels. (A) Cross-linking and porosity of cryogels is manipulated to allow for controlled release from cryogel walls. (B) Polymers with specific drug interaction sites are mixed with the cryogels to slow down drug release. (C) Heparin interacts with growth factors and can be incorporated to obtain sustained growth factor release. (D) Incorporation of existing controlled release systems in cryogels. .

Table 1. Classification of hydrogels.

Characteristics	Variants			
Cross-linker type	Physical	Chemical		
Polymer network type	Homopolymeric	Copolymeric	Multipolymeric	
Polymer network charge	Nonionic	Cationic	Anionic	Zwitterionic
Polymer network configuration	Crystalline	Semicrystalline	Amorphous	
Particle network type	None	Nanocomposite	Microcomposite	
Gel morphology	Film	Microsphere	Matrix	
Porosity	Microporous	Mesoporous	Macroporous	Supermacroporous

Table 2. Modes of adjusting cryogel synthesis to customize cryogels.

Parameters	Effects
Cross-link type and concentration	<ul style="list-style-type: none"> Physical cross-links: yield gels with insufficiently large pores whose strength is inversely correlated with thawing rate Chemical cross-links: yield gels with sufficiently large pores despite their potential cytotoxicity
Cryogelation temperature	<ul style="list-style-type: none"> When increased: increased pore size and pore wall thickness and density
Polymer molecular weight	<ul style="list-style-type: none"> When increased: increased gel stiffness When decreased: increased pore size
Cryo-concentration	<ul style="list-style-type: none"> When increased: increased elasticity When decreased: increased gelation time
Cooling rate	<ul style="list-style-type: none"> When increased: decreased pore size

Author biographies:

Prof. Adnan Memic completed his Ph.D. in Chemistry with emphasis in biochemistry from Wayne State University under Prof. Mark Spaller (currently at Dartmouth). Next, he was a postdoctoral fellow working on generating neuromodulating nanoparticle platforms (NNPs) in the lab of Prof. Brian Kay at the University of Illinois. Previously, he was a Visiting Assistant Professor of Toxicology and Pharmacology at Dartmouth's Geisel Medical School. He joined King Abdulaziz University in 2010, was promoted to Associate Professor of Nanotechnology, and is concurrently a part-time Lecturer on Medicine at Harvard Medical School and a visiting Associate Professor in the Department of Chemical Engineering at Northeastern University, Boston. His research focuses on translating micro and nanotechnologies into medicine.



Dr. Thibault Colombani graduated from University of Nantes with a MS in Biotechnology in 2013 and a Ph.D. in Immunology in 2017. He is currently working as a Postdoctoral Research Associate in immunoengineering in Prof. Sidi A. Bencherif Laboratory at Northeastern University, where he is focusing on developing biomaterials for Tissue Engineering and Immunotherapy. He has a special interest in modulating cancer microenvironment and enhancing immune cell stimulation via immunomodulators to optimize current anti-cancer strategies.



Prof. Sidi A. Bencherif received in 2009 a Ph.D. degree in Chemistry from Carnegie Mellon University. Following his PhD, he was initially appointed from 2009 to 2012 as a postdoctoral researcher and later from 2012 as a researcher associate in the laboratory of Prof. David Mooney at Harvard University and the Wyss Institute for Biologically Inspired Engineering. In 2016, he joined the department of Chemical Engineering at Northeastern University as an Assistant Professor. His research interests include developing naturally derived biomaterials that can be used for tissue engineering, drug delivery, immunotherapy, and studies into fundamental cell-biomaterial interactions. Prof. Bencherif has authored and co-authored over 50 journal articles in top journals (Science, PNAS, Nature Materials, Nature communications, etc), international conference proceedings, reviews and patent applications, and is the recipient of several fellowships, honors and awards.



In this review, the versatility of cryogel materials for biomedical applications is presented. This unique class of polymeric hydrogels possess a sponge-like morphology combined with remarkable and tunable physicochemical properties. An extensive literature overview is covered on the latest applications of cryogels including bioseparation, tissue engineering, drug delivery, and more recently immunotherapy. Current challenges and future perspectives are also discussed.

Keywords: cryogels; biomaterials; bioseparation; tissue engineering; immunotherapy

*Adnan Memic, Thibault Colombani, Mahboobeh Rezaeeyazdi, Loek Eggermont, Joseph Steingold, Zach Rogers, Kasturi J. Navare, Halimatu S. Mohammed, Sidi A. Bencherif**

Latest Advances in Cryogel Technology for Biomedical Applications

